PADERBORN UNIVERSITY

FACULTY OF
COMPUTER SCIENCE,
ELECTRICAL ENGINEERING
AND MATHEMATICS

ENERGY MANAGEMENT AND OPTIMAL GRID PLANNING FOR RURAL ELECTRIFICATION IN AFRICA

To the Faculty of Electrical Engineering, Computer Science and Mathematics of Paderborn University

for the attainment of the academic degree

Doctor of Engineering (Dr.-Ing.)

submitted dissertation
by

M.Sc.-Ing. Joseph Sisala Mwakijale
Born on January 03, 1989, in Dar es Salaam

PADERBORN UNIVERSITY

FACULTY OF
COMPUTER SCIENCE,
ELECTRICAL ENGINEERING
AND MATHEMATICS

ENERGY MANAGEMENT AND OPTIMAL GRID PLANNING FOR RURAL ELECTRIFICATION IN AFRICA

To the Faculty of Electrical Engineering, Computer Science and Mathematics of Paderborn University

to obtain the academic degree

Doctor of Engineering (Dr.-Ing.)

approved dissertation
by

M.Sc.-Ing. Joseph Sisala Mwakijale

First Reviewer: Prof. Dr.-Ing. Henning Meschede

Second Reviewer: Prof. Dr.-Ing. Stefen Krauter

Date of the dissertation defense: 13. April 2026

Paderborn 2026

Diss. EIM-E/400

ABSTRACT

Access to clean, affordable, sustainable, and reliable energy remains a major global challenge. The United Nations established Sustainable Development Goal 7 (SDG 7) to ensure universal access to modern energy services by 2030. Despite global efforts, about two billion people lack access to commercial energy sources, nearly one billion in Sub-Saharan Africa. Strategies such as grid extension, microgrids, Solar Home Systems (SHS), and swarm grids (SG) have been implemented to address this gap. Swarm grids, formed by interconnecting multiple SHS into autonomous networks, remain at an early development stage. Key challenges include energy dispatch strategies, optimal grid planning, energy management systems, security and privacy, and the cost-effectiveness of converters and communication transceivers.

This research investigates two questions: (1) How can a smart transceiver be developed for rural swarm grid implementation? (2) How can solar-based swarm grids be optimally planned considering investment, operational costs, and local constraints? Additional focus is placed on: (a) identifying tools for efficient deployment of solar swarm grids, (b) integrating the tool with common computer applications for easy use by non-experts, and (c) evaluating driving and threshold parameters for selecting distribution lines in swarm grid implementation.

An integrated framework is proposed to address these questions. First, a LoRa-based smart communication transceiver is designed, with functionality validated through Python simulations and laboratory prototyping. Second, an optimization-based planning model is developed using mixed-integer linear programming to determine cost-effective swarm grid configurations while considering network topology, energy demand, power flow, and infrastructure costs. To enhance usability for users with diverse technical backgrounds, the model is integrated with Microsoft Excel. The framework is evaluated using a test case of ten houses in Kitame village, Tanzania.

Results show that the transceiver effectively manages communication, dispatches energy, records transactions, and detects unauthorized requests. The planning model improves energy deficits by 56.2% and reduces surpluses by 84.9%. Grid stability can be enhanced using either a centralized energy storage system (ESS), achieving 100% improvement at high cost, or demand-side management (DSM), achieving 81% improvement. The study concludes that combining ESS and DSM is essential for stabilizing swarm grids and enabling reliable, cost-effective decentralized electrification.

Declaration

I hereby declare that I have written this thesis independently and have not used any sources or aids other than those specified. I also declare that I have complied with the general principles of scientific work as laid down in the Guidelines for Safeguarding Good Research Practice of the German Research Foundation.

Paderborn, 20.04.2026 

DEDICATION

I truly and deeply dedicate this thesis to my beloved daddy, who sadly passed away during my PhD journey. The love, sacrifices, and unwavering belief in me continue to inspire everything I do. Daddy, your persistence in pushing me to accomplish this academic achievement will never leave my mind until we meet again. May your soul continue to rest in eternal peace!

ACKNOWLEDGEMENT

Firstly, I am deeply grateful to God Almighty for the strength, grace, and persistence that have sustained me throughout this PhD journey.

I would like to express my genuine gratitude to my supervisor, Prof. Henning Meschede, for his invaluable guidance, trust, continuous support, tolerance, and insightful feedback. The mentorship has been helpful in shaping both this research and my academic carrier.

I would also like to acknowledge and thank my first supervisor, Prof. Ulrich Hilleringmann, who not only guided the first part of this research before retiring but also made my journey to Germany possible. The initial support, trust and encouragement laid the foundation for this work, and I remain exceptionally grateful for the contributions.

To the faculty and staff of Sensor Technology department and Energy and System Technology department, thank you for creating an enriching academic environment and for providing the resources that enabled this work.

To my lovely wife, Jesca Mwakijale and our kids, words cannot fully express my gratitude. Your patience, prayers, love, strength, and constant encouragement have been my anchor. Thank you for walking beside me with steady support, even when the path was difficult.

To my mother, siblings, in-laws, and extended family - your prayers, love, and support have carried me from the very first day until the moment, I'm concluding this journey. I'm deeply thankful.

To my friends and colleagues, Lukas, Jenipher, Julia, Ramon, Kevin and Henning, few to mention, thank you for your companionship, academic input, and emotional support throughout this journey. May the Almighty God bless you all.

To the Government of United Republic of Tanzania through the Ministry of Education, Science and Technology under the UDSM HEET project, thank you for the financial and institutional support, which made this research possible.

Lastly but not the least, I am thankful to my employer - the University of Dar es salaam (UDSM) and the staff of college of Engineering and Technology (CoET), for the financial, social, emotional and institutional support that have encouraged me to this achievement.

Table of Contents

Chapter 1: INTRODUCTION

Access to clean, affordable and reliable energy is still a global challenge yet to be 100% solved. The United Nations, through its New York Conference in 2015, established a clear directive by setting Sustainable Development Goal 7 (UNSDG 7). This goal aims to ensure universal access to clean, affordable, reliable, and sustainable energy by the year 2030 (Prechtl, 2023). Currently this challenge is being accelerated by climate change caused by high carbon emission (Solomon et al., 2009). Approximately one billion people in the Global South, particularly in Sub-Saharan Africa, still live without access to clean, affordable, and reliable electricity for basic needs (Adenle, 2020; Ashetehe et al., 2024). Additionally, around 2 billion people worldwide lack access to commercial energy sources (Cabello-Vargas et al., 2021).

The World bank indicator of access to electricity show that most of the under electrified countries are in African continent and few from Asia as demonstrated in Figure 1.1.

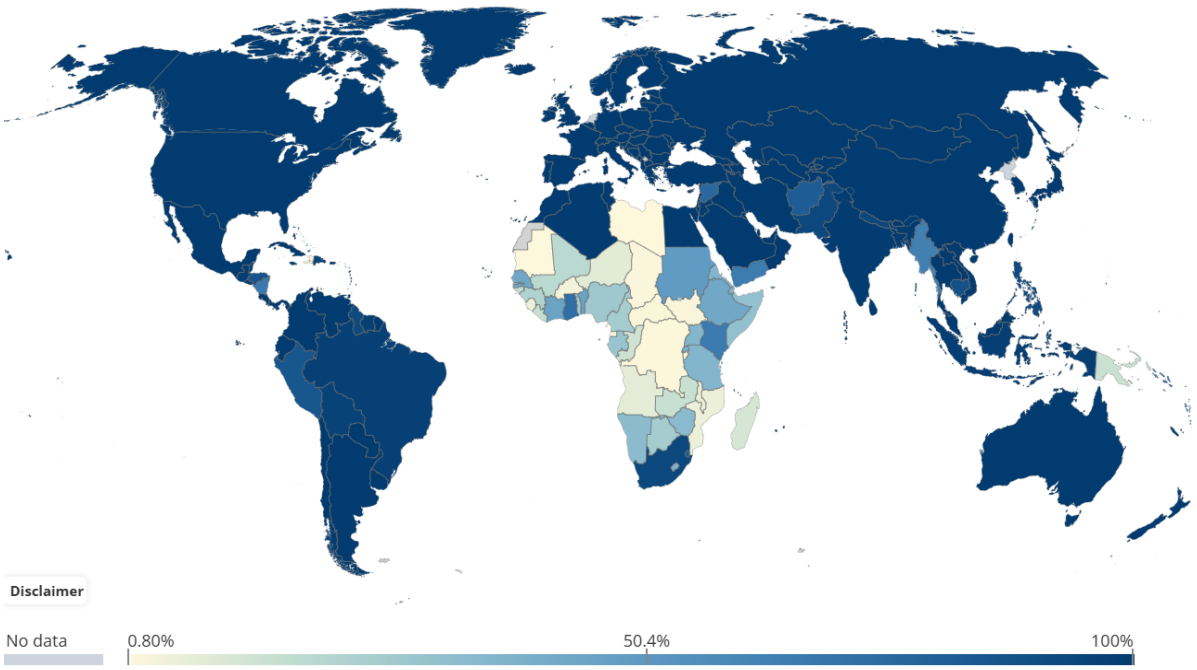

Figure 1.1: Rural Energy Access Rate: Source *(*Indicator | Access to Electricity (% of Population) | World Bank Data360*, n.d.)*

Access to energy, being the steppingstone towards sustainable human socio-cultural development in the aspect of education, finance, healthcare, safety, food security, and the general welfare of any society, needs to be taken care of at all levels (Kulkarni et al., 2019).

While energy access challenge is not a topic in the developed countries, climate change, increased in fossil fuel cost, depletion of fossil fuel reserves, global warming, geopolitical and military conflicts and the need for environmentally friend source of energy are their subjects of concentration (Asif & Muneer, 2007). Therefore, in the developed countries the main challenge in energy sector is to have clean and sustainable energy in which the focus is on the renewables.

In Sub-Saharan Africa (SSA) and some parts of rural Asia such as rural India, Bangladesh, etc., the energy access issue is mitigated using different strategies including the extension of the national grid, establishment of the mini grids and the use of solar home systems (Javadi et al., 2013). These strategies have got different shortcomings which hinders the fully reliance onto them. The extension of national grid involves running of poles and cables several kilometres and installation of transformers towards the remote rural areas. Since, in the rural areas of developing countries their electrical usage is only for the basic needs then most of the governments find it uneconomical to facilitate such projects. While financial viability remains the primary barrier to grid extension, additional challenges include project uncertainty, difficult terrain, the presence of unsurveyed areas and of late the climate change which causes drought in most of dams in hydropower plants and hence causes load shading even in urban areas (Temesgen et al., 2024). The introduction of mini grids was thought to be the best approach in combating the energy access question, but it has also got some challenges hindering its reliance. The challenges facing mini grids include, the risk associated with investors in the case of arrival of the national grid at the village, the risk associated with the interruption of the political leaders in establishing the electricity price without considering or discussing the matter with the investor, government regulatory issues, low electricity demand in rural areas (causing high levelized cost of energy, LCOE), high payment default rates and over-optimistic demand projections (Peters et al., 2019). On the other hand, people in rural areas were encouraged to depend on off-grid solar home systems as their main source of electricity. Solar home system comprised a connected network of the solar PVs, storage batteries, inverters and charger controllers. In the village most of them are the poorest hence cannot afford to have their own solar home systems (SHSs). While some cannot purchase their own SHSs those who can own are using them for the basic needs only (Stojanovski et al., 2017). Since in most of the sub-Saharan countries the availability of sun is almost constant throughout the year, and the electricity production is exceeding the consumption (Fuchs et al., 2023). According to Groh et al. (2014), the amount of generated electricity by the SHSs being dumped as excess is 39.1% of the total generated power. And of course, this occurs during the day when there is plenty of solar power.

The excess energy production results from either high solar output or the oversizing of SHSs, which are designed to ensure reliable operation during autonomous days. This excess production could be monetized by selling it to neighbours or by using it to run small home-based businesses. Trading electrical energy between neighbours in an off-grid SHSs needs an autonomous standalone grid, known as swarm grid (SG).

The concept of swarm grid originated from natural phenomena such as shoaling of fish, colony of organisms and flocking of birds (Kirchhoff, 2013). This concept is now used in renewable energy sources (solar power in this case) to enhance electrification in rural areas by interconnecting the households with standalone SHSs to those with or without SHSs in solving the power demand and the sustainable energy access challenges (Kirchhoff, 2013). The swarm grid concept has got different names due to its formation nature, the names include swarm electrification, peer to peer rural electrification, bottom – up, Ad hoc Grid, Organic Microgrids, et cetera (Groh et al., 2014; Soltowski et al., 2019; Unger & Kazerani, 2012). Figure 1.2 describes the formation of the swarm grid.

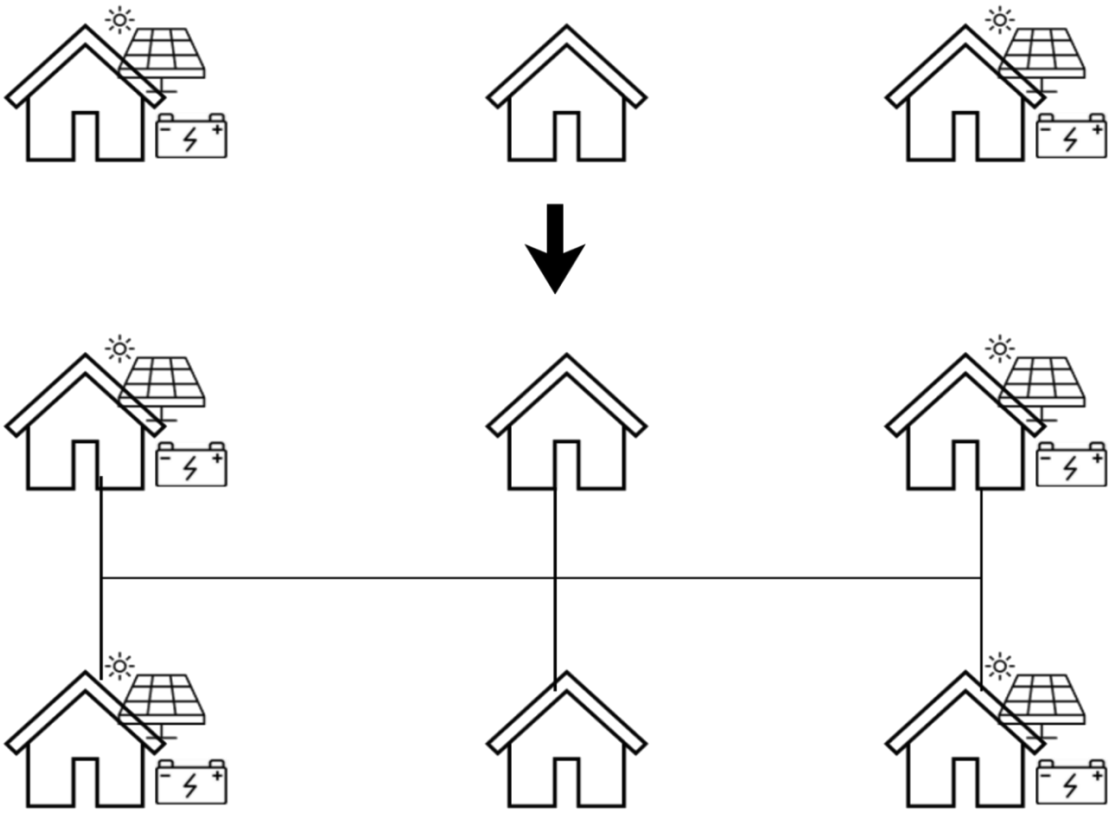

Figure 1.2: Formation of Swarm Grid from SHSs

Drawing from UNSDG 7, financial status of the people in the developing countries, sunny availability in the SSA and the climate change this work is motivated at contributing to solve

the energy access challenges in rural Africa. In the context of swarm grid, the available body of knowledge can be categorized in three groups namely: optimization, security and privacy, and communication technologies (CT) and power electronics (PE) across the grid as illustrated in Figure 1.3. This work is aimed at bringing the knowledge gap in the aspect of optimization, Communication technologies and Security and privacy.

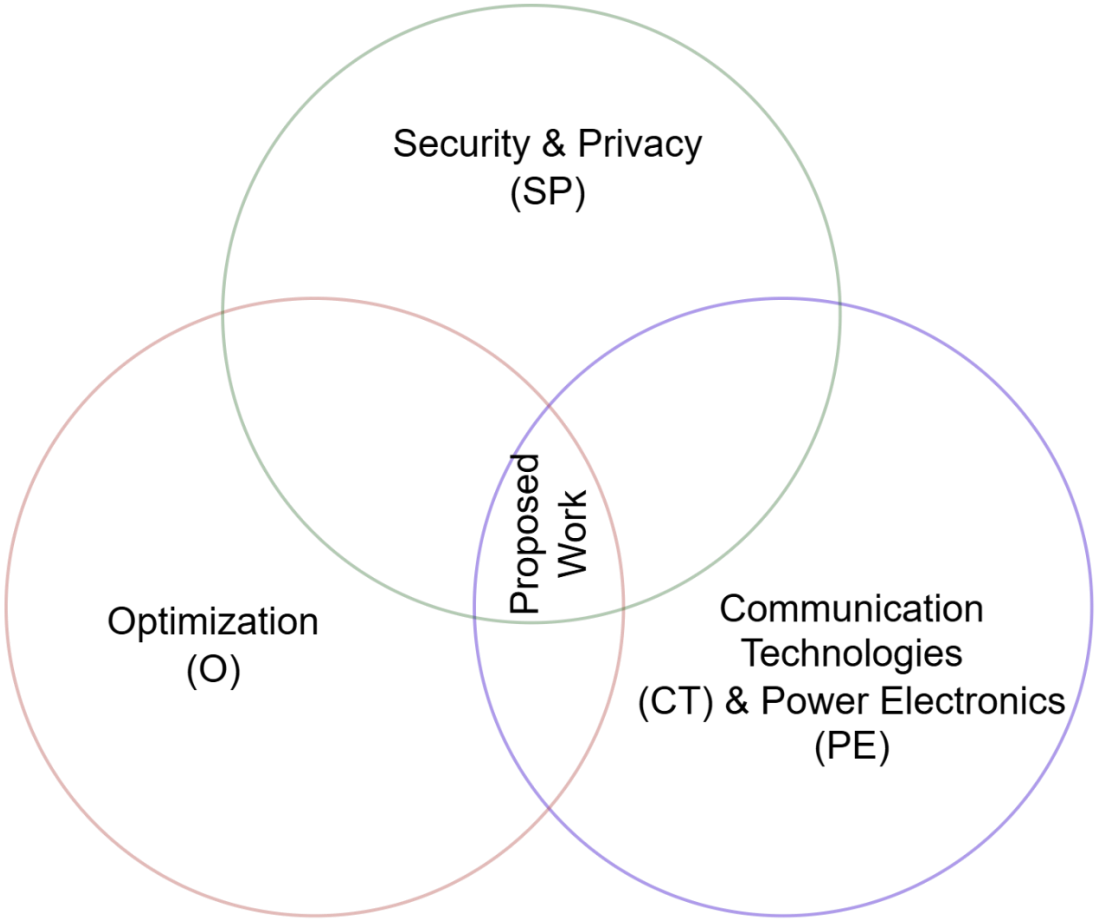

Figure 1.3: Rationale of the Proposed work on Swarm Grid Technology

In addressing energy access challenge different approaches such as extension of national grid, establishment of mini and micro grids, swarm grid and the use of solar home systems have been deployed. However, swarm grid deployment faces diverse challenges including energy dispatch strategies, optimal grid deployment, smart systems for energy management, security and privacy issues, cost effectiveness of converters and many more. These challenges highlight the need for further research to speed-up the universal energy access. This study aims to study and propose solutions on the development of smart transceivers for energy management and optimal grid planning and deployment tools towards SG implementations.

The primary goal of this study is to examine and address the challenges hindering the implementation of swarm grids in reducing energy poverty across rural regions of Africa with the focus of rural Tanzania. This primary goal is achieved through the following specific objectives:

i. To determine the suitable ad hoc communication technology for rural implementation of swarm grid
ii. To develop a smart transceiver for energy management in the swarm grid using the communication technology in (i) above
iii. To develop an optimization tool for effective and efficient deployment of the solar swarm grids
iv. To evaluate the performance of the optimization tool developed in (iii) above
v. To integrate the tool described in (iii) with common computer application program, enabling easy interaction and use by novice

In line with the stated primary goal and specific objectives, this research was conducted in the rural areas of Africa to investigate energy access challenges and provide a cost-effective solution for the existing and newly or prospective deployments of solar swarm grids. Since most areas of SSA countries are rich in solar power, this work restricts its discussion to only solar swarm grids. Furthermore, this work narrows down to discuss only communication technologies required in the rural settings, optimization strategies and the impact of thresholding parameters in the swarm grid deployments. Towards the end of this study alternative approaches to mitigate energy access challenges will be proposed and consequently the living standards in rural areas could be improved.

The remainder of this thesis is structured as follows. Chapter 2 reviews the relevant literature and related works. Chapter 3 describes the methods and design of the proposed solution. Chapter 4 presents the transceiver design, and development. Chapter 5 discusses the optimal swarm grid planning and designing tool. Finally, Chapter 6 concludes the thesis with a summary of findings and recommendations for future research.

Chapter 2: LITERATURE REVIEW

2.1 Introduction

In combating energy challenges, especially in rural areas of developing countries, different approaches have been implemented. In the field of solar swarm grids (SG) there are gaps that still need to be solved for full reliance on technology.

The purpose of this review is to investigate and identify the unresolved challenges in the deployment and implementation of swarm grids (SGs). To achieve this, the review focuses on studies that discuss existing ad hoc communication technologies including those previously applied in swarm grids, the types and functionalities of transceivers used in energy management, the types and scope of distribution networks currently in use, and finally, the planning and implementation strategies and tools being employed.

This chapter is organized as follows: Section 2.1 introduces the chapter. Section 2.2 presents the related works, followed by Section 2.3, which discusses the simulation and optimization of energy systems. Section 2.4 describes the Swarm Grid concept for energy access, while Section 2.5 focuses on communication technologies for rural applications. Section 2.6 covers smart transceivers for energy management, and Section 2.7 explores distribution network design and thresholding parameters. Section 2.8 addresses user-friendly tools and interfaces. Finally, Section 2.9 concludes the chapter by summarizing the identified challenges and research gaps.

2.2 Related Works

This subsection presents various scientific studies on rural electrification in developing countries, with a focus on swarm grid deployment, design, technological perspectives and applications.

Bowes et al. (2017), discuss the energy access status in developing countries and present the advantages and disadvantages of different approaches. These approaches include solar homes systems, mini-grids, and extension of the main grid. Grid extension focusses on expanding the national grid but more often struggle with economic feasibility in remote areas. Mini-grids have the advantage of offering community-scale solutions but face regulatory and operational challenges. The stand-alone solar home systems provide a rapid deployment but with limited power capacity and waste useful energy.

Sheridan et al. (2023) present a comprehensive literature review on electrical swarm grids, describing the state of the art, along with the technology's advantages, disadvantages, and key challenges. Among the challenges discussed are the difficulties of implementing swarm grids in remote areas where mobile network coverage is either unavailable or unreliable due to local terrain; the lack of quantitative evidence on the technology, particularly regarding power losses in peer-to-peer interconnections; the absence of modern methods for grid design and planning; limited exploration of power line communication (PLC) within swarm grids; and insufficient studies on hybrid generation systems in the swarm grid context, among others.

Inam et al. (2015), analysed the architecture and system design of microgrids applying the swarm grid concept. A key focus of their discussion is the method of household interconnection-whether through AC or DC grids. After evaluating few factors such as grid size, generation type, safety, stability, and load characteristics, they conclude that DC grids offer a more suitable solution for swarm grid applications. However, despite its valuable theoretical contributions, the study is limited to small-scale scenarios, considering only low power loads (25 W) and short inter-household distances (approximately 5 meters). In practice, many rural villages may have households separated by greater distances and consume significantly higher power than 25 W.

Ebrahim et al. (2021) discuss the interconnection of nano-grids - referred to as swarm grids in this context - to form a large-scale network known as the Open Energy Distribution Network (OEDN). This interconnection is achieved via a DC bus, managed through sophisticated control algorithms for power management and coordination. However, the study overlooks the internal connectivity and operational challenges within each nano-grid, assuming that the nano-grids are fully functional and reliable prior to interconnection. Some critical issues such as communication mechanisms, privacy, network design etc must be addressed at the nano-grid level before large-scale integration can be realized. Furthermore, although the proposed advanced control algorithms may enhance system coordination it acts as additional load due to high power requirement for its operation. The high-power requirement solutions are discouraged in in solar-powered nano-grids, where energy efficiency is paramount.

Giraneza et al. (2021) propose a swarm grid concept referred to as the interconnection of nano-grids. In this system, surplus energy from each nano-grid is fed into a shared network and stored in a central energy storage unit named as the energy bank. The stored energy can then be redistributed to various stakeholders, including nano-grid members, households without solar home systems, and commercial clients such as milling operators, traders, and to the business

centres. In the case of competing demand, priority is given to nano-grid members. Despite the well-conceived formulation of the centralized storage concept, the study does not address how energy management is performed within the system also it lacks practical sense in a sparse village.

The optimization of networks and technologies is a fundamental factor in achieving high performance at a reasonable cost. In the context of rural electrification, different optimization techniques have been widely employed to minimize costs and enhance overall system performance. In the following paragraphs, the literatures are presented.

The work of Steven Nolan et al. (2017) employs Multi-objective Particle Swarm Optimization (MOPSO) to perform the optimization. The study first formulates the cost minimization of distribution lines as a Capacitated Minimum Spanning Tree (CMST) problem, solved using the Esau-Williams method. It then extends this by considering multiple cable sizes and distributed power source locations, reformulating the problem as a Multi-Level Capacitated Minimum Spanning Tree (MLCMST), which is solved using a Genetic Algorithm (GA) with Prim-Ped encoding. While this approach represents a significant contribution to grid optimization, its application is restricted to conventional microgrids, where the control architecture is centralized. Swarm grids, in contrast, are decentralized networks where peer-to-peer energy exchange, autonomous node behaviour, and communication uncertainty play critical roles. The optimization methods in employed do not account for these complexities, nor do they address the flexible, evolving nature of swarm grid topologies. Therefore, directly applying the approach of Steven Nolan et al. (2017) to swarm grids would be inadequate without substantial modification. This highlights the need for optimization methods specifically tailored to swarm grids.

Magnasco et al. (2016) attempted real-time optimization of swarm nanogrid using a Genetic Algorithm (GA) - based approach, supported by a real-time data monitoring tool. Their formulation considers n separate cost-reduction objective functions each targeting cost minimization at the household level and one additional objective function to minimize the network's excess energy, giving a total of $n + 1$ objective functions, where n represents the number of households in the village. However, this approach has got two challenges. First, it entirely overlooks the optimization of network layout and deployment costs. Second, the design becomes increasingly impractical as the number of households grows; managing $n + 1$ objective functions for large communities leads to excessive computational complexity. Such

a fragmented optimization structure is unsuited for real-world swarm grid deployments, where solutions must be both time and cost-effective.

To minimize the cost of consumed energy in smart cities, Kerboua et al. (2020) employed a particle swarm optimization technique to develop an energy management tool. This tool is designed to manage two types of loads: shiftable and non-shiftable. Since the city incorporates both renewable energy sources (solar and wind, in this case) and the national grid, it was straightforward to categorize the loads in this manner. Although the tool has proven to be highly effective, it cannot be directly applied to swarm grid applications due to differences in the involved stakeholders. This highlights the need for the development of smart tools specifically for swarm grid systems to support rural electrification.

According to the review conducted by Sheridan et al. (2023), there is limited research on the communication technologies required for swarm grid electrification, highlighting a significant opportunity for further investigation in this field. Available contributions are presented in the subsequent sections.

Unger & Kazerani (2012) propose transceiver module for the exchange of control information in the swarm grid. The module operations rely on the cellular network as their communication technology. This solution faces challenges due to its reliance on the cellular network. In most of rural areas especially of Africa and Asia the cellular coverage is not there and if present the operation cost is high. Therefore, the instant deployment of the solution is questionable. This calls for alternative solutions that can serve the needs of the present situation.

Kulkarni et al. (2019) propose a pay-as-you-go (PAYGO) methodology for implementation in swarm grids, utilizing Bluetooth-based communication technology. In this approach, transceivers installed in each household exchange information with servers via the GAMMA cloud. However, due to the limited range of Bluetooth, it became necessary to employ personnel equipped with special devices to extend the communication range. These personnel are required to pass near the households at least once a day. The solution faces challenges due to its reliance on human intervention, making it less reliable and not cost-effective.

Narvios et al. (2021) propose an Internet of Things (IoT)-based swarm grid that utilizes Wi-Fi, internet connectivity, controllers, and sensors to enable communication across the grid. While this approach is well-suited for developed countries or large cities in developing countries, it is not practical for rural areas where even basic voice cellular network coverage remains a challenge.

Privacy and security are the other parameters which need to be taken care of in the swarm grid electrification because when obtaining a customer's real time information, it is easier to taper with their security and privacy. There is very limited literature discussing privacy and security in the swarm grid even those which tries to explain they embed it to the features of the employed communication technology. This is because swarm grids mostly deal with low power loads and most of the privacy and security algorithms are computationally expensive and seem to add unnecessary load to the grid.

Zhu et al. (2011) developed a secure energy routing mechanism to enhance security and enable optimal sharing of renewable energy in smart microgrids. They make use of the energy routers to ensure the security against internally generated attacks does not destroy the grid. The involved encryption and decryption algorithms are still computationally expensive and hence pave a way for more improvements.

Kirchhoff & Strunz (2019) identify five key drivers to encourage prosumer participation in swarm grids: operational simplicity, clear ownership roles for generation and storage assets, scalability, ability to meet all energy demands, and financial compensation for shared energy. However, despite the clarity of these drivers, their application remains largely theoretical. There is a need to move beyond theory and develop practical solutions that address these drivers.

The deployment of swarm grids has sparked discussions around two main approaches: AC and DC distribution lines, each with clear advantages and disadvantages. AC distribution lines are advantageous for their ease of voltage transformation for long-distance transmission using conventional technologies, minimizing power losses. AC is already familiar to most electricity users, making user integration straightforward. It also easily supports small rural enterprises such as milling machines and water pumping projects. Moreover, AC components are widely available in the market, and for high-voltage systems, AC is safer than DC in cases of accidental contact. Importantly, AC grids can seamlessly integrate with the national grid once it reaches the village. Conversely, DC swarm grids present significant cost benefits. Their deployment is cheaper since no AC-to-DC conversion is required, as they power DC appliances directly. Given the proximity of homes in most rural swarm grid setups, ohmic losses in DC lines are minimal. Additionally, with typical operating voltages of 24V or 48V, DC systems are inherently safer for human contact compared to higher AC voltages (Daniel Philipp et al., 2020) .

Despite these known advantages, there is a critical research gap regarding the simulations, laboratory analysis and practical limitations of each approach. There is no set-up threshold to move from one distribution type to another. The thresholds are essential for determining where and when AC or DC should be applied in swarm grid deployments. Without this knowledge, the optimal design of swarm grids remains uncertain, limiting their effectiveness in rural electrification.

The study by Huang et al. (2014) demonstrates how electricity costs can be minimized through the deployment of an energy-sharing grid. In their study, authors developed algorithms to support decision-making by a central controller, using a time-of-use (TOU) pricing model to achieve cost reductions. The energy-sharing grid was interconnected with the main grid and supplied power to the village when needed. However, the work does not address important aspects such as the communication protocols required to implement the controller's decisions. Furthermore, the reliance on a centralized controller introduces some risks: (i) the possibility of a total blackout in the event of controller failure, as seen in large-scale blackouts in the USA, (ii) high computational demands at the central controller, leading to significant energy consumption; and (iii) unresolved questions regarding who in the community is responsible for providing the energy and maintenance needed to sustain the central controller's operation. Given these challenges, there is an urgent need to transition from centralized to distributed control systems. Distributed controllers can eliminate single points of failure, reduce energy consumption, and distribute control responsibilities among local prosumers. This approach would significantly enhance the resilience, efficiency, and sustainability of energy-sharing grids in rural communities.

The works discussed this section have tried to contribute to resolving swarm grid challenges under different contexts and set-ups. However, there are still unsolved issues that need to be addressed before full reliance of the solar swarm grid. Table 2.1 provides summary of the existing literature and the unsolved research challenges for quick reference. While the studies summarized in Table 2.1 primarily present scientific works addressing optimization, deployment strategies, and operational challenges of swarm grids, effective implementation in rural contexts also depends on the availability and suitability of enabling technologies. To complement the scientific works, Table 2.2 summarizes the state of technical knowledge related to communication technologies, optimization approaches, and grid design considerations relevant to swarm grid deployments.

Table 2.1: Summary of the Research Gaps

Reference	Issue being Addressed	Methodology	Assumptions (if any)	Challenges and / or Limitations
Giraneza et al. (2021)	Energy Management	Centralized storage	All HHs have access to the energy bank	Difficult to implement in a sparse village
Kerboua et al. (2020)	Minimization of the cost for consumed energy	PSO	The SG is Grid connected	In the remote areas the Grid is not available hence the approach is in-appropriate
Zhu et al. (2011)	Privacy and Security	Algorithm development	None	The algorithms are computationally expensive
Kirchhoff & Strunz (2019)	Drivers for participation in SG	Theoretical analysis	None	Lacks practical applications
Daniel Philipp et al. (2020)	SG deployment approaches (AC or DC)	Theoretical analysis on the advantages and disadvantages	None	Simulation, laboratory analysis and practical realizations are missing
Huang et al. (2014)	Cost minimization in the Grid tied SG	Central control equipped with the developed algorithm based on time of use (TOU) pricing model	None	-Communication protocol involved is missing -Reliance on central controller put the entire grid at risk

Table 2.2: Summary of the Technical knowledge Gaps in the deployment of SG

Reference	Issue being Addressed	Methodology	Assumptions (if any)	Challenges and / or Limitations
Inam et al. (2015)	Determination of distribution type between AC and DC	Evaluation of grid size, generation type, safety, stability, and load characteristics	HHs separation is 5 m only and the maximum power is set at 25 W	In practical and real cases, the HHs separation is beyond 5 m, and the power requirement can go up to kW
Steven Nolan et al. (2017)	Grid Optimization	MoPSO and GA	Applied to Micro-grids (centralized approach)	Can not directly be applied to swarm grid (need decentralized approach)
Magnasco et al. (2016)	Network Optimization	GA, formulated n cost-minimization at HH level, and 1 function for minimization of network's excess energy making a total of $n + 1$ objective functions	None	-Complexity grows as the number n of HHs increases. -Optimization of the entire network layout is missing
Unger & Kazerani (2011)	Communication	Cellular network	Availability of cellular coverage	The reliance in cellular network lack practicability in remote areas without cellular coverage
Kulkarni et al. (2019)	Communication	Bluetooth, personnel and	None	Reliance in Bluetooth makes the solution not realistic while

		GAMMA clouds		human intervention makes it not only less cost effective but also less reliable
Narvios et al. (2021)	Communication	Wi-Fi and Internet	Availability of internet	Reliance on internet makes it irrelevant for remote applications where there is no internet

2.3 Simulation and Optimization of Energy Systems

Simulation and optimization are essential tools in analysing and improving the performance of energy systems, including Swarm Grids (SGs). In the context of SGs, where system growth is organic and decentralized, these tools support informed investment planning (what components to install and where) and dispatch decisions (how to operate available resources efficiently). Both aspects can be formulated as optimization problems, but the primary goal is to simulate realistic system behaviour rather than to achieve purely mathematical optimality.

Early research in off-grid and hybrid energy systems commonly employed software such as HOMER (Hybrid Optimization of Multiple Energy Resources) to identify least-cost configurations of renewable energy sources. While HOMER remains popular for techno-economic assessment, it provides limited flexibility in modelling network interactions, operational constraints, or decentralized energy exchanges typical of swarm grids. Consequently, recent studies have shifted toward more advanced simulation and optimization approaches.

For instance, Samende et al. (2021) developed an optimization-based model to minimize power losses in transmission and storage systems, while Watson et al. (2018) incorporated historical weather data to optimize system sizing under varying resource conditions. Similarly, Masenge & Mwasilu (2020) applied Mixed-Integer Linear Programming (MILP) to reduce energy storage costs and improve the overall cost-effectiveness of hybrid systems. These studies highlight a broader trend: optimization methods are increasingly integrated into simulation models to improve both investment and operational decision-making. In the literature, optimization approaches are generally grouped into three categories:

1. Classical (Mathematical) Optimization – methods such as Linear Programming (LP), MILP, and Nonlinear Programming (NLP) are used to determine cost-optimal system configurations under well-defined constraints.
2. Heuristic Methods – problem-specific strategies (e.g., greedy or decomposition approaches) that provide feasible solutions efficiently, often used in network layout or microgrid design.
3. Metaheuristic Methods – general-purpose algorithms inspired by natural processes, such as Genetic Algorithms (GA), Particle Swarm Optimization (PSO), and Grey Wolf Optimization (GWO), which are particularly useful for complex, non-linear, and multi-objective energy problems.

Among these, PSO and GWO are frequently applied in swarm grid and rural electrification studies due to their balance between convergence speed and solution accuracy. However, a key limitation across many studies is the lack of integration between investment and operational (dispatch) layers, as well as limited treatment of uncertainties such as demand fluctuations, weather variability, and technical constraints.

2.4 Energy Access and Swarm Grid Concept

Swarm grid is a technology that is getting much attention recently due to its easy creation of diversity generation and storage. In this technology, the owner of a standalone Solar Home System (SHS) is allowed to connect nearby households and sell surplus electricity. This not only generates income for the SHS owner but also expands energy access to others. Figure 2.1 shows an architecture of the swarm grid concept with the two main players: Prosumer and consumer. The grid operations are facilitated by means of GSM network for transferring control signals across the grid.

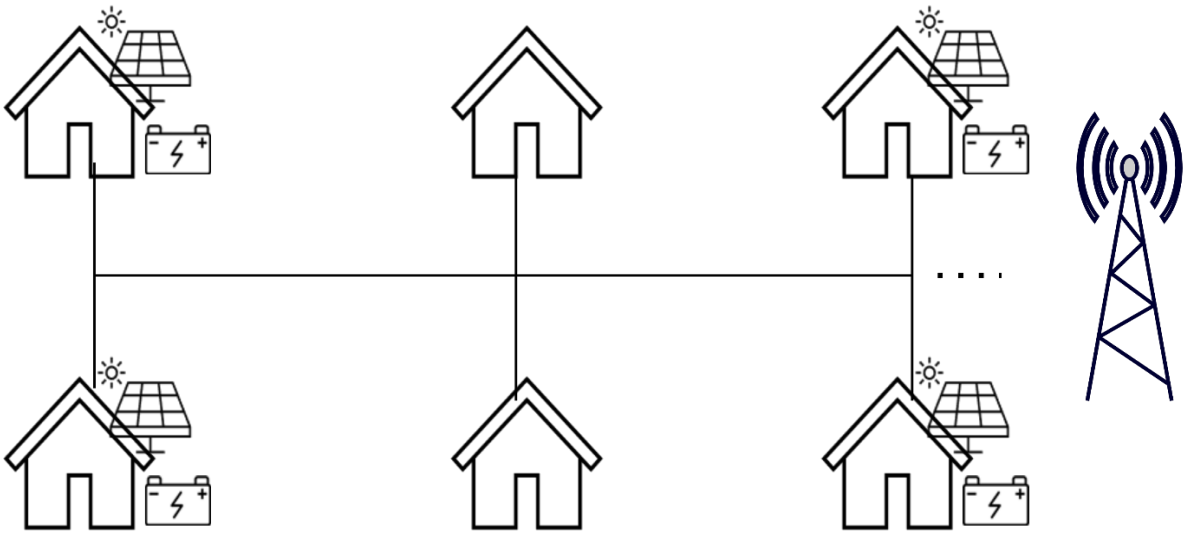

Figure 2.1: Swarm Grid Concept and Operations: Source (Inam et al., 2015)

The consuming unit can only purchase electricity from the grid and pay for what it has been consumed. The consuming unit is commonly known as consumer. On the other hand, the Generating unit can both purchase and sell electricity from and to the grid. The generating unit is commonly known as prosumer. According, Groh et al. (2014) and Kirchhoff (2015) most standalone SHSs owners generate significantly more energy than they consume. For instance, in the case of Tamil-Nadu, India, research has shown almost 40% of the generated solar energy is in excess (Groh et al., 2014).

Swarm grid technology has been successfully demonstrated in different countries such as India, Rwanda (through field trials), and Bangladesh, where it has proven effective in increasing energy access in areas without grid connections (Fairley, 2018). This technology is expected to be one of the most effective solutions for addressing energy access challenges in both rural and urban areas, particularly where solar irradiance remains constant throughout the year. However, the SG faces various challenges in different aspects such as security and privacy, optimization, grid stability and reliability, modelling, power electronics, communication systems, control systems and the clear architecture development (Sheridan et al., 2023). These challenges need to be addressed for full reliance on the technology.

2.5 Communication Technologies for Rural Swam Grids

Effective communication infrastructure is a critical component in the deployment and management of solar swarm grids, which rely on decentralized, peer-to-peer energy trading between distributed energy resources placed in the different households (Agrawal et al., 2023).

In rural and remote environments, conventional communication infrastructure (like fibre optic cable and telephone systems) is often difficult to deploy due to its terrain and financial affordability of the users. In such situations the choice of appropriate ad hoc communication technology plays a pivotal role in ensuring system reliability, scalability, affordability and efficiency. In this section different ad-communications technologies are discussed.

2.5.1 Overview of Ad Hoc Communication Networks

Ad hoc communication networks are self-configuring systems of wireless nodes that can dynamically establish communication without requiring a fixed infrastructure (Agrawal et al., 2023). These networks are particularly suited for applications, where the nodes (households in this case) may be geographically dispersed and the network topology may change from time to time due to variability in energy, consumer and prosumer participation. The key attributes necessary in the implementation of the rural solar swarm grid communication system include:

- *Low power consumption*
- *Long-range connectivity*
- *Robustness to node failures*
- *Low deployment and maintenance cost*
- *High privacy and security*

2.5.2 Contender Technologies

Different wireless communication protocols have been explored for energy-related applications in off-grid contexts. The most relevant to the rural swarm grids include:

(a) Bluetooth and BLE

Bluetooth, and particularly Bluetooth Low Energy (BLE) is designed for ultra-low power communication over very short distances (ideally up to 100 m but practically serves only 10 m). Bluetooth has had several releases since 1999, starting with Bluetooth v1.0 which was aimed at connecting devices typically working together, devices like cell phones, headsets, laptops, mouse, keyboards, mouse, et cetera presents low data rate, up to 1 Mbps. The latest version is Bluetooth 4.0 which was completed in 2010. Bluetooth 4.0 is fully compatible with 1.0 but provides high data rates up to 24 Mbps. Bluetooth is ideal for intra-household communication and energy management or device level communication. It lacks the range and scalability required for the implementation of swarm grid (Augustin et al., 2016)

(b) Cellular networks (GSM/3G/4G)

Cellular networks offer wide coverage and reliable data transfer at high speed. However, they are dependent on mobile network availability, which is often limited, and have coverage issues due to the terrain of the rural areas or nonexistence in most of the underserved rural areas. Additionally, the high deployment cost, operational costs (SIM cards, data plans and servicing of the Base stations) and energy consumption pose barriers for large scale rural deployment (Mekki et al., 2019).

(c) LoRa and LoRaWAN

LoRa (Long Range) is a sub-GHZ wireless technology offering long-range communication (Up to 20 km and 5 km in rural and urban settings, respectively without a need for repeaters) at low data rates (Centenaro et al., 2016). It uses the unlicensed portion of the internationally reserved radio band for industrial, scientific and medical (ISM), i.e., 433 MHz in Asia, 868 MHz in Africa, 868 MHz in Europe, and 915 MHz in North America. The chirp spread spectrum (CSS) modulation used by LoRa to spread a narrow band signal into wider channel bandwidth supports its bidirectional communication. Also, this CSS results in a signal of low noise level, high interference resilience, and high security (i.e., difficult to jam or detect) (Reynders et al., 2016). Furthermore, LoRa has ability to adapt the data rate and range trade-off between devices facilitated using six spreading factors (SF7 – SF 12). This is to say, LoRa is highly energy-efficient, cost effective, and ideal for sparse, large-area deployments, making it one of the most promising candidates for rural swarm grids.

LoRaWAN is the LoRa based communication protocol standardized by the LoRa-Alliance. It supports star and mesh-like topologies with centralized gateways. It uses the time difference of arrival (TDOA) technique to localize end devices. Furthermore, LoRaWAN supplies diverse classes of end devices to deliver the different needs of IoT applications, e.g., low power requirements (Murdyantoro et al., 2019). Currently three classes of end devices exist, however all of them support bidirectional communications. Their distinctions are as follows (Mekki et al., 2019):

- *Class A devices:* Devices in this class support the uplink transmission followed by two short downlink windows (*see* Figure 2.2). Mostly, the communication needs by the end device are used to determine the transmission lot schedule while in rare cases a random time basis is used. At any time, the downlink communication will have to wait until the next uplink message occurs in the same device. By allowing short

duration of downlink after uplink has occurred, devices in this class are considered as the lowest power consumption devices for all three classes.

- *Class B devices:* in accumulation to the random receive windows supplied by class A devices, class B devices provide extra receive windows occurring at scheduled times.
- *Class C devices:* contrary to devices in Class A and B, devices in this class have an always open receive windows which close only during the uplink. Therefore, devices in this class are considered to have the highest energy consumption compared to the other two classes.

Figure 2.2: LoRaWAN Communication for Class A devices (Mekki et al., 2019)

(d) Wi-Fi (IEEE 802.11)

Wi-Fi is widely available and supports high data throughput, up to hundreds of Mbps depending on the channel condition. Wi-Fi is built on top of the IEEE 802.11 standards and provides a range of up to 1 km with evasion broadcast power of 200 mW. The minimum data rates that Wi-Fi can support can be as low as 4 Mbps. It is power hungry when compared with other narrow bands (Nb) Ad-hoc communication technologies. Its reliance on continuous power supply and infrastructure (routers/access points) makes it less ideal for remote applications such as rural swarm grid (Augustin et al., 2016). More details about Wi-Fi and the corresponding protocol architecture can be found in (Adame et al., 2014).

(e) ZigBee (IEEE 802.15.4)

ZigBee is a communication technology built on top of the IEEE 802.15.4 standard which can support data rates up to 250 kbps in a short range. The range of Zigbee is environmentally dependent, in a clear line of sight (LOS) up to 1 km is possible. The low-power, short-range, and low data rates made it widely used in smart metering and home automation. However, its limited range and susceptibility to interference make it less suitable for widely spread rural applications unless repeaters are used exclusively (Augustin et al., 2016).

2.5.3 Comparative Analysis of Ad hoc Comm. Technologies

Having gone through all the candidate ad-hoc technologies, a thorough comparative analysis based on the attributes mentioned earlier in this sub section is conducted. Table 2.3 outlines the properties of each communication technology and the corresponding level of suitability towards SG implementation. Figure 2.3 compares those technologies in terms of bandwidth and range requirements.

Table 2.3: Comparative Analysis of Ad hoc Comm Tech (Mekki et al., 2019)

Technology	Range	Power Consumption	Topology	Cost	Suitability for SG
ZigBee	Low	Very Low	Mesh	Low	Limited (need repeaters)
LoRaWAN	High	Very Low	Star	Low	Highly suitable
Wi-Fi	Medium	High	Star	Medium	Not ideal
BLE	Very Low	Very Low	Point-to-point	Low	Not suitable
GSM/3G/4G	High	Medium-High	Star	High	Conditional

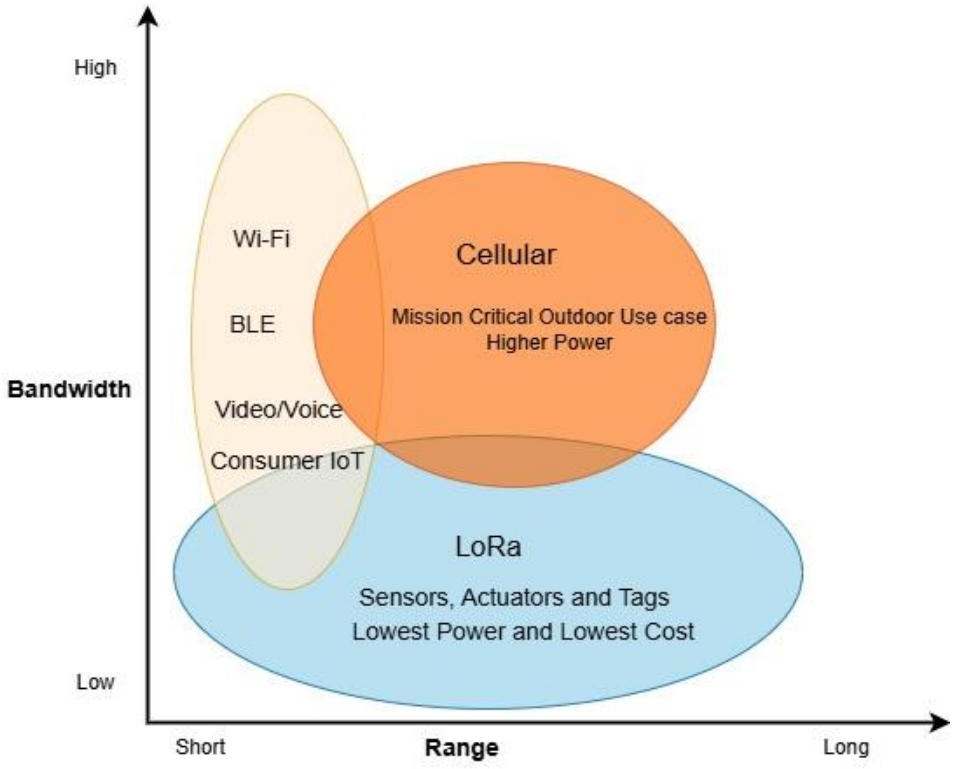

Figure 2.3: Bandwidth and Range Comparison of the Comm Tech (Mekki et al., 2019)

2.6 Smart Transceivers for Energy Management

The energy industry is currently transitioning from conventional methods to more modern approaches through mimicking human muscular and never systems (Georges Akhras, 2000). A key feature of modern methods is the ability to reduce human involvement in the operation, management, and control of energy systems and subsystems. Since modern methods can operate without human intervention, they reduce human errors and are therefore referred to as smart systems, tools, or methods. Therefore, a smart transceiver is devices that can operations such as billing, energy management, demand side management, commit a request or receive of energy etc without the need for human intervention.

2.6.1 Role of Smart transceivers in energy systems

Smart transceivers play multiple roles in energy systems. In the context of off-grid implementations, they are used to transmit and receive signals related to billing information, power consumption, power delivery, total payment required, total revenue generated, fault detection and notifications, user identification, request types, power demand, and connection setup or termination (Kulkarni et al., 2019; Narvios et al., 2021). These smart transceivers can also be integrated into demand-side management (DSM) systems to enable intelligent load control. They facilitate real-time decision-making by determining which loads should remain energized and which should be temporarily disconnected, based on factors such as priority level, demand-response signals, time-of-use pricing, or system constraints. For instance, in an off grid microgrid scenario, non-critical loads like air conditioning or water heating may be shed during peak demand periods, while critical loads such as lighting and medical equipment remain powered. This dynamic load management helps optimize energy usage, enhance system stability, and extend the availability of limited energy resources (Mwammenywa et al., 2022).

2.6.2 Smart communication modules

Smart communication modules are integral parts of any modern energy grid including the off grids. By incorporating the communication technologies such as Zigbee, Wi-Fi, GSM, LoRa or Bluetooth, these modules allow for seamless exchange of data between subsystems. According to (Georges Akhras, 2000), any smart communication architecture is comprised of five components (*summarized in* Figure 2.4) called smart communication modules:

- *Control unit (Controller):* This is also referred to as the brain of the system. The function of this module is to control and manage the whole system by performing data manipulation and analysis, followed by determining the appropriate actions to be

taken. Example of these controllers include Microcontrollers (e.g., Arduino, STM32 etc.), Programmable Logic Controller (PLC), PID controller algorithm and Embedded system running control software, etc.

- *Data acquisition (Sensor):* The role of this module is to collect the required raw data for sensing, monitoring and control. There are various types of sensors in the world, few to mention, including: water level sensors, current sensors, voltage sensors, temperature sensors, humidity sensors, light sensors etc.
- *Data transmission:* This is the channel for raw data transfer from the data acquisition module to the local control units.
- *Data instructions:* Its role is to transmit the decisions and corresponding instructions from the control unit to the appropriate components of the system.
- *Action devices (Actuator):* The function of these devices is to act by triggering the controlling devices. It mostly converts electrical signals into mechanical movements. Example of actuators include, electric motor, solenoid valve, Hydraulic piston, relay etc.

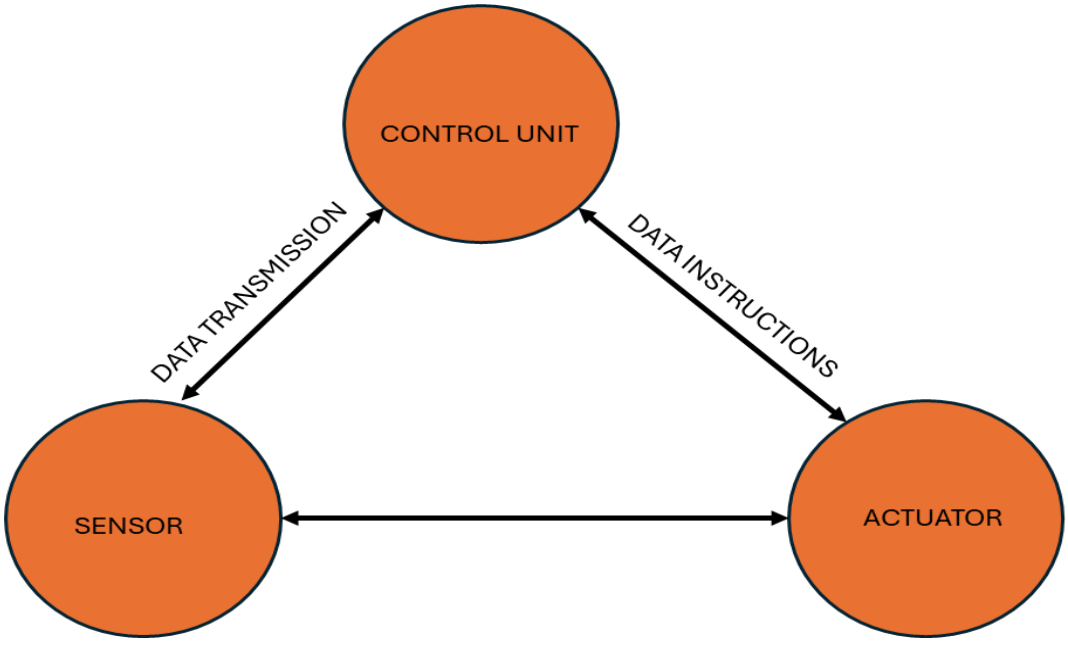

Figure 2.4: Smart Communication Architecture (Georges Akhras, 2000)

2.7 Distribution Network Design and Thresholding parameters

In the design of power distribution networks in rural areas, several factors are considered in selecting an appropriate system architecture. However, regardless of the number of factors

involved, the outcome typically results in the choice between an AC or a DC distribution system. This decision can be guided through the application of thresholding, which refers to the setting of upper or lower limits to support the selection among available options. Paserba & Cunningham (2024) pointed out to this as the war of electric current. The research conducted by Inam et al. (2015) outlines six factors that can be considered in choosing between the two distribution networks. These factors include:

1. *Type of power generation*
2. *Safety*
3. *The span of the distribution system (size of the grid) as well as separation distance between houses*
4. *Types of end user's appliances (types of loads)*
5. *Stability*
6. *Skills required and the cost of deployment*

The work of Starke et al. (2008) uses the types of loads in the network to compare losses between the two distribution systems in the main grid. In that study at different ratio of loading type each different system is better than the other, for example, if the loading type is 100 % AC and 100 % for each system then AC was found to better than DC the vice versa happen when the loading is 50 % for each. Furthermore, line power losses are directly related to the length (span) of the distribution line. From the utility's perspective, real power losses are given significantly greater attention than reactive power losses (Ramesh & Chowdhury, 2009).

Since the grid may consist of open loops or radial strands without any parallel lines, the current flow is clearly defined. Therefore, the calculation of active and reactive power losses can be performed independently. Moreover, since the grid is in an isolated area, the assumptions used in the calculations remain valid. Consequently, equations (2.1) and (2.2) represent a highly simplified model of the actual grid, used to determine total real power loss and reactive power loss, respectively.(Ramesh & Chowdhury, 2009)

$$P_{loss} = \sum_{i=1}^{n_{br}} |I_i|^2 r_i \tag{2.1}$$

$$Q_{loss} = \sum_{i=1}^{n_{br}} |I_i|^2 x_i \tag{2.2}$$

Where $|I_i|$ is the amplitude of the current flowing in branch i, n_{br} indicates the total number of branches in the distribution system, r_i and x_i is the resistance and reactance of branch i, respectively.

2.8 User friend Tools and Interfaces

The user friend tools and interfaces have been known for different applications by proving a good huma-machine interaction. User friendliness plays a vital role in the design and effectiveness of engineering tools. It focuses on creating intuitive, efficient and user-friendly interfaces that enable engineers and non-engineers to interact seamlessly with complex software systems (Van Der Meer et al., n.d.). Different approaches have been used to integrate engineering solutions to user friend interfaces. Narvios et al. (2021) developed a mobile phone graphical user interface (GUI) to enable households to request energy, authorize energy dispatch, and obtain an overview of power flow within the swarm grid. To provide a better understanding of the various parameters affecting the swarm grid, Hollberg (2015) developed and integrated a model into MS Excel for simulating electricity flow and line losses. Furthermore, to demonstrate the ramp behaviour of renewables, the work of Mishra & Palu (2016) developed a user interface tool using MATLAB software for visualizing and analysing power variation events. Additionally, to enable novice users to design their own solar PV systems, the work of Alfaris & Almutairi (2024) developed a user-friendly interface that offers a higher degree of flexibility for conducting PV assessments.

2.9 Research Questions

This study provides contribution to field through proposition of transceiver and grid designs for deployment of swarm grids. Towards achieving the desired objectives, this study seeks to address the following research questions.

i. How can a smart transceiver for swarm grid implementation be developed using a communication technology suitable for rural settings?
ii. How can a solar swarm grid be planned under consideration of investment and operation costs as well as local specifications?
    a. Which tools are applicable for effective and efficient deployment of solar swarm grids?
    b. How to integrate the tool with common computer application program, enabling easy interaction and use by novice?

c. How can driving and thresholding parameters for the selection of distribution line in the implementation of swarm grid be evaluated?

Chapter 3: RESEARCH METHODOLOGY

This chapter draws the procedural used to explore and address challenges facing the deployment, planning and maintenance of the swarm grid. The aim of this research is to investigate and solve the challenges facing the deployment of swarm grids toward the eradication of energy poverty in rural Africa.

Due to the organic and distributed generation and storage nature of the swarm grid and inherited deployment complexities, this study opts for a hybrid methodology comprising laboratory prototyping and testing, and software simulations. The choice of this methodology is motivated by the need to capture both the deployment and maintenance challenges, and scenarios facing the swarm grid.

3.1 Research Design

This study adopts a quantitative research methodology, focusing on a decentralized, simulation and laboratory prototyping-based framework to develop solutions for swarm grid implementation. Building on the gaps identified in the literature on rural energy access and decentralized grids, the research methodology is structured around two main components: (i) the development of a smart transceiver prototype and (ii) the construction of an optimization tool for swarm grid implementation.

To inform and validate these methodological steps, a field study was conducted in three representative villages in Tanzania: Kitame, Kinduli, and Mpale. The goal of the study was to collect data and gain insights into the challenges facing swarm grid deployment and the rural energy access landscape. A summarized design framework of this methodology is described in Figure 3.1.

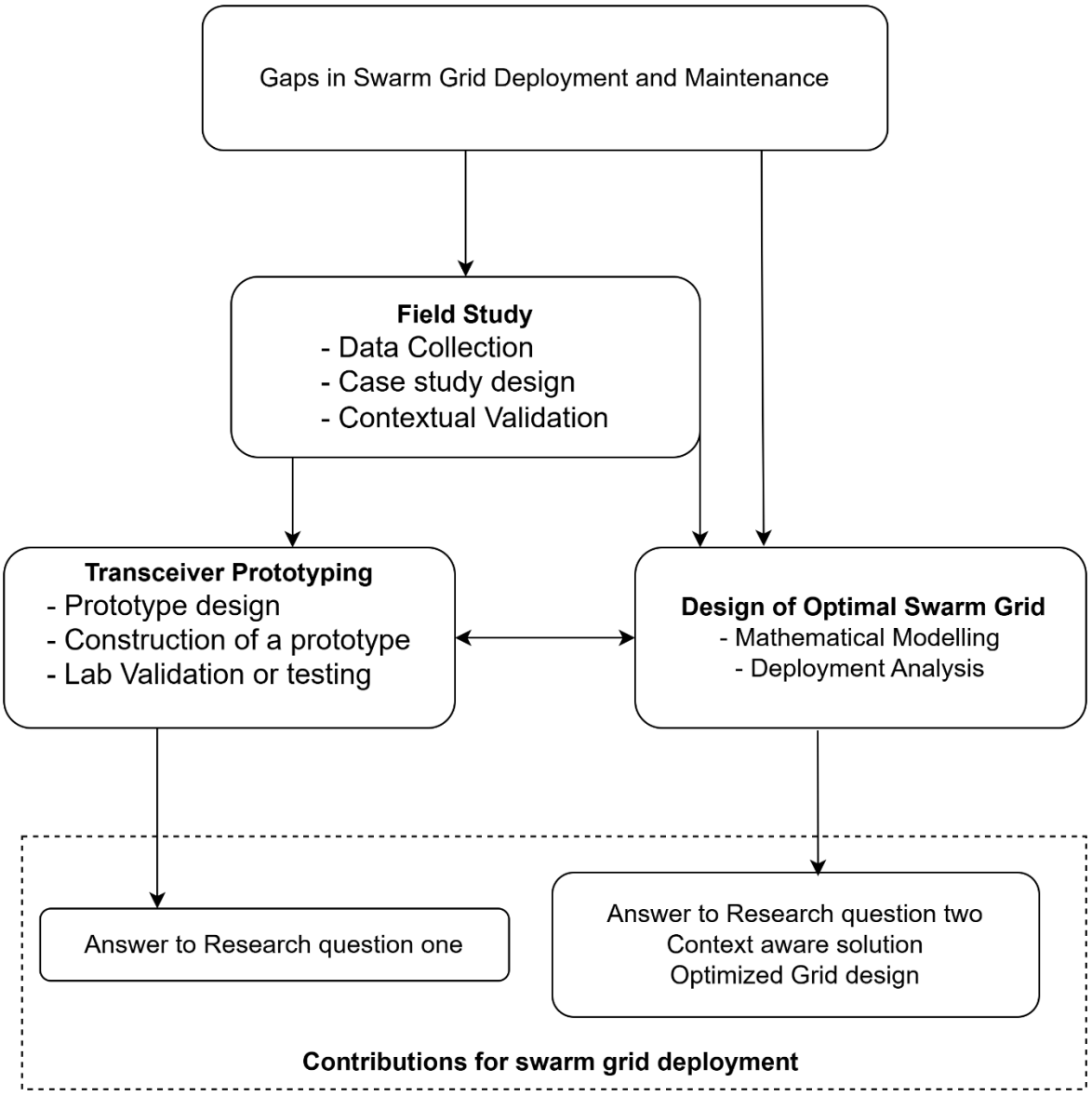

Figure 3.1: Research Methodology Framework

3.2 Field Study

This section outlines the data collection procedures carried out as part of this study. Given the nature of this research, a fieldwork for data collection was conducted in three villages in Tanzania: Kitame (6°12'3.11"S, 38°51'31.12"E), Mpale (4°59'52.94"S, 38°28'13.30"E), and Kinduli (5°52'45.30"S, 36°30'20.27"E). Figures 3.2 through 3.4 present the aerial views of each village as seen in Google Earth.

Figure 3.2: Aerial view of Kitame village

Figure 3.3: Aerial view of Mpale village

Figure 3.4: Aerial view of the Kinduli Village

Data were collected through guided interview questions aimed at determining the number of households in each village, the annual solar pattern, the average daily energy consumption per household, the available energy generation and storage units per household, and the geospatial data. The data collection was conducted over a four-month period, from September to December 2024. A summary of the socio-economic and energy access data for each village is presented in Table 3.1. The data collected at the individual household level were used as inputs for simulations in the developed network optimization tool, as presented in Chapter Five.

Table 3.1: Summary of the Socio-economic and energy access data

Village Name	**Number of HHs**	**Economic Activity**	**Source of Electricity**	**Distance from Main Grid (Approx)**
Kitame	80	Fishing and Salt farming	SHS	30 km
Mpale	220	Farming	Microgrid	0 km
Kinduli	55	Farming	SHS	50 km

3.3 Transceiver Prototyping Tools

This section describes the laboratory materials and tools employed to support hardware design, simulation and construction of the smart transceiver. These materials and tools are categorically divided into two main types: hardware and software.

The hardware included: Variable electronic load for varying the demand/energy consumption during prototype testing, programmable DC supply used in realizing storage unit (charging and discharging) at the laboratory during prototype testing, breadboards used for building of transceivers, Arduino microcontrollers used as the central processing unit of the transceiver, current and voltage sensors used in the detection on the state of charge in the energy storage unit and in the distribution line, LoRa modules used to send and receive data across the grid, a memory for data storage to be retrieved for billing purposes, a display used for displaying the amount of energy shared to other household, two resistors for controlling the amount voltage at the LoRa module input pins, a relay for connection and disconnection purposes, and the connecting wires for connecting all transceiver components according to the design. Specifications for all transceiver components are described in Chapter Four.

The software tools used in this work to support system design, simulation, analysis, and documentation. Proteus was used to simulate the transceiver circuit prior to hardware prototyping, while draw.io was employed for preparing system design drawings and schematic diagrams. Python, integrated with the Gurobipy optimization solver, was used to simulate the transceiver network, analyse different power distribution scenarios, and solve the developed mathematical models. In addition, Microsoft Excel was used for data entry and visualization of the optimization results. Microsoft Word supported the overall thesis write-up, while Microsoft Teams facilitated effective communication and collaboration with the supervisor and colleagues during consultation sessions.

3.4 Optimal Swarm Grid Design

This study employs classical (mathematical) optimization methods to model and solve the energy system planning and operation problems associated with swarm grids. These methods provide a transparent, computationally efficient, and well-established framework for handling constrained energy system problems. These methods rely on a rigorous mathematical formulation that guarantees the identification of an optimal solution within a well-defined feasible region, provided that the problem satisfies certain convexity and continuity conditions.

In the context of energy systems, classical optimization is particularly suitable for problems involving investment decisions (e.g., determining optimal capacities or network layouts) and operational dispatch (e.g., scheduling generation, storage, and power flow). The approach allows for the systematic incorporation of technical, economic, and physical constraints into a single optimization framework. The general form of a mathematical optimization problem can be expressed as in equation (3.1).

$$\begin{aligned} \text{Minimize / Maximize:} \quad & f(x), x = (x_1, x_2, \dots, x_n)^T \in \mathbb{R}^n \\ \text{Subject to:} \quad & \phi_j(x) = 0, j = 1,2, \dots, M \\ & \psi_i(x) \geq 0, i = 1,2, \dots, N \end{aligned} \tag{3.1}$$

where:

- $f(x)$represents the objective function, such as total system cost or energy loss,
- $\phi_j(x)$denote the equality constraints, such as power balance or energy conservation,
- $\psi_i(x)$denote the inequality constraints, such as capacity or operational limits, and
- x represents the decision variables, which may be continuous, discrete, or a mixture of both.

3.4.1 Types of Mathematical Optimization

Depending on the nature of the objective and constraint functions, several subclasses of classical optimization methods can be identified:

- Linear Programming (LP): All relationships in the model are linear. LP is commonly used when the system's cost and constraints vary linearly with decision variables.
- Quadratic Programming (QP): The objective function is quadratic, while constraints remain linear.
- Mixed-Integer Linear Programming (MILP): Some decision variables are restricted to integer values, allowing discrete investment or operational choices (e.g., binary connection decisions or unit commitment) but the problem is still linear.
- Nonlinear Programming (NLP): Either the objective function or the constraints are nonlinear, capturing complex physical relationships in power flow or component efficiency.
- Dynamic Programming (DP): Decomposes sequential decision-making problems into simpler subproblems, often used for multi-period or temporal optimization.

Among these, MILP is a commonly applied technique in swarm grid and energy system modelling due to its flexibility in representing both continuous variables (e.g., power flows, state of charge) and discrete decisions (e.g., installation of cables or components).

3.4.2 Application in This Study

In this work, the energy system optimization problem is formulated as a Mixed-Integer Linear Programming (MILP) model and solved using the Gurobi optimizer. The MILP formulation allows the simultaneous optimization of investment and operational decisions within a unified framework.

The general objective of the model is to minimize total system cost while satisfying technical and operational constraints. The decision variables represent energy flows, storage operations, and component installation decisions. The Constraints include:

- Power flow balance at each node: ensuring demand–supply equilibrium
- Component capacity limits: defining upper bounds for power generation, storage, and transmission
- Component cost: defining the cost for pole, cables and other supporting infrastructure.
- Battery operation constraints, ensuring feasible charging and discharging schedules; and
- Network connectivity and flow constraints, ensuring that energy can only flow through installed links.

Chapter 4: TRANCEIVER DESIGN AND DEVELOPMENT

This chapter describes the procedures involved in the design, simulations and laboratory construction and testing of the energy dispatch transceiver. It is organized into three main sections. Section 4.1 presents the design procedures and the working principles of the transceiver, Section 4.2 presents simulation results and discussion. Section 4.3 discusses laboratory prototype development and testing. The conclusion and chapter summary are presented in section 4.4. It is worth mentioning that portions of this chapter have already been published by the author through the IEEE Power Africa Conference, held in Marrakech, Morocco (2023), and Johannesburg, South Africa (2024).

4.1 Transceiver Design Procedures

As established in the literature review (Subsection 2.5) and summarized in Table 2.3, LoRaWAN emerges as the most appropriate ad hoc communication technology for rural sub-Saharan African (SSA) contexts. Building on this, the conceptual layout of a typical village is depicted in Figure 4.1.

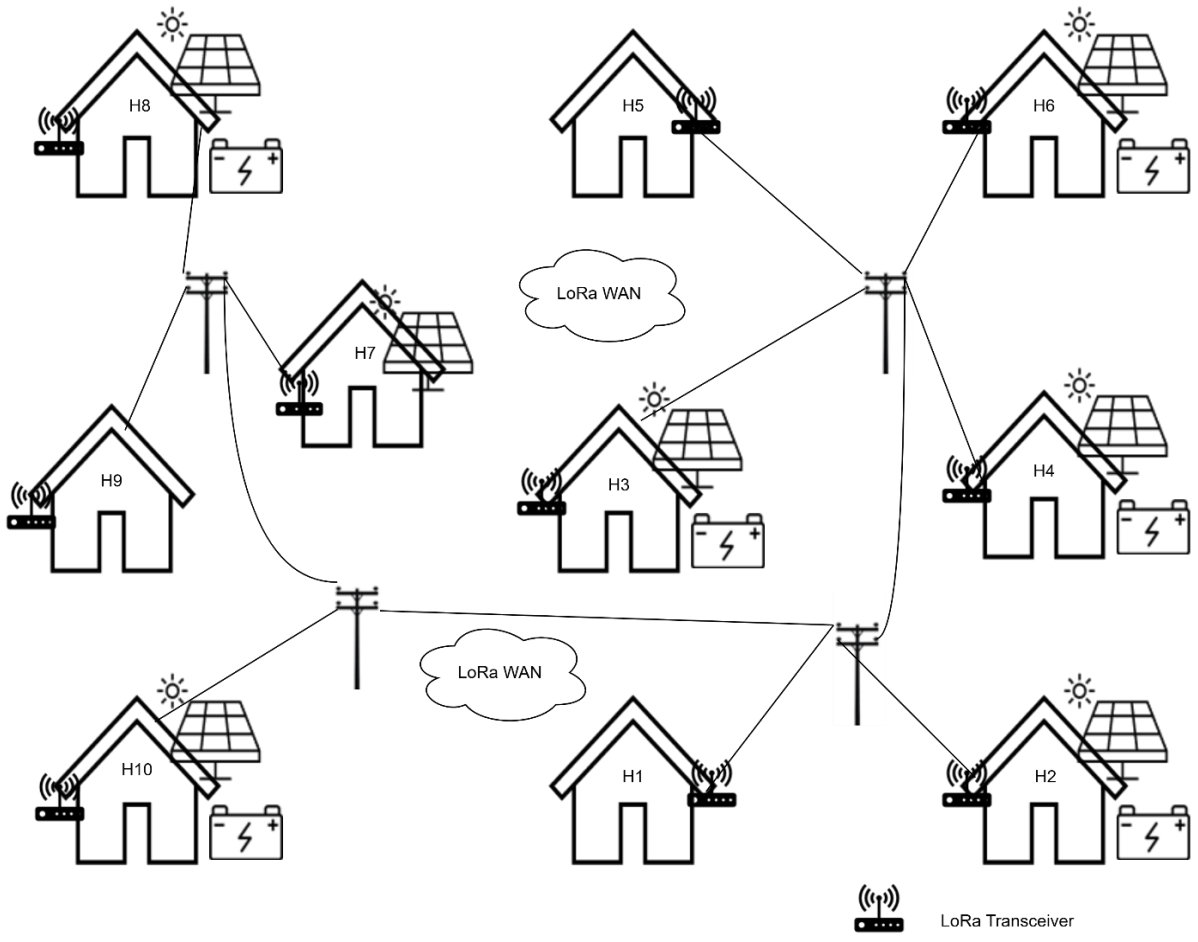

Figure 4.1: Typical Swarm Grid Village utilizing LoRa WAN Technology

In this configuration (see Figure 4.1), each household participating in the swarm grid is equipped with a LoRa-based transceiver to enable effective communication within the decentralized energy network. Having identified the appropriate communication technology, this section discusses the design and development of the transceiver for energy sharing and trading. The proposed transceiver incorporates additional security features beyond those provided by the native LoRaWAN protocol. Additional security and privacy features are presented in subsection 4.1.1. The architecture of the developed transceiver is illustrated in Figure 4.2.

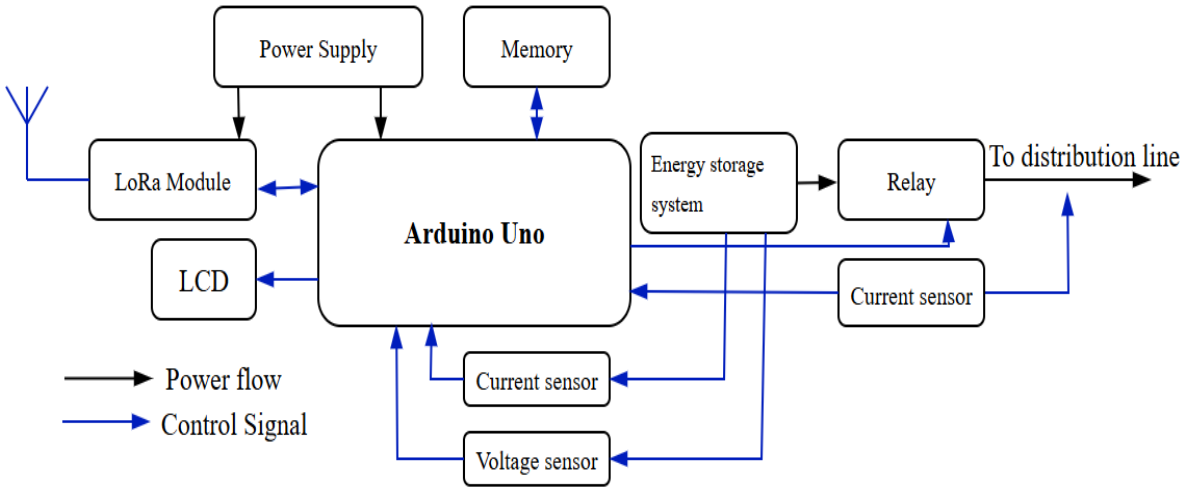

Figure 4.2: Architecture of the Developed Transceiver

The transceiver comprises of the Arduino uno microcontroller for data processing and decision making of the transceiver, it serves as the brain of the transceiver. The other key components include: LoRa module for enhancing wireless communication across the grid, two sensors (voltage and current) connected to the energy storage system (ESS) to detect the available energy level, a relay for establishing connection and disconnection, an additional current sensor placed after the relay to determine the amount of power discharged, which is then be priced as per agreed billing system, , an LCD display for indicating the energy level status, a memory unit for data storage, and a power supply for powering the microcontroller and LoRa module.

4.1.1 Security and Privacy Feature of the Developed Transceiver

In a peer-to-peer energy sharing grid, security and privacy are of critical importance to be addressed. During the process of sending an energy request or delivering energy, sensitive information about stakeholders may be revealed through their energy profiles. If such information is captured by adversaries, it could negotiate both privacy and security.

Furthermore, malicious transceivers may attempt to eavesdrop on the network or even receive energy illegally.

As reviewed in the literature, many existing swarm-grid transceivers do not adequately address security and privacy issues. They often assume that all stakeholders are trustworthy and will not tamper with grid information. However, this assumption is not always valid, creating the need for explicit safeguards. While many strong security algorithms are available in smart grid systems, they cannot be directly applied to swarm-grid implementations because they are power-hungry. Since rural swarm grids operate at low voltage and are designed for low-power consumers, lightweight security mechanisms are essential.

In this work, the developed transceiver incorporates a lightweight security layer on top of the standard LoRa security features, making it more secure than conventional designs. The security mechanism operates as follows:

When transceiver i in household i detects an energy deficit, it generates an Energy Request (ER_i) defined as

$$ER_i = EL - Ea \tag{4.1}$$

Where:

Ea is the available energy in the storage system,

EL is the energy required by the current active loads.

This energy request value is then encapsulated into a secured Energy Request Message (ERM):

$$ERM_i = (ER_i, K_i, T) \tag{4.2}$$

Where:

ER_i, is the amount of the requested energy by household i,

K_i is the security key, and T is the timestamp at which the message was generated.

The security key K_i is generated using a lightweight encryption mechanism such that meets the equation (4.3).

$$K_i = ER_i \oplus MAC_i \tag{4.3}$$

Where: MAC_i is the MAC address of the requesting transceiver, and $\oplus$ denotes the exclusive-or (XOR) operation.

By doing so, the identity of the requestor is concealed from adversaries, and only authorized transceivers with prior configuration can interpret the message.

Upon receiving an ERM, another transceiver (say transceiver *j*) verifies authenticity by recomputing the MAC_i:

$$MAC_i' = K_i \oplus ER_i \tag{4.4}$$

and comparing the result with the stored information. If a match is found, the message is authenticated; otherwise, it is discarded. After this preliminary check, the timestamp is validated. A validity period of one millisecond is used, which is sufficient to account for the LoRa transmission latency of ±20 microseconds (Devalal & Karthikeyan, 2018).

If authentication is successful and the receiving transceiver has surplus energy, it generates an Energy Feedback Message (EFM):

$$EFM_j = \left(ES_j, K_j, T\right) \tag{4.5}$$

Where:ES_j is the amount of energy that transceiver *j* can supply, and K_j is the security key for the feedback message.

The feedback key is defined as:

$$K_j = MAC_j \oplus MAC_i \tag{4.6}$$

This ensures that only the original requestor (transceiver *i*) can decode the feedback. In the case of multiple requests, a first-come, first-served principle is applied while in the case of multiple responses the one with high amount of energy to be shared is given high priority, otherwise the first-come, first-served principle is applied. Figure 4.3 summarizes the message authentication procedures used to ensure security and privacy control.

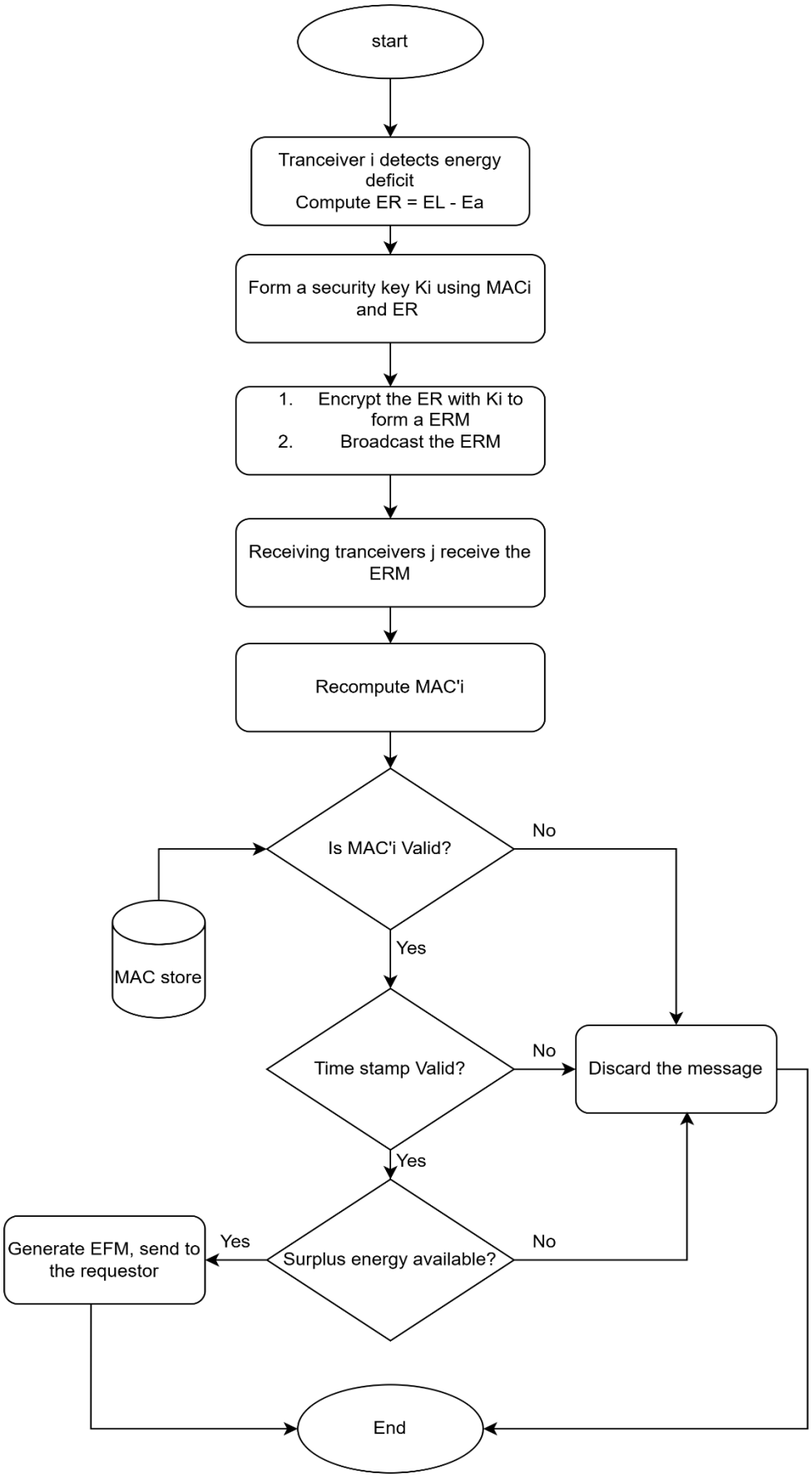

Figure 4.3: Message Authentication in Swarm Grid

4.1.2 Working principle of the Transceiver

The transceiver operates under the assumption that the household load remains constant over a one-hour window. It determines energy status relative to this one-hour demand.

- When the available energy in the ESS falls below 75% of the demand, the transceiver identifies an energy deficit condition.
- When the available energy exceeds 125% of the demand, it identifies an energy excess condition.

This safeguard prevents unnecessary switching due to minor fluctuations in load or supply. The detailed sequence of operation is as follows:

1. Deficit condition: The transceiver calculates the energy request using (4.1) and transmits it as a secured ERM (4.3).
2. Reception: Any receiving transceiver authenticates the ERM as described above (subsection 4.1.1).
3. Surplus check: If the receiver meets the excess-energy condition, it generates the available energy surplus:

$$ES = Ea - 1.25 * EL \tag{4.7}$$

   where Ea is the available energy and EL the current load demand.

4. Handshake: The responding transceiver returns the secured EFM (4.6), indicating the amount of shareable energy.
5. Acknowledgment: The requesting transceiver acknowledges one prosumer at a time by including its MAC address in the acknowledgment message. Only the acknowledged transceiver is authorized to supply its surplus energy.
6. Normal monitoring: In the absence of deficit or surplus events, the transceiver continues monitoring the energy level against active loads.

Figure 4.4 and Figure 4.5 summarize the working principle of the proposed transceiver.

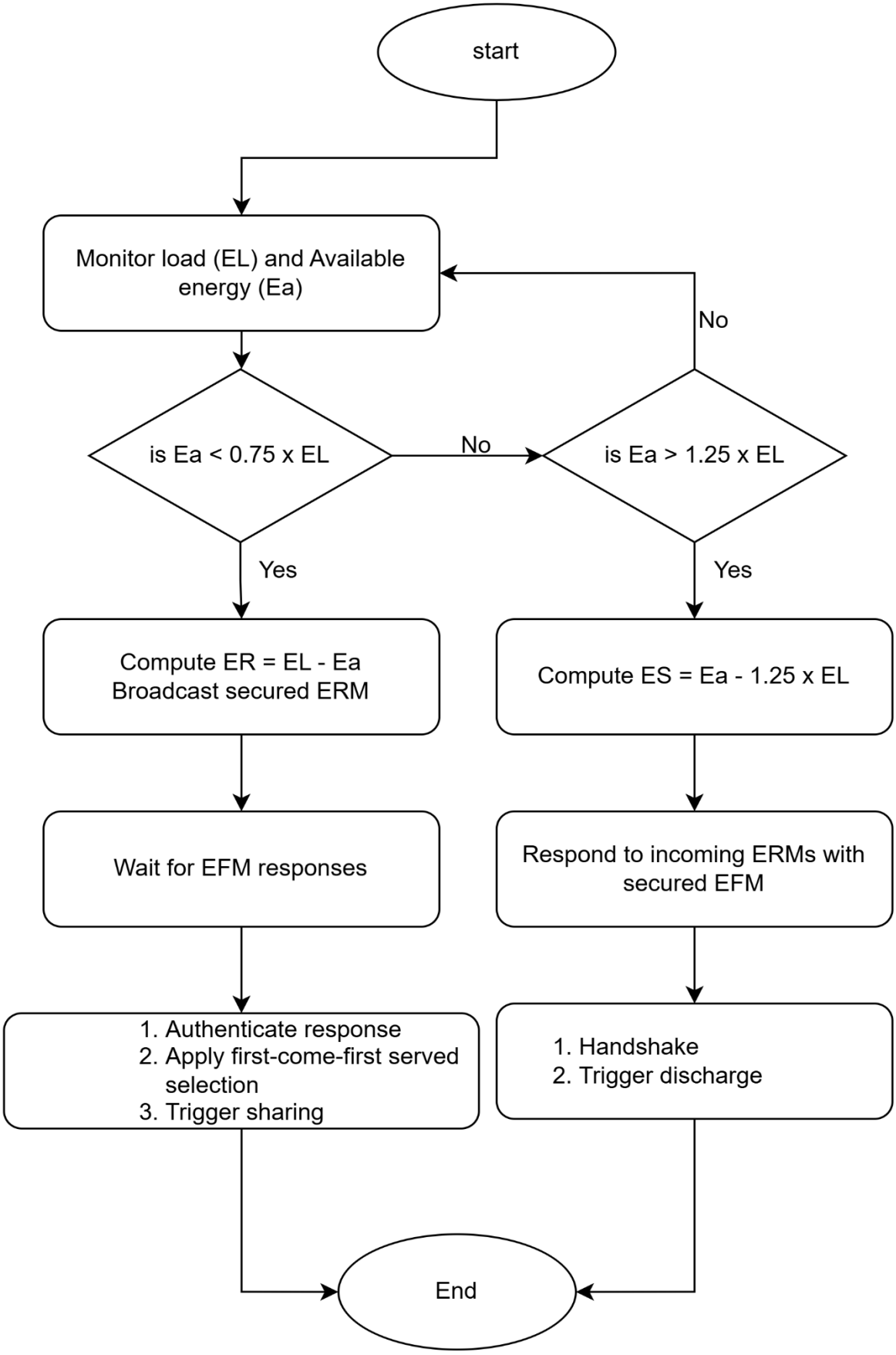

Figure 4.4: Working Principle of Transceiver

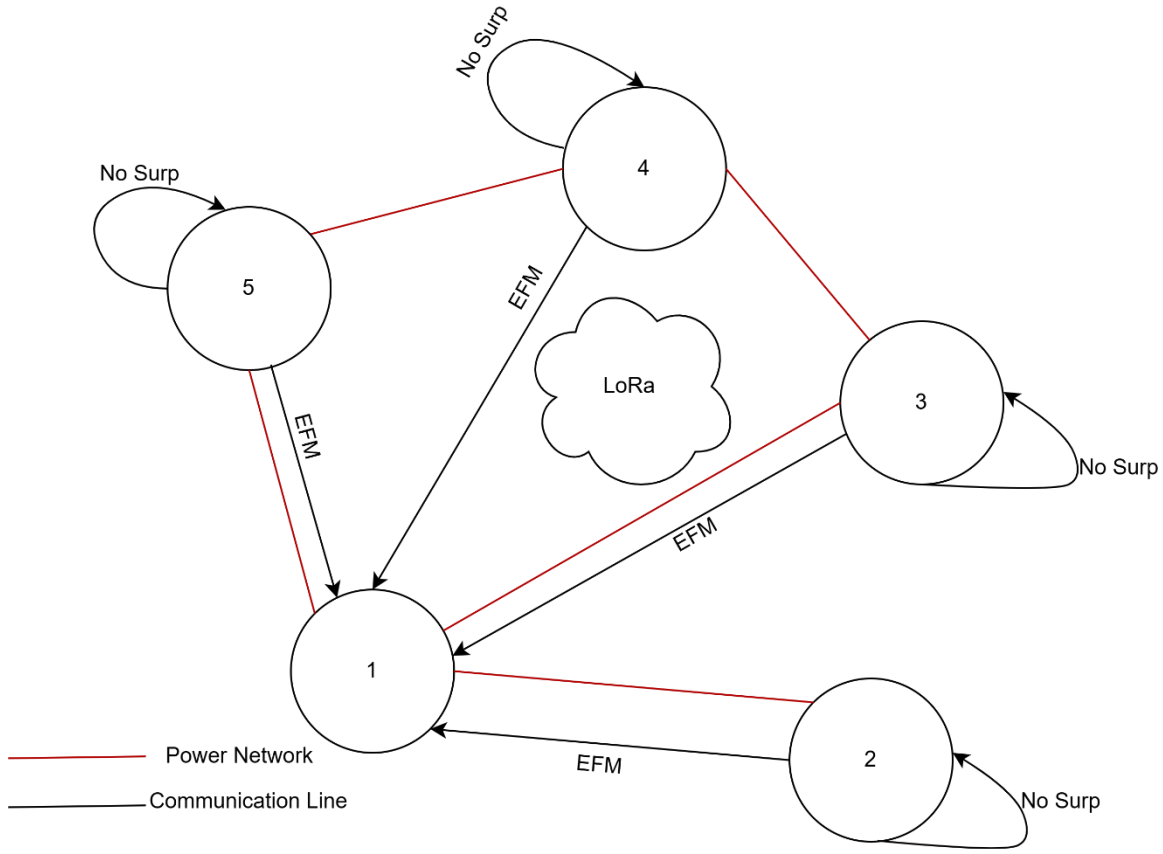

Figure 4.5: State decision diagram: Assuming the Request is from node number 1

4.2 Simulation Results and Discussion

4.2.1 Simulation Setup

The simulation was designed to model and visualize the energy exchange dynamics among interconnected households within a secure transceiver network. The primary objectives were to evaluate (i) the energy exchange processes among nodes, (ii) the security and reliability of message exchanges, and (iii) the effectiveness of the network in identifying and blocking adversarial activities (iv) the ability of transceiver to choose among multiple options.

A network comprising a total of 10 transceivers were deployed in the simulation environment like the one depicted in Figure 4.1, each representing an individual household node. Among these, one transceiver (H4) was configured as an adversary to simulate malicious behaviour within the network. The remaining nine transceivers operated as cooperative nodes, some equipped with solar generation capability to emulate distributed renewable energy sources.

The simulation was executed for a total duration of 24 hours, with a time step of one hour. At each time step, the transceivers performed different actions, including local energy checks, energy request message (ERM) broadcasts, energy found message (EFM) and exchanges, and the message authentication. To capture the randomness of the electrical demand profile, the load demand was randomly set between 0 and 800 Wh in each time step. The initial energy stored in the energy storage system was randomly set between 400 Wh and 1.2 kWh. Each household was assumed to have energy storage system with the maximum capacity of 2.4 kWh. Solar power generation was assumed to occur between 10:00 and 17:00, with average hourly production ranging from 0 to 960 Wh. The adversarial node was configured to broadcast falsified messages at four-hour intervals, whereas deceptive feedback messages were transmitted randomly during network communications.

Table 4.1: Transceiver Simulation Parameters

Parameter	**Description/Value**
Total No of Transceivers	10 (representing 10 households)
Adversarial Node	1 transceiver (H4), configured as malicious
Cooperative Nodes	9 Transceivers (Normal operation)
Solar PV – Equipped Nodes	5
Simulation Duration	24 hours
Time step	1 hour
Node Actions per Time Step	1. Local energy checks, • ERM (Energy Request Message) broadcasts, • EFM (Energy Found Message) replies, 2. Message authentication
Load Demand Profile	Randomly set between 20 – 800 Wh
Initial Stored Energy	Half of the maximum storage capacity
Energy Storage Capacity	2.4 kWh per household
Solar Generation Period	Between 10:00 and 17:00
Average Solar Generation	0 – 960 Wh per hour during generation period
Adversarial Behaviour	Broadcast falsified messages every after four hours

The key performance indicators obtained from the simulation include the number of ERM and EFM messages exchanged, the behavioural patterns of the adversarial transceiver, and the overall performance of the network in maintaining secure and efficient energy sharing among nodes.

4.2.2 Simulation Results

This section presents and describes the results obtained from the transceiver network simulation. The outcomes are used to evaluate the performance of the proposed transceiver's working principle and the authentication mechanism. The results highlight the behaviour or role of each transceiver over the 24-hours simulation period. The focus is on the success rate of energy request and feedback messages (ERM/EFM) and the overall network performance under the presence of adversarial node. Graphical plots are provided to further illustrate the findings followed by subsequent analysis and discussion.

Figure 4.6 shows the detected energy deficit conditions in some of the transceivers, which subsequently broadcast energy request messages (ERMs). The occurrence of ERMs triggers the generation of energy feedback messages (EFMs) to transceivers with excess energy. Figure 4.7 demonstrates the corresponding EFMs, showing the amount of energy available to resolve each ERM. Although EFM replies may originate from multiple transceivers, Figure 4.7 presents only the successful transfer.

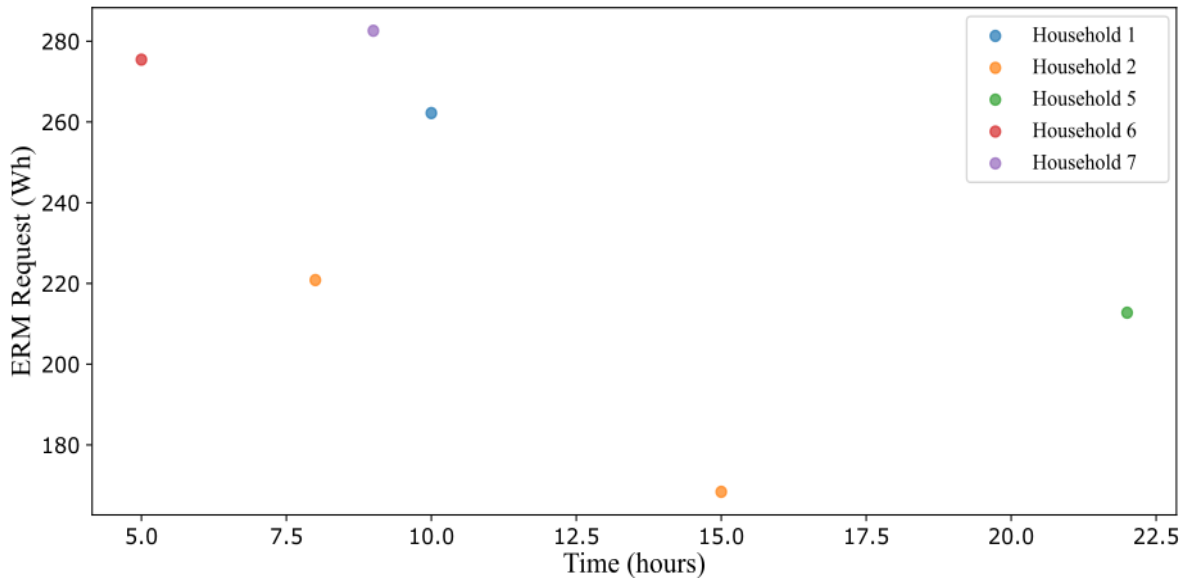

Figure 4.6: ERM Occurrence over time

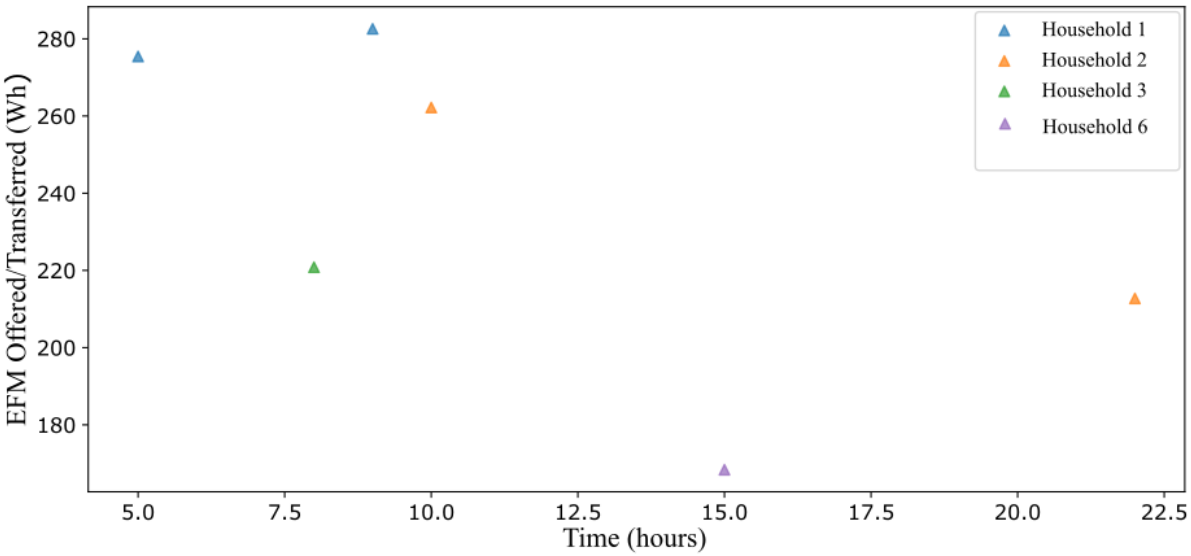

Figure 4.7: EFM Occurrence Over time

In the case of multiple replies, the requesting transceiver tends to select the response from the node whose surplus energy at least meet its demand or the combination of more than one supplier to clear its deficit. Figure 4.8, Figure 4.9 and Figure 4.10 provide snapshots of this process, showing the decision-making behaviour happened under different conditions. Figure 4.11 illustrates the energy exchange data for each transceiver, providing the necessary information required for precise and transparent billing computations.

```
10: Household 1 DEFICIT (SoC=417.49, Load=679.69)
10: Household 1 broadcasts ERM = 262.20 Wh
10: Household 2 replies with EFM = 262.20 Wh
10: Household 4 (ADVERSARY) sends FAKE EFM (bogus key)
10: Household 1 discards EFM from Household 4 (auth failed)
10: Household 5 replies with EFM = 262.20 Wh
10: Household 9 replies with EFM = 153.23 Wh
10: Household 10 replies with EFM = 40.36 Wh
10: Household 1 needs 262.20 Wh, 4 offers received
   Household 2 transfers 262.20 Wh → Household 1
       Updated SoC: Household 2=495.66, Household 1=679.69
10: Household 1's deficit fully met by 1 prosumer(s)
```

Figure 4.8: Ability of the transceiver to choose among available suppliers

```
1: Household 2 DEFICIT (SoC=418.63, Load=595.20)
1: Household 2 broadcasts ERM = 176.58 Wh
1: Household 1 replies with EFM = 54.52 Wh
1: Household 4 (ADVERSARY) sends FAKE EFM (bogus key)
1: Household 2 discards EFM from Household 4 (auth failed)
1: Household 7 replies with EFM = 65.84 Wh
1: Household 2 needs 176.58 Wh, 2 offers received
   Household 7 transfers 65.84 Wh → Household 2
       Updated SoC: Household 7=878.65, Household 2=484.47
   Household 1 transfers 54.52 Wh → Household 2
       Updated SoC: Household 1=919.91, Household 2=538.99
1: Household 2 still short of 56.22 Wh after received from 2 prosumer(s)
```

Figure 4.9: Ability of the transceiver to grasp the available amount of energy

```
4: Household 6 DEFICIT (SoC=441.92, Load=621.63)
4: Household 6 broadcasts ERM = 179.70 Wh
4: Household 2 replies with EFM = 81.38 Wh
4: Household 4 (ADVERSARY) sends FAKE EFM (bogus key)
4: Household 6 discards EFM from Household 4 (auth failed)
4: Household 7 replies with EFM = 62.48 Wh
4: Household 10 replies with EFM = 46.99 Wh
4: Household 6 needs 179.70 Wh, 3 offers received
   Household 2 transfers 81.38 Wh → Household 6
       Updated SoC: Household 2=698.08, Household 6=523.30
   Household 7 transfers 62.48 Wh → Household 6
       Updated SoC: Household 7=608.26, Household 6=585.78
   Household 10 transfers 35.85 Wh → Household 6
       Updated SoC: Household 10=484.71, Household 6=621.63
4: Household 6's deficit fully met by 3 prosumer(s)
```

Figure 4.10: Transceiver receiving energy from more than one supplier

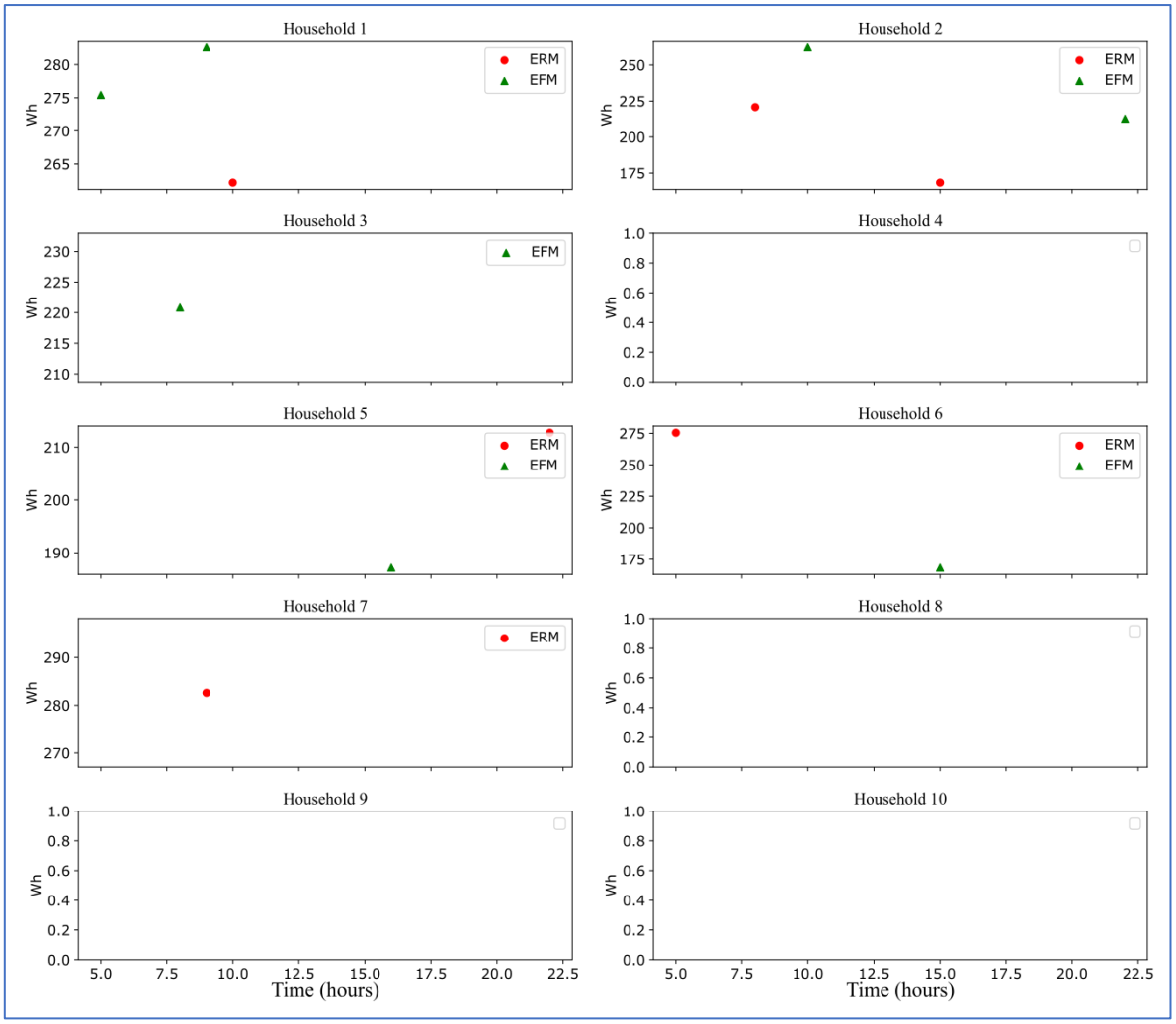

Figure 4.11: Energy exchange records for each household

In the event of adversarial messages, all transceivers in the network reject any requests or offers originating from unknown or unverified sources. Figure 4.8 - Figure 4.10 and Figure 4.12 present the network performance showing how the adversarial messages were detected and blocked.

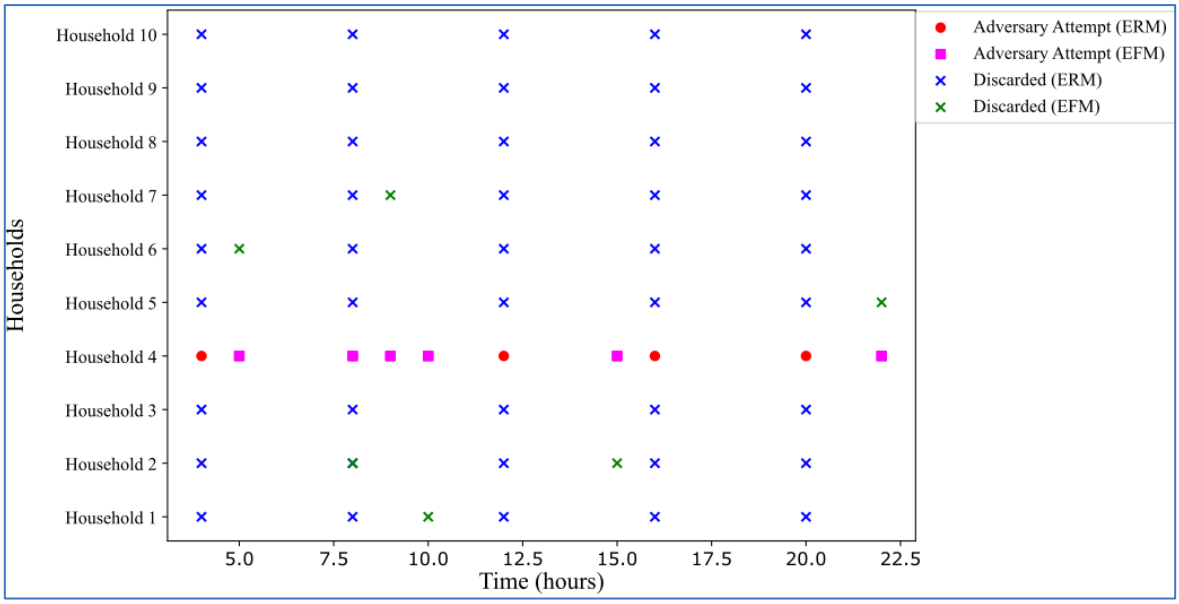

Figure 4.12: Adversary behaviour and Network nodes Response

4.2.3 Discussion

The simulation results demonstrate the effectiveness of the proposed transceiver in facilitating a secure energy exchange between participants in the swarm grid. The transceivers can detect the three conditions, i.e. normal, deficit and surplus operations. For the 24-hour simulations the transceivers in households 1,2,5,6, and 7 at different times detect the energy deficit condition and broadcast the energy request message (ERM), see Figure 4.6. On the other hand, transceivers in households 1, 2, 3, and 6 reply with energy found message (EFM) after detecting the energy surplus condition, see Figure 4.7. The consumer – supplier pair can be deduced from these two figures and summarized in Table 4.2.

Table 4.2: Consumer - Supplier Pair

Consumer (Household No.)	Supplier (Household No.)
1	2
2	3 and 6
5	2
6	1
7	1

When multiple EFMs were received, the consumer transceiver effectively selected the most optimal supplier(s) based on the available energy levels, as shown in Figure 4.8 through Figure

4.10. This adaptive decision-making ensures balanced energy distribution without overloading the network with multiple exchanges within specified window. Transceivers that are neither in the ERM nor EFM state are operating under normal condition. For the simulated period, this category includes the transceivers in households 8, 9, and 10. Accordingly, their energy exchange records shown in Figure 4.11 contain no (zero) entries. However, at each individual time step, any transceiver that does not appear in the ERM or EFM state is also regarded as operating in a normal state for that specific time step. The record for Household 4 is also zero, as it was classified as an adversary; consequently, its data are excluded from billing considerations.

The privacy and security of the SG participants is captured and tested in two scenes: (i) the adversary was allowed to send a fake energy request message every after four hours (ii) randomly responding to the ERMs by sending EFMs replies. The authentication mechanism implemented in the proposed transceiver successfully detected and blocked both adversary scenarios, preventing any operations on it. As shown in Figure 4.12 all transceivers in the network discard (marked in blue crosses) ERM messages from the adversary. On the other hand, a transceiver in a network with deficit in energy had discarded (marked in green crosses) fake EFMs from the adversary. This prevented energy misallocation, disclose of the participant status, and preserved trust among legitimate participants. There is no successful breach was recorded throughout the simulation period, indicating robustness of the proposed transceiver solution.

Although the proposed transceiver performed effectively under simulated conditions, laboratory prototype and real word deployment would require dynamic communication delays, complex hardware implementation and more complex adversarial strategies. In the following subsection a prototype of the transceiver is constructed and tested in the laboratory environment.

4.3 Transceiver Prototyping and Testing

4.3.1 Transceiver Prototyping

(a). Components Selection and Configurations

Towards realization of the proposed transceiver in the laboratory, a thorough component selection process was conducted based on their technical specifications and standards. Table 4.3 presents a summary of the components used in the construction of a transceiver; detailed

descriptions are provided in the subsequent subsections. The transceiver was built using the architecture shown in Figure 4.2

Table 4.3: Components for Prototype Construction

S/N	Component Name	Specifications	Description/Purpose
1	Reyax RYLR998: 868/915MHz LoRa UART Transceiver Module	Frequency band: 868 MHz / 915 MHz Input Voltage:2.3 V - 3.6 V	It uses ISM license free frequency of 868 / 915 MHz. In Europe 863-870 MHz band has been allocated. Used for wireless communication between nodes.
2	Elegoo Mega R3 Microcontroller	Input/Output voltage: 5 V I/O Digital pins: 54 Analog input pins: 16	The MCU board is cheap and allows for network scalability It was used as the brain of the transceiver to interpret and decide on different signals.
3	Current Sensor (AC712)	Voltage supply: 5 V DC Current Range: 5 A	It was used to sense the energy status in the energy storage system. It was also used to determine the amount of discharge electrical energy.
4	Relay Module	Current Range: 5 A	It was used for connection and disconnection purposes. During charging or discharging it connects otherwise kept disconnected.
5	LCD Display	16x2 Display LCD with I2C Interface Operating voltage: 5 V DC	It was used to display the amount of power charged or discharged (negative if charged, otherwise positive).

6	SD card Module	Storage size: 5 MB	For data storage to be used for billing purposes and security matters.
7	Jumper wires	30 cm long	Connecting the components.

1. Reyax RYLR998 LoRa Module

The RYLR998 transceiver module is composed of Semtech LoRa engine and Nuvoton MCU which operates in the unlicensed frequency range of 868/915 MHz. This module facilitates high interference resistance, improved power efficiency and hence long-range communications of up to 15 km. Unlike other modules, this module has an integrated antenna and headers connected to it that eliminates the need for soldering and makes it plug and play as shown in Figure 4.13.

Figure 4.13: RYLR 998 LoRa Module source: (LoRa Datasheet, (2021))

This is a class A type of device and hence it guarantees the life span of the energy storage system by drawing very little amount of power for its operations. The device requires input power supply of 2.3 V to 3.6 V. It has five pins, with descriptions as shown in Table 4.4. Other technical specifications can be found in (Lora Datasheet, (2021))

Table 4.4: Pin Description of RYLR998 (LoRa Datasheet, (2021))

S/N	Pin Name	Pin Type	Function
1	VDD	Input	Power Supply
2	NRST	Input	Reset (Active low), Internal pull up, pull down at least 100 ms
3	RXD	Input	UART Data Input
4	TXD	Output	UART Data Output
5	GND	N/A	Ground

Connecting to the Microcontroller

Since the module requires an input voltage of 2.3 - 3.6 V, while the Arduino provides 5 V, a voltage reduction using a potential divider circuit was implemented to ensure the module's safety. The voltage division circuit is as shown in Figure 4.14, a LoRa module was connected at point "L" following the pin connections shown in Table 4.5

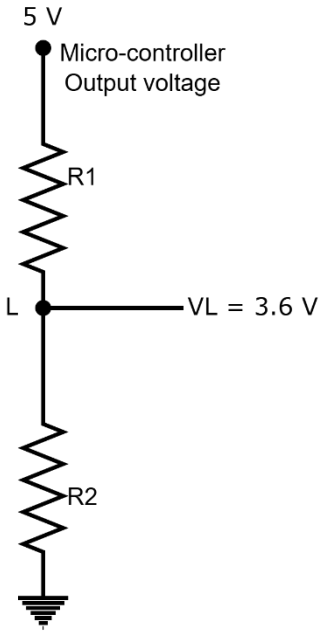

$$V_l = \left[\frac{R_2}{R_2 + R_1}\right] \times V_m$$

$$V_l = 2.3 \text{ to } 3.6\ V, V_m = 5V$$

On solving,

$$\frac{R_1}{R_2} = 1.174 \text{ to } 0.389$$

∴ For safety and sensitivity reasons it is not recommended to operate at extreme values, so the value of 6.2 kΩ and 5.6 kΩ for resistor R_1 and R_2, respectively were used.

Figure 4.14: Voltage divider circuit to Reduce voltage going to LoRa Module

Table 4.5: Pin Connections between RYLR998 and Microcontroller

Arduino	**RYLR998**
5 V	VDD (Via R_1 & R_2)
TX0	TX
RX0	RX
GND	GND

Another advantage of this module is that it can easily be configured using the AT (Attention) commands. The commands are transmitted to the module from the host device such as a USB TTL module or a microcontroller through a serial UART connection. Essential AT commands are described here-under while the supplementary commands can be found in (LoRa Datasheet, (2021))

i. AT+ADDRESS

This command is used to set up the address of the LoRa module and hence the transceiver's address which for this case was the household number. The address can take any value ranging from 1 to 65535, meaning that the maximum number of transceivers that can communicate in the given grid is 65535. Address 0 is reserved as the broadcast address and cannot be assigned to any transceiver. In this work, it was used during the energy request process. The syntax for the command is as shown below

AT+ADDRESS = <Address>

For example, to set up an address of 1 to a node of household 1, below command was used.

AT+ADDRESS = 1

An OK response was displayed back once the command is successful. Following this syntax all transceivers were accordingly configured. To confirm the configured address the AT+ADDRESS command was used followed by a question mark as shown below. The

command gave back the configured address in the module. Generally, any command followed by a question mark gives back the configured parameter associated to that command.

AT+ADDRESS?

ii. AT+NETWORKID

This command is used to assign the network or group identification of the LoRa network. For the modules to communicate they must be in the same network i.e., having the same network ID. The network ID can have any value ranging from 3 to 15, although the default network ID is 18. In this work a network ID of 5 was used. The syntax for this command is:

AT+NETWORKID = <Network ID>

For example, to set up a network ID of 5 to transceivers in the prototype a below command was used in all four transceivers.

AT+NETWORKID = 5

iii. AT+BAND

This command is used to configure the band's centre frequency. For effective communication, the transmitter and receiver must use the same frequency band. The ISM frequency band for Europe is 868 MHz however the default frequency band for this module is 915 MHz. The syntax for this command is as shown below alongside with the configured frequency.

AT+BAND=<Parameter>, <Frequency Memory>

AT+BAND=868000000,M

iv. AT+PARAMETER

This command is used to configure the RF parameters of the module. These parameters need to be the same for both transmitter and receiver. The parameters as indicated in the angle brackets include:

<*Spreading Factor*> which can take any value between 5 and 11 with 9 being the default value. The spreading factor varies direct as the sensitivity and inversely to the transmission time, 8 was used.

<*Bandwidth*> this varies proportional to the transmission time an inversely to the sensitivity. It can be configured as the number among 7, 8 and 9 to represent 125 kHz, 250 kHz and 500 kHz respectively, 8 was used.

<*Coding rate*>, the coding rate can be set as any number between 1 and 4 with 1 being the highest and default coding rate, 2 was used.

<*Programmed Preamble*>: this account for data loss security, if the preamble code is bigger, it will have less possibility of losing data. It is recommended that the value set is above 10 but not greater than 24, 17 was used.

v. AT+SEND

This command is used to send data to either a specific node or to the entire network. The command has the syntax as shown below:

AT+SEND=<Receiver's address>, <Payload Length>, <Message or Data>

Provided that all the configurations from i to iv, are okay, if the receiver's address is set to 0 then all transceivers will receive the message otherwise the specific transceiver will receive the intended message. The maximum payload length is 240 bytes, and the data are transmitted in ASCII format. To adhere with the command syntax the component of the message described in Chapter 3 were concatenated to form a string.

2. Arduino Microcontroller

The Arduino Mega board with ATMega2560 microcontroller as the primary processor serves as the brain of the transceiver. It possesses 54 digital input - output pins 15 out of them can be used for PWM outputs, and 16 analogue input pins. Its compatibility with LoRa RYLR998 and wide range of connectivity choices made it more appropriate to this work. Furthermore, the board has 8 kb of SRAM and 256 kb of flash memory which tends to increase the processing and storage capability of the transceiver. Figure 4.15 shows the board that was used in the prototyping of the transceiver.

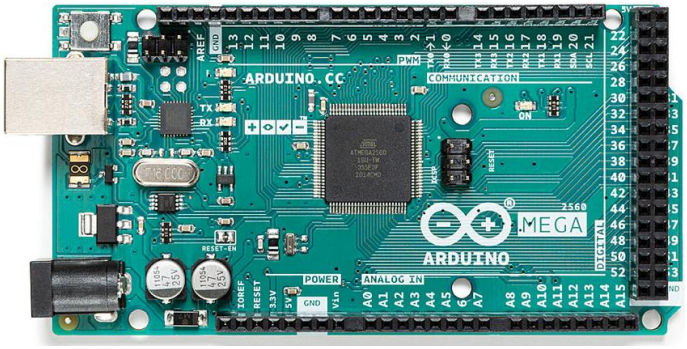

Figure 4.15: Arduino Microcontroller with AT Mega 2560 processor

3. Current Sensors and Relay Module

The two current sensors were used for two different purposes, one was to detect the instantaneous amount of energy in the energy storage system, while the other was used to determine the amount of energy traded between two transceivers. For prototyping purpose, a system voltage of 24 V was used (as mainly used in the real SHSs) and the maximum energy exchange per unit hour allowed to be 600 W. The required current rating of the current sensor was then calculated as shown in equation (4.8). The ACS712 was then chosen due to its wide input range and linearity, ability to measure high current up to 25 A, low output error of 15%. Similarly, the corresponding relay module was chosen based on the ratings of the current sensor. The two modules are shown in Figure 4.16 and Figure 4.17.

$$I = {}^{P}/_{V} = {}^{600}/_{24} = 25\ A \tag{4.8}$$

Figure 4.16: ACS712 Hall effect Based current sensor

Figure 4.17: Single Channel 5 V 10 A Relay Module

(b).Prototype development

Based on the components detailed prior to this section, the connections between them were conducted according to the pin description of each component and the transceiver design as illustrated in Figure 4.2. The MCU and LoRa module was programmed and configured using the C programming language and the AT commands, respectively. Figure 4.18 shows the constructed transceiver prototype.

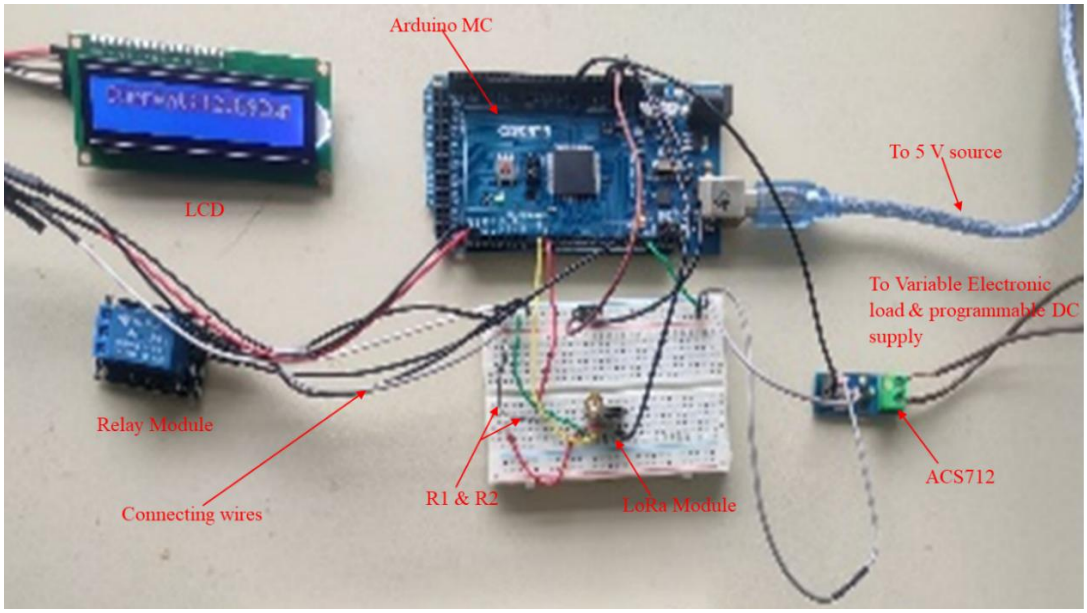

Figure 4.18: Transceiver Prototype

A total of five transceivers were constructed labelled HH1…, HH5. Four transceivers were configured using the proposed encryption and decision-making mechanism, while the fifth served as an adversary, with same configurations as in Section 4.2.1.

4.3.2 Transceiver Testing

Two transceivers (HH 2 and HH 5) were connected to variable electronic loads to represent consumers, while the other two (HH 1 and HH 3) were connected to both a programmable DC supply and an electronic load to represent prosumers. Variations in load demand were simulated using the electronic loads, whereas surplus energy production was simulated using the programmable DC supply. The swarm grid was not physically constructed; instead, programmable DC power supplies were used to emulate the energy storage system, and electronic DC loads were used to emulate the demand, as illustrated in Figure 4.19. Relay closing and opening were used to emulate the actual connection to and disconnection from the grid. Various test cases were conducted in an hour-window for each as described in Table 4.6, and the corresponding results are summarized in Figure 4.20.

Figure 4.19: Variable electronic Load and Programmable DC Supply used at the laboratory

Table 4.6: Transceiver Testing Cases

Case	Set up	Expectation	Observation
1	The supply was set to 100 Wh and the demand to 70 Wh, in all transceivers	No node should request energy; therefore, no relay responses should occur.	No relay activity was observed, indicating normal operation was ongoing.
2	The programmable DC supply of HH3 was increased to 180 Wh, while other nodes maintained a supply of 100 Wh and a demand of 70 Wh. HH5 was present.	No node should request energy; a surplus alone does not trigger energy export. All relays should remain open.	No relay activity was observed.
3	HH3 maintained a supply of 180 Wh, creating surplus. The demand in HH2 was increased by 70 Wh, creating a deficit.	HH2 broadcasts an encrypted energy request. Only nodes with surplus energy (HH3 and H1 in this case)	After a short delay (assumed to be a decision time), the relays at HH2 and HH3 closed, indicating readiness for energy sharing. They reopened after

		respond but only one to close.	the reducing the demand at HH2.
4	With HH3 at 180 Wh the demand for HH5 increased by 70 Wh, other transceivers kept at case 1 state	Relays for HH3 and HH5 to be closed	Relays for HH3 and HH5 get closed within few seconds

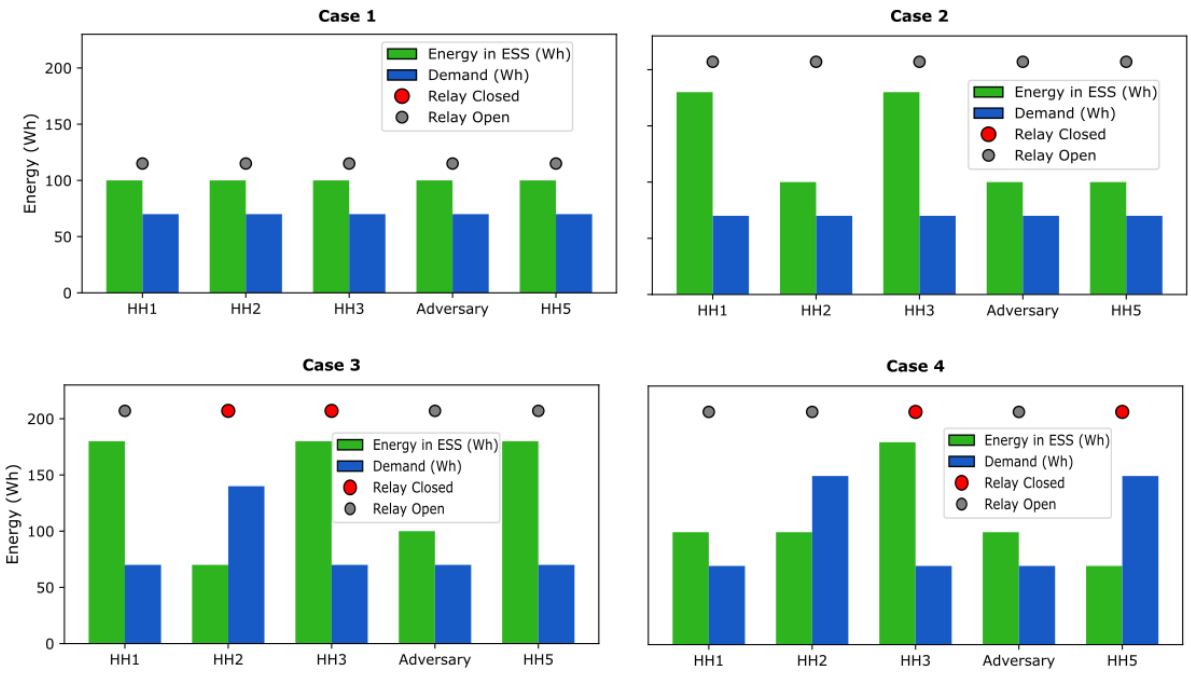

Figure 4.20: Laboratory testing Results of the Transceiver in four cases

The laboratory test results demonstrate that the developed transceiver effectively operates according to the designed working principles and the implemented data encryption mechanism. However, real-world implementation is essential to validate the actual energy exchange process. In practical applications, issues such as voltage rise at certain nodes may occur; therefore, appropriate voltage balancing measures will need to be implemented.

4.4 Chapter Summary

In this chapter, a smart transceiver for energy sharing and potential trading among swarm grid participants has been developed. The transceiver incorporates basic privacy and security mechanisms to enhance the protection of information exchanged between stakeholders against potential adversarial threats, although comprehensive testing against real-world and

sophisticated cyberattacks has not yet been conducted. In addition to its functional capabilities, the proposed design emphasizes cost-effectiveness, ease of installation, and the use of readily available components, making it practical and scalable for deployment in underserved areas such as rural Tanzania, where affordability and accessibility are critical factors.

Simulation results and laboratory tests have been conducted to validate the performance and reliability of the designed transceiver. Since the swarm grid concept is still in its early stages, there is limited literature available for comparison. However, the transceiver developed by (Mwammenywa et al., 2022) employs LoRa technology for transmitting control signals within a microgrid, focusing solely on demand-side management without addressing energy trading or security features. The present work therefore establishes a baseline for future enhancements and advancements in smart transceiver design for swarm grid technology. Possible future developments include the integration of real-time energy pricing, customer-based trading, and other advanced functionalities. The following chapter discusses the model for optimal swarm grid planning and design, where transceiver units are integrated into all participating households.

Chapter 5: SWARM GRID PLANNING AND DESIGN TOOL

This chapter describes the development of a planning and design tool for the implementation of a swarm grid. It is organized into seven sections. Section 5.1 presents an overview of the design methodology, while Section 5.2 describes the model for designing and developing the optimal grid layout. Section 5.3 addresses post-design grid stability control and related measures, and Section 5.4 explains the integration of the proposed model into a standard computer program. Section 5.5 discusses the methodological approaches for selecting distribution lines, Section 5.6 presents simulation results and their discussion, and Section 5.7 summarizes the chapter. It is worth noting that portions of this chapter have already been published by the author through the IEEE Power Africa Conference, held in Johannesburg, South Africa (2024) and Sustainable development of Energy, Water and Environmental Systems (SDEWES) conference held in Oujda, Morocco (2025).

5.1 Methodological Overview of Swarm Grid Design

The goal of this section is to provide an overview on methods and strategies that has been used to develop an optimized network planning tool. The model development proceeds through the following steps. Initially, two extreme conditions in terms of power demand and supply for each household in the rural area are identified over the course of 24 hours. In most villages peak demand occurs at night, while maximum solar power generation occurs during the day. Using these extreme conditions together with the materials specifications and costs, geo and spatial data of the households, an optimal network deployment model is formulated to accommodate both day and night scenarios.

Once the grid is generated, it is evaluated using time-series demand and supply data. If the evaluation reveals unmet demand or surplus are beyond the specified design range, the model regenerates the grid using updated values of the tuning parameters. This process repeats iteratively until either an optimal grid configuration is achieved, or maximum allowable iteration has reached. Furthermore, performance improvement and stability control are achieved by implementing an appropriate energy management strategy, such as demand-side management or the integration of an energy storage system. Figure 5.1 presents a high-level summary of the sequence.

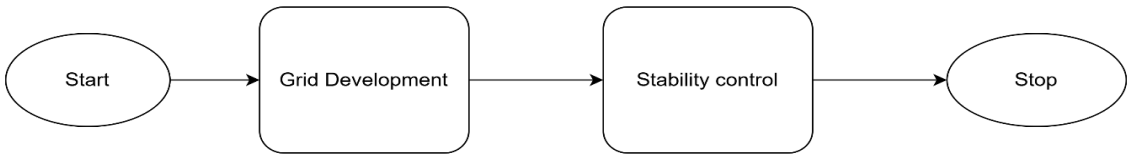

Figure 5.1: Overview of Grid Development and Management

5.2 Grid Design and Development

5.2.1 Grid layout

The primary goal of developing this tool is to minimize investment costs and promote efficient network design in swarm grid implementation, which may indirectly contribute to reduced electrical losses. The model evaluates network configurations under predefined technical and economic constraints. Figure 5.2 illustrates the overall workflow of the proposed highlighting the key steps from data input until the printout of the optimized grid configuration.

Within this optimization framework, the design of the swarm grid layout is governed by three main factors that must be carefully considered to ensure network reliability, scalability, and a proper balance between supply and demand. These factors include the specifications, types, and costs of locally available materials, particularly cables and poles. To systematically incorporate these considerations into the planning process and achieve the stated objective, the objective function defined in Equation (5.1) was formulated.

$$min \sum_{i \in N} \sum_{j \in N, j \neq i} \sum_{k \in K} \left(c_k \cdot d_{i,j} + cp \cdot mp_{ij} \cdot y_{ij}\right) \cdot 0.5 * x_{ij,k} + \sum_{i}^{N} \left(aP_{i,d}^{D} + bP_{i,d}^{S}\right)_{day,night} \quad (5.1)$$

Where c_k is the cost of conductor type k in TZS/m, d_{ij} is the Euclidean distance between house i and j in m, cp=cost per pole in TZS/pole and mp_{ij} is the number of poles necessary between house i and j, $x_{ij,k}$ and y_{ij} are the decision variables, while a 0.5 accounts for the bidirectional cable connections between house i and j, N is the total number of houses in the village, K is the total number of cable types available, $P_{i,d}^{D}$.is the demand penalty of house i during grid development $P_{i,d}^{S}$ is the surplus penalty of house i during grid development, a and b are the tunning parameters. These penalty terms are included in the objective function to guide the optimization toward solutions that balance supply and demand while minimizing both energy shortfalls and unnecessary excess generation.

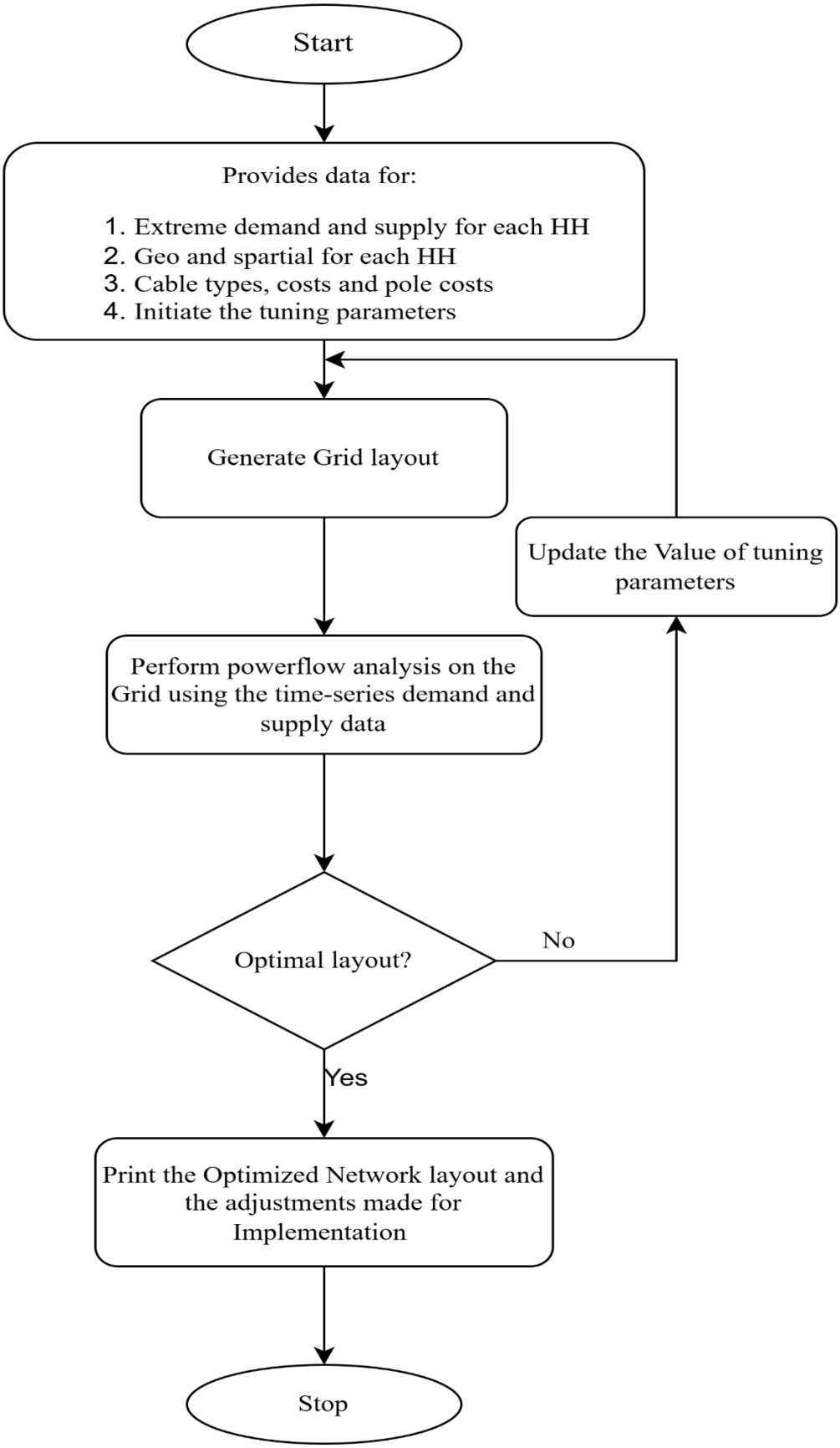

Figure 5.2: Optimized Grid Development

Decision variables to the model are as indicated in (5.2) and (5.3) such that the value is 1 if cable of type k is installed between house i & j or a pole is installed, and 0 otherwise. The day and night in (5.4) ensure that the same network topology is used during the surplus production - low demand scene (referred as day) and low production - high demand (referred as night). The objective function was then bounded to different constraints as presented in subsection i through v.

$$x_{ij,k} = \begin{cases} 1: Connection\ exist \\ 0: Otherwise \end{cases} \tag{5.2}$$

$$y_{ij} = \begin{cases} 1: A\ pole(s) have\ been\ chosen \\ 0: Otherwise \end{cases} \tag{5.3}$$

$$\left(x_{ij,k}\right)_{night} = \left(x_{ij,k}\right)_{day} \tag{5.4}$$

i. Flow Equilibrium for each Household

From the principle of energy conservations, it is required that the total amount of electrical energy flowing towards house i to be the same as the deficit required by house i, as shown in (5.5).

$$\sum_{j \in N, j \neq i} f_{ji} - \sum_{j \in N, j \neq i} f_{ij} + PV_i + B_i + P_i^D = D_{i,} + P_i^S \quad \forall i, j \in N \tag{5.5}$$

Where PV_i is the average day time electricity generated by solar PV from house i in Watts, D_i is the electricity demand from house i in Watts, f_{ji} is power flows from house i to house j in Watts, f_{ij} is the power flows from house j to house i in Watts and B_i is the average amount of power supplied by the energy storage system of house i at night in Watts, P_i^D represents the unmet demand penalty, which quantifies the cost or impact of not supplying the required energy to household i, P_i^S represents the surplus penalty, accounting for the inefficiency or cost associated with producing energy beyond the household's demand. N is the total number of houses in the village.

ii. Capacity Limitation for Cables

This constraint is to ensure that an appropriate cable type is chosen depending on the amount of electrical energy that is expected to be flowing between the two houses. The constraint equation is as seen in (5.6).

$$f_{ij} \leq c_c \cdot x_{ij,k} \quad \forall i,j \in N, c \in K \tag{5.6}$$

Where c_c is the Capacity of cable type c in kilowatts (kW) and other symbols carry the meaning as previously defined in this work.

iii. Connectivity Constraints

To restrict the pairing between houses it is mandatory to ensure that only one cable is chosen while doing the pairing. In ensuring this constraint is attained equation (5.7) is used while the symmetrical condition i.e. a cable connecting house i to j is the same as that connecting house j to i is taken care of by (5.8), all symbols carry their pre-defined meaning.

$$0 \leq \sum_{k \in K} x_{ij,k} \leq 1 \quad \forall i,j \in N, i \neq j \tag{5.7}$$

$$x_{ij,k} = x_{ji,k} \quad \forall i,j \in N, k \in K \tag{5.8}$$

iv. Non-negativity Constraints

The negative input to the model could result in false optimal network design; to overcome such scenarios the model is bounded by the non-negativity constraints equations as defined in (5.9) and (5.10).

$$f_{ij} \geq 0 \quad \forall i,j \in N \tag{5.9}$$

$$f_{ji} \geq 0 \quad \forall i,j \in N \tag{5.10}$$

v. Pole Placement Constraints

An extra pole may be chosen if and only if there is a cable connection between houses and the distance between them meets a certain threshold, configured directly on the model as it is country dependent. Currently, the threshold is set to be 30 m (standard distribution line span for Tanzania expecting that the arrival of national grid should use the existing infrastructure). Equation (5.11) displays the pole constraints used for the objective function of this model. It is also worth noting that each household has a pole beneath the house called inlet pole.

$$\sum_{N,K,i\neq j} x_{ij,k} \leq \sum_{N,i\neq j} y_{ij} \tag{5.11}$$

5.2.2 Power Flow Analysis

In the power flow analysis, time-series demand and supply data are fed in the generated grid to evaluate its performance. In this subsection mathematical modelling for power flow analysis in the grid are presented. The output of the power flow analysis includes the number of connected nodes, unmet demand and surplus production in the entire grid. These outputs are then compared with the desired or expectations to decide if tunning is needed or not. Equations (5.12) to (5.25) show how the analysis and updating of the tunning parameters are conducted.

i. Power Flows Balance

Equation (5.12) represents the house power balance for each household $i \in N$at every time step $t \in T$. It enforces the principle of conservation of energy by ensuring that total power inflows are equal to total power outflows at each node:

$$S_{i,t}^{pv} + S_{i,t}^{bat(dis)} + \sum_{j\in N} f_{j,i,t} + P_{i,t}^{D} = D_{i,t} + S_{i,t}^{bat(chg)} + \sum_{j\in N} f_{i,j,t} + P_{i,t}^{S} \tag{5.12}$$

Where, $S_{i,t}^{pv}$ is the Supply from the solar PV at node *i* at time *t,* $S_{i,t}^{bat(dis)}$ is the Supply due to battery discharge at node i at time t, $f_{j,i,t}$ is the Power flow from node i to j at time t, $D_{i,t}$ is the Demand due to load at node i at time t, $S_{i,t}^{bat(chg)}$ is the Demand due to charging of the battery at node i in time t, $f_{i,j,t}$ is the Power flow from node i to j at time t, $P_{i,t}^{D}$ is the Unmet demand penalty, $P_{i,t}^{S}$ is the Surplus penalty, and N is the total number of houses in the village

ii. Energy Balance for Battery

To ensure compliance with the principle of conservation of energy, the battery energy at any time step t must be equal to the energy stored at the previous time step adjusted for charging and discharging activities. Accordingly, Equation(5.13) defines the intertemporal energy balance of the battery.

$$E_{i,t+1}^{b} = \beta E_{i,t}^{b} + \left(\eta_c S_{i,t}^{bat(chg)} - \frac{S_{i,t}^{bat(dis)}}{\eta_d} \right) \Delta t \tag{5.13}$$

Where $E_{i,t+1}^{b}$ is the stored energy in the battery at node i at time $t+1$, $E_{i,t}^{b}$is the stored energy in the battery at node i at time t, $S_{i,t}^{bat(chg)}$ is the Battery charging power at time t, $S_{i,t}^{bat(dis)}$ is the Battery discharging power at time t, η_c, η_d is the Battery charging and discharging efficiency, respectively and β is the Battery self-discharge factor

iii. Battery Capacity Limits

To prevents overcharging and deep discharge of the battery, the battery energy level for all houses at any time t is governed by equation (5.14).

$$E_i^{bmin} \leq E_{i,t}^{b} \leq E_i^{bmax}, \qquad \forall i \in N, t \in T \tag{5.14}$$

Where E_i^{bmin} is the Minimum allowable battery energy of node i, $E_{i,t}^{b}$ is the Battery energy of node i at time t, E_i^{bmax} is the Maximum allowable battery energy of node i

iv. Battery Charge/Discharge Limits

To ensure that the battery is neither discharged below zero nor beyond its maximum allowable discharge capacity, and simultaneously not charged above its maximum charging capacity, Equation (5.15) is introduced to bound the battery's state of charge within its technical limits. Furthermore, to ensure that battery discharge remains proportional to the available demand, Equation (5.16) is implemented to restrict discharge to the level of existing demand.

$$0 \leq S_{i,t}^{bat(chg)} \leq C_i^{bat(chg)}, \qquad 0 \leq S_{i,t}^{bat(dis)} \leq C_i^{bat(dis)} \tag{5.15}$$

$$S_{i,t}^{bat(dis)} \leq D_{i,t} \quad \forall i \in N \;\; t \in T \tag{5.16}$$

Where: $C_i^{bat(chg)}$ is the maximum battery charging power, $C_i^{bat(dis)}$ is the maximum battery discharge power, other symbols retain the same meaning as previously defined in this document.

v. Battery Operation Constraint

During energy sharing, simultaneous charging and discharging of the battery is prohibited using Equation (5.17). This constraint effectively implements a logical "AND" condition to ensure that the battery can either charge or discharge at any given time, but not both simultaneously.

$$NOT\left(S_{i,t}^{bat(chg)}\ AND\ S_{i,t}^{bat(dis)}\right) = 1 \tag{5.17}$$

vi. Flow Constraint

The power flow between any pair of houses should occur only if there is a cable connection between them. To restrict this condition equation (5.18) is used. Furthermore, to limit the looping in the power flow between each pair of houses equation (5.19) is introduced.

$$f_{j,i,t} = -A_{i,j} f_{j,i,t}\ \ ,\forall i,j \in N\ \ t \in T$$

$$A_{i,j} = \begin{cases} 1\text{: Connection exist} \\ 0\text{: No connection} \end{cases} \tag{5.18}$$

Where $A_{i,j}$ is the element in adjacency matrix drawn from the optimized grid, all other symbols retain the same meaning as previously defined in this document.

$$NOT\left(f_{j,i,t}\ AND\ f_{i,j,t}\right) = 1\ \ ,\forall i,j \in N\ \ t \in T \tag{5.19}$$

vii. Capacity Constraint

The power flowing between houses should not exceed the maximum capacity of the cable connecting the two houses. To ensure this is attained equation is (5.20) introduced.

$$f_{j,i,t} \leq C_c\ \ ,\forall i,j \in N\ \ c \in K \tag{5.20}$$

Where C_c is the capacity of the cable present in the optimized grid for the given connection. K is the number of cable types available.

viii. Unmet demand Constraint

To prevent the solver from allocating unmet demand that exceeds the actual household demand, Equation (5.23) is introduced. This constraint restricts the model from assigning deficit values greater than the corresponding demand. All symbols retain the same meaning as defined previously in this document.

$$P_{i,t}^{D} \leq D_{i,t} \ , \forall i,j \in N, t \in T \tag{5.21}$$

ix. Battery Cyclic Constraint

To ensure that no artificial or "free" energy is introduced into the swarm grid (SG), a cyclic condition is imposed requiring the battery's state of charge at the beginning of the simulation to be equal to its state at the end. This constraint prevents the model from exploiting non-physical energy imbalances and ensures consistency with the principle of conservation of energy. All symbols retain the same meaning as defined previously in this document.

$$E_{i,t=0}^{b} = E_{i,t=T}^{b} \ , \qquad \forall i \in N, t \in T \tag{5.22}$$

x. Objective Function (Minimization of Penalties)

The operational penalties are optimized using the right-hand side of Equation (5.1), where the objective now minimizes the cumulative penalty over the entire operational horizon $T$and across all N houses in the network. The a and b are the same as those in equation (5.1). The minimization of operation penalties is realized using equation (5.23).

$$min \sum_{t \in T} \sum_{i \in N} \left(a P_{i,t}^{D} + b P_{i,t}^{s} \right) \tag{5.23}$$

xi. Own Demand Prioritization

In the energy trading environment, the price for selling electricity to the grid is cheaper than purchasing from it. This difference will in turn cause unnecessary cost of purchasing electricity from the grid. Also, if the battery discharge and charging occur more frequent place additional stress on the battery, reducing its lifespan. Therefore, own demand prioritization is one solution to be incorporated in the model to cater for the forementioned challenges. To effect this in the developed model additional mathematical modelling as described in equation (5.24) and (5.25)

are considered. Alongside with these additions, the modification of the battery discharge limits of equation (5.15) is required.

$$P_{G,i}(t) = \max\left(0, E_{i,t}^{b} - \sum_{\tau=t}^{t+\tau} D_i(\tau)\right) \tag{5.24}$$

Where $P_{G,i}(t)$ is the energy discharged by house i to the grid at time t, $E_{i,t}^{b}$is the available energy in the battery of house i at time t, $\sum_{\tau=t}^{t+\tau} D_i(\tau)$, is the future demand term, τ is the forecasted time period in hours. The corresponding constraint for maximum discharge is as shown in equation (5.25). All symbols and notations carry their usual meaning as defined in this study.

$$S_{i,t}^{bat(dis)} \leq \min\left(C_i^{bat(dis)}, P_{G,i}(t)\right) \tag{5.25}$$

5.2.3 Updating the Tuning Parameters (a, b)

During power flow analysis the stability of the grid in terms of total unmet demand and surplus is evaluated. If the designed grid does not meet the targeted unmet demand or surplus, then turning parameters are updated and the grid gets redesigned. Equations (5.26) and (5.27) provide guidance on how to update the turning parameters.

$$a_{k+1} = a_k\left[1 + \gamma\frac{U - U^d}{U^d + \epsilon}\right] \tag{5.26}$$

Where a_k, and a_{k+1} is the current and next value of parameter "a" respectively, U^d is the designer unmet demand level required, U is the total unmet demand from the power flow analysis, γ is step size, small (around 0.1) to avoid oscillations and ϵ, is the very small number (in the order of 1e-6) to avoid division by zero.

$$b_{k+1} = b_k\left[1 + \gamma\frac{S - S^d}{S^d + \epsilon}\right] \tag{5.27}$$

Where b_k, and b_{k+1} is the current and next value of parameter "b" respectively, S^d is the designer surplus level required, S is the total surplus obtained from the power flow analysis, γ is step size, small (around 0.1) to avoid oscillations and ϵ, is the very small number (in the order of 1e-6) to avoid division by zero.

5.3 Grid Stability Control in the Post-Design Phase

After completion of the network design and optimization phase, maintaining grid stability during operation becomes an important task. In the post-design phase, different control strategies are employed to balance supply and demand, hence regulating power exchange between SG participants. These strategies ensure reliable and grid operation under varying load and generation conditions. Figure 5.3 presents the sequence of activities for grid stability control.

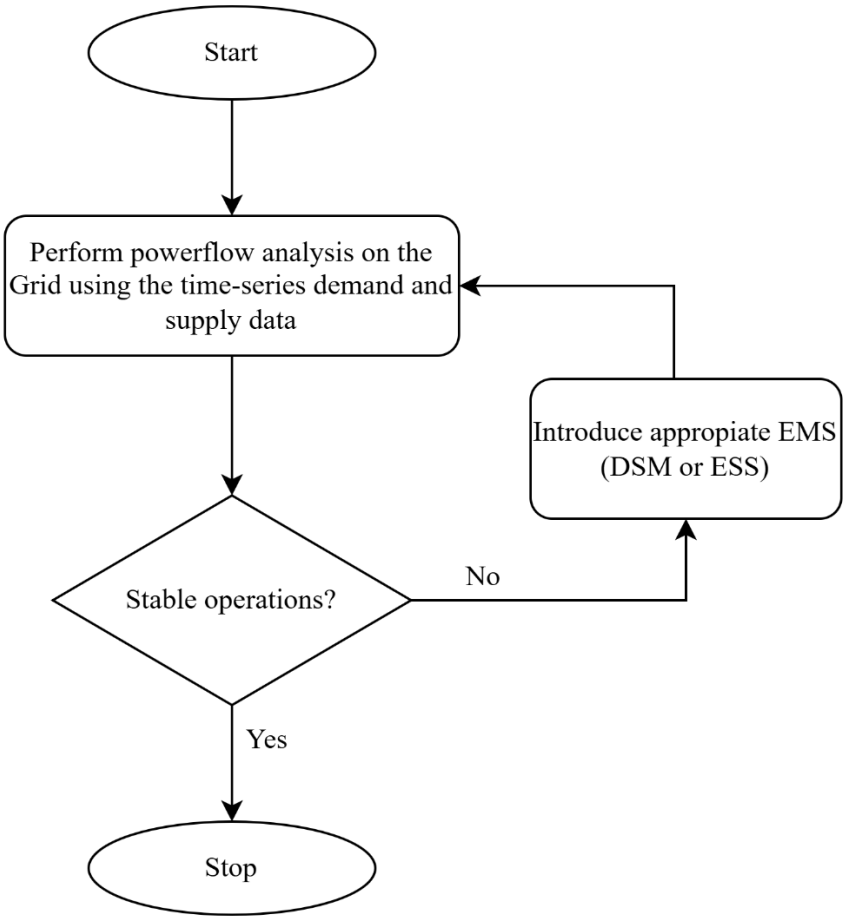

Figure 5.3: Grid Stability and Control Approaches

As introduced in Section 5.1, the control strategies or energy management solutions can be categorized into two main groups: the integration of energy storage systems and the

implementation of demand-side management. The integration of energy storage systems is typically carried out after assessing the total deficit and surplus in the grid and is generally performed once. In contrast, demand-side management can be implemented without prior knowledge of the exact magnitude of unmet demand or surplus, although understanding the general trend remains important.

5.3.1 Introduction of Centralized Energy Storage System

The integration of a centralized energy storage system (ESS) into the swarm grid (SG) network is one of the strategies that can be used to improve energy management, stability, and reliability. Once the swarm grid has been established and the power flow analysis has been conducted, the optimal size of the ESS can be determined using different optimization methodologies. In this study, a model is proposed to determine the optimal ESS capacity for the system. The centralized ESS is designed to store excess energy generated within the network and discharge it later to cover energy deficits. Specifically, the ESS is charged using available surplus energy and discharged when local household ESS units and network power flows are unable to fully meet the demand as depicted in Figure 5.4.

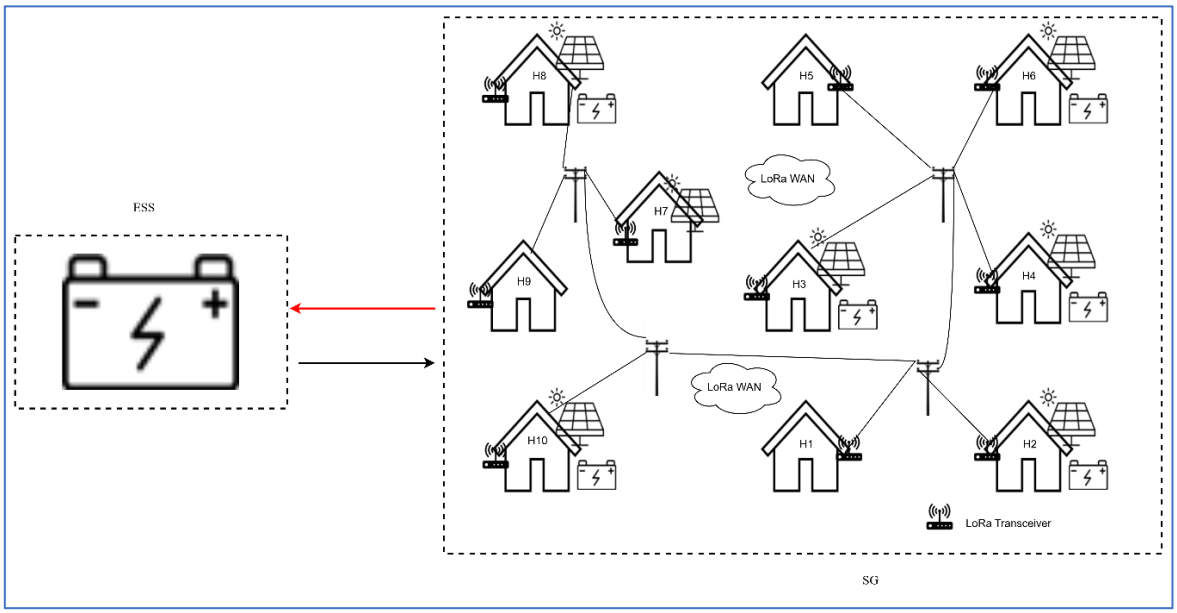

Figure 5.4: Outlook of the introduction of ESS to SG

The objective of this approach is to ensure that all energy demand is satisfied while maintaining the ESS capacity at an optimal and economically feasible level. Equation (5.28) provides the objective function for this task.

$$\min \sum_t \sum_i \omega U_{i,t} + \lambda B \ , t \in T \ i \in N \tag{5.28}$$

Where ω is the penalty to ensure the model covers the entire deficit, $U_{i,t}$ is the deficit of house i in time t after the introduction of centralized ESS, λ is the cost for the battery (ESS), B is the capacity in kWh of the optimal battery required. As explain above the battery is to be charged from the available surpluses in the SG, then equation y holds.

$$S_t^{PV\_surplus} = \sum_{i \in N} \max\left(S_{i,t}^{pv} - D_{i,t}, 0\right) \tag{5.29}$$

Where $S_t^{PV\_surplus}$, is the surplus required to charge the centralized ESS at time t, $S_{i,t}^{pv}$ is the supply from PV for house i at time t, and $D_{i,t}$, is the demand of house i at time t. The model is the bounded to the following constraints.

To prevent simultaneous charging and discharging of the ESS equation (5.30) is introduced. Where CB_t^{chg} is the charging of centralized battery, CB_t^{dis} is the discharge of the centralized battery.

$$NOT\left(CB_t^{chg} \ AND \ CB_t^{dis}\right) = 1 \tag{5.30}$$

The centralized battery will only be charged from the available surplus in the SG, as bounded by equation (5.31). All symbols retain the same meaning as defined in this section.

$$CB_t^{chg} \leq S_t^{PV\_surplus} \tag{5.31}$$

The state of charge in the centralized battery cannot exceed the capacity of the battery, also can never be less than zero. Equation (5.32) ensure the conditions are met. All symbols retain the same meaning as in this section.

$$0 \leq SOC_t \leq B \ , \forall t \in T \tag{5.32}$$

The centralized battery should discharge the amount of energy same or less that the total sum of the deficit in the grid at any given time as instructed by the equation (5.33)

$$CB_t^{dis} \leq \sum_{i \in N} P_{i,t}^D, \forall t \in T \tag{5.33}$$

The energy in the centralized battery at any time t is governed by equation (5.34)

$$CB_{i,t+1}^b = \beta CB_{i,t}^b + \left(\eta_c CB_{i,t}^{chg} - \frac{CB_{i,t}^{dis}}{\eta_d}\right)\Delta t \tag{5.34}$$

The discharged energy from the centralized battery is allocated proportionally among households experiencing unmet demand. Each household receives a share of the discharged energy corresponding to its contribution to the total network deficit at that time step. This proportional allocation ensures fair distribution of available stored energy while reducing the remaining unmet demand across the network.

Let

$$P_t^{\text{total}} = \sum_{i \in N} P_{i,t}^D \tag{5.35}$$

Where $P_{i,t}^D$ is the unmet demand penalty obtained from the optimized grid in the SG. Then for each household condition in equation (5.36) shall hold true.

$$U_{i,t} \geq \begin{cases} P_{i,t}^D - CB_t^{\text{dis}} \cdot \dfrac{P_{i,t}^D}{P_t^{\text{total}}}, & \text{if } P_t^{\text{total}} > 0 \\ P_{i,t}^D, & \text{if } P_t^{\text{total}} = 0 \end{cases} \tag{5.36}$$

The other decision variables to the model are the non-negative constraints as presented in equation (5.37) to (5.40). All symbols retain the same meaning as defined in this section.

$$CB_t^{\text{ch}} \geq 0 \tag{5.37}$$

$$CB_t^{\text{dis}} \geq 0 \tag{5.38}$$

$$B \geq 0 \tag{5.39}$$

$$U_{i,t} \geq 0 \tag{5.40}$$

5.3.2 Introduction of Demand Side Management (DSM)

Another option for stabilizing the grid, apart from the introduction of energy storage systems (ESS), is the implementation of appropriate demand side management (DSM) strategies. Demand side management focuses on modifying or controlling electricity consumption patterns on the consumer side to improve the balance between supply and demand. Through DSM, certain flexible loads can be shifted from one time to another depending on the strategy applied. This allows electricity demand to be redistributed across different hours of the day, helping to reduce peak loads, improve the utilization of renewable energy, and enhance overall grid stability.

As discussed by Rasheed et al. (2020), there are three main types of demand side management (DSM) strategies commonly applied in electricity grids: load shifting DSM (also referred to as incentive-free DSM or demand rescheduling), Time-of-Use (TOU) pricing, and Real-Time Pricing (RTP). Each of these strategies aims to influence electricity consumption patterns to better align demand with available supply.

In this work, the focus is placed on the load shifting type of demand side management. This approach allows flexible electricity demand to be redistributed across different time periods without altering the total daily energy consumption. By shifting loads from periods of high demand to periods of lower demand or higher renewable generation, the deployed grid can be operated in a more controlled and balanced manner. The overall objective is to minimize the energy deficit and surplus as described in equation (5.41)

$$\min \left(c^u \sum_{i,t} P_{i,t}^D + c^Q \sum_{i,t} Q_{i,t} + c^s \sum_{i,t} P_{i,t}^s \right) \tag{5.41}$$

Where $P_{i,t}^s$, is the surplus of house i at time t, $P_{i,t}^D$, is the deficit or unmet demand of house i in time t, $Q_{i,t}$ is the amount of demand that can be shifted of house i at time t, c^u is the cost of unmet demand, c^Q is the cost of shifted deficit account for unnecessary shift or inconvenience in shifting the load, and c^s is the cost of surplus. It is required to shift some demand whenever convenient hence equation (5.42).

$$Q_{i,t} \geq D_{i,t}^{Q} \geq 0$$
$$Q_{i,t} \geq 0 \tag{5.42}$$

Where $D_{i,t}^{Q}$ is the shifted demand of house i at time t. Power flow from on house to another and Battery charging and discharging variables as well as state of charge defined earlier still hold in the DSM. Other variables include those in (5.43).

$$P_{i,t}^{D} \geq 0$$
$$P_{i,t}^{s} \geq 0 \tag{5.43}$$
$$PV_{i,t}^{use} \geq 0$$

In shifting the demand there should be a conservation of the total demand for the entire day such that no demand is left unallocated. Equation (5.44) constraint the model to that condition.

$$\sum_{i,t} D_{i,t}^{Q} = \sum_{i,t} D_{i,t} \ , \forall i \in N, t \in T \tag{5.44}$$

Where $D_{i,t}$ is the demand of house i at time t, N is the total number of houses in the grid. The magnitude of the shifted demand is governed by equation (5.45).

$$Q_{i,t} \geq \ \left|D_{i,t}^{Q} - D_{i,t}\right|, \forall i \in N, t \in T \tag{5.45}$$

During the day PV generation is always expected to in large amount which might result into surplus. So, the PV used and the surplus should add-up to the total PV generated, equation (5.46) holds

$$PV_{i,t}^{use} + \ P_{i,t}^{s} = S_{i,t}^{pv}, \qquad \forall i \in N, t \in T \tag{5.46}$$

Where $S_{i,t}^{pv}$ is the total energy generated by house i at time t, $PV_{i,t}^{use}$ is the amount of solar PV energy consumed by house i in time t. Also, the PV used cannot exceed the available PV generation.

$$PV_{i,t}^{use} \leq S_{i,t}^{pv}, \qquad \forall i \in N, t \in T \tag{5.47}$$

At each node there should always be energy balance i.e., the energy supplied must equal the energy consumption as governed by (5.48). All symbols retain the same meaning as defined in this document.

$$PV_{i,t}^{use} + S_{i,t}^{bat(dis)} + \sum_{j \in N} f_{j,i,t} + \ P_{i,t}^{D} \ = \ D_{i,t}^{Q} + S_{i,t}^{bat(chg)} + \sum_{j \in N} f_{i,j,t} + \ P_{i,t}^{s} \tag{5.48}$$

In this section, a brief overview of the demand side management (DSM) modelling has been presented. The other associated equations, decision variables, and constraints related to battery operation, energy flows, and network interactions, as defined in Section 5.2, also apply here. This DSM model serves as the framework to demonstrate how the swarm grid (SG) can benefit from demand flexibility in achieving operational stability, enhanced reliability, and improved integration of distributed energy resources.

5.4 Implementation and Usage of the Tool

After successfully completing the model design, the tool's interface was subsequently developed. The primary objective in creating the tool's interface was to ensure accessibility and ease of use for stakeholders with diverse educational backgrounds and levels of technical expertise. In support of this, the study by Maria Mahmud et al. (2024) suggests that Microsoft Excel is one of the most suitable options to consider. The integration could increase not only the user-friendliness but also number users of the tool by allowing users to interact with the tool through a common and familiar interface. Since the tool was developed in Python then Visual Basic for Applications (VBA) was chosen as an effective intermediary to facilitate communication between Python and Excel. As a result, all data inputs and performance visualizations are handled within the Excel environment. A piece of code used to establish the linkage between Python and Excel through VBA, as discussed by Mergel (n.d.) is presented below.

```
sub PerformDataVisualization ()
        Dim vbaShell As Object
        Set vbaShell=VBA.CreateObject("Wscript")
        vbaShell.Run """ file_path_to_python executable""" & """file_path_to_paython
script"""
End Sub
```

The outlook of the developed interface is as shown in Figure 5.5, in which users will only be required to input data via the button named "*Enter Household Data"* and choose the visualization operation among the five available options. After clicking that button, an excel sheet named time-series data will be created. The workbook will have three spreadsheets named, "Supply_PV", "Battery" and "Load_demand". In the "Supply_PV" sheet as shown in Figure 5.6, the columns with numbers 0 to 23 stand for time so it can be time of the day, days of the month, months of the year or number of years. The rows with H1 to H10 represent the number of houses so the nomenclature should be adhered to. In this sheet a user will be required

to enter average solar power in (W) production for each household. In a similar manner, the load demand data are to be entered in the sheet titled “Load_demand,” as shown in Figure 5.7.

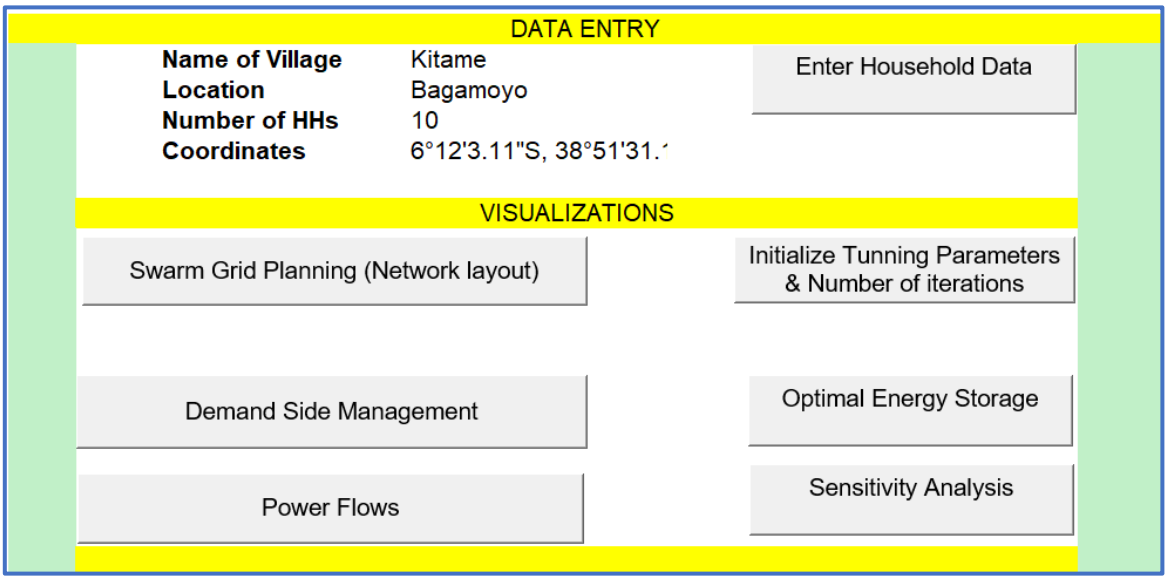

Figure 5.5: MS Excel Interface of the Developed Tool

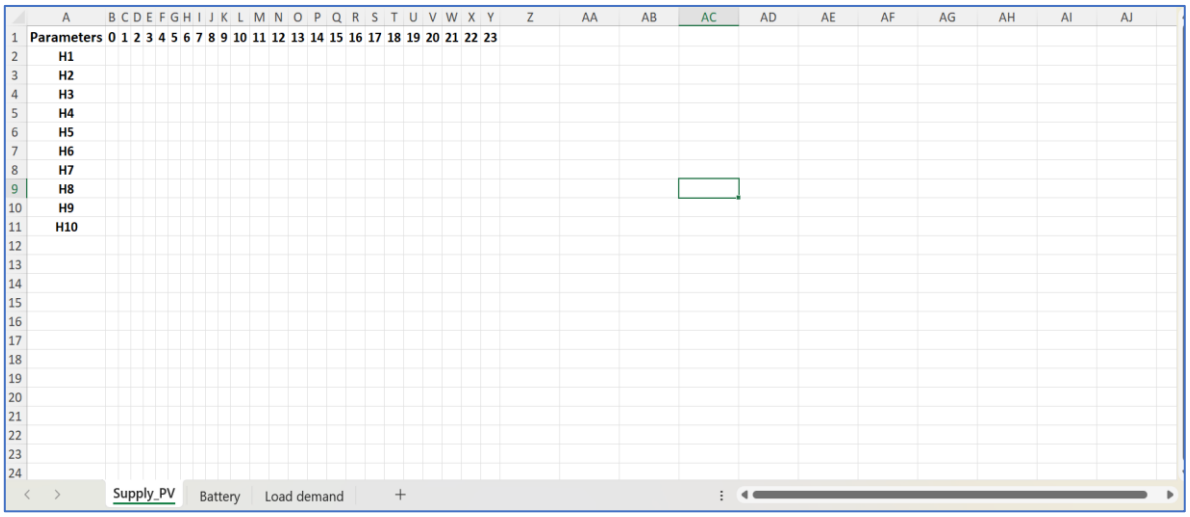

Figure 5.6: Excel Workbook for entering solar power data for each household

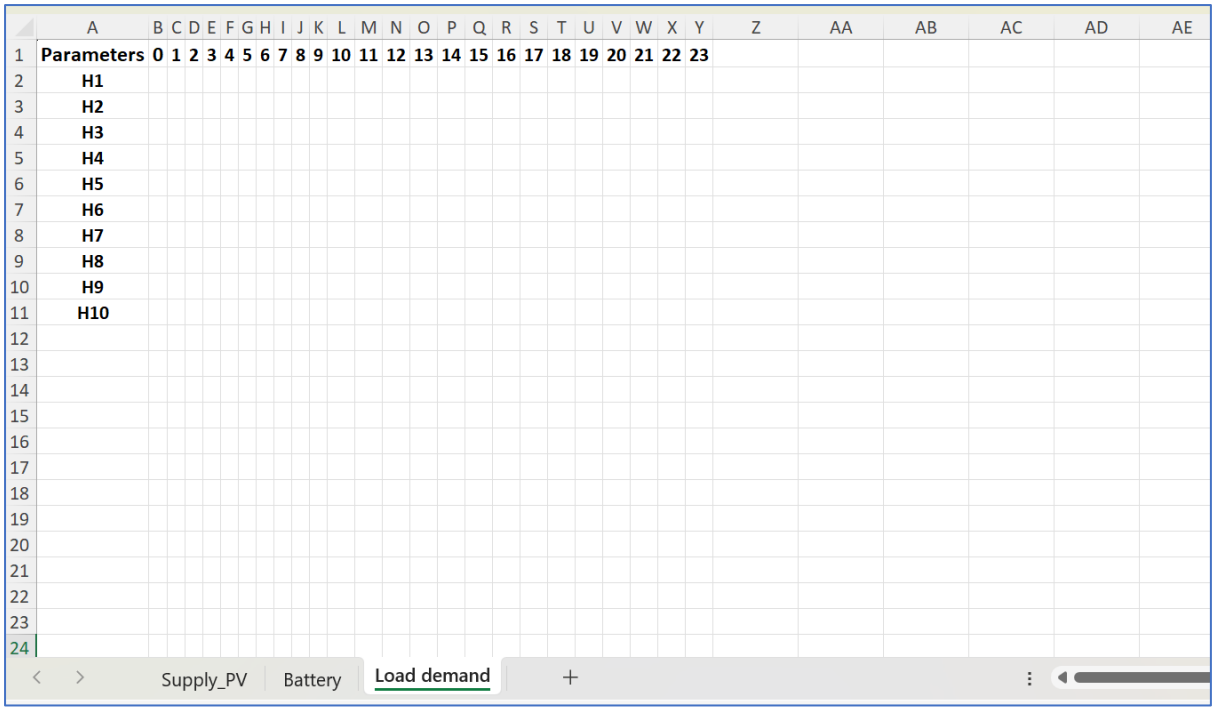

Figure 5.7: Excel Workbook for entering demand data for each household

Moreover, the sheet named “Battery” will be used to enter energy storage particulars for each household. Figure 5.8 illustrates the energy storage particulars that need to be supplied to the model. These parameters include the battery capacity, charging and discharging power limits, and the minimum and maximum allowable energy levels.

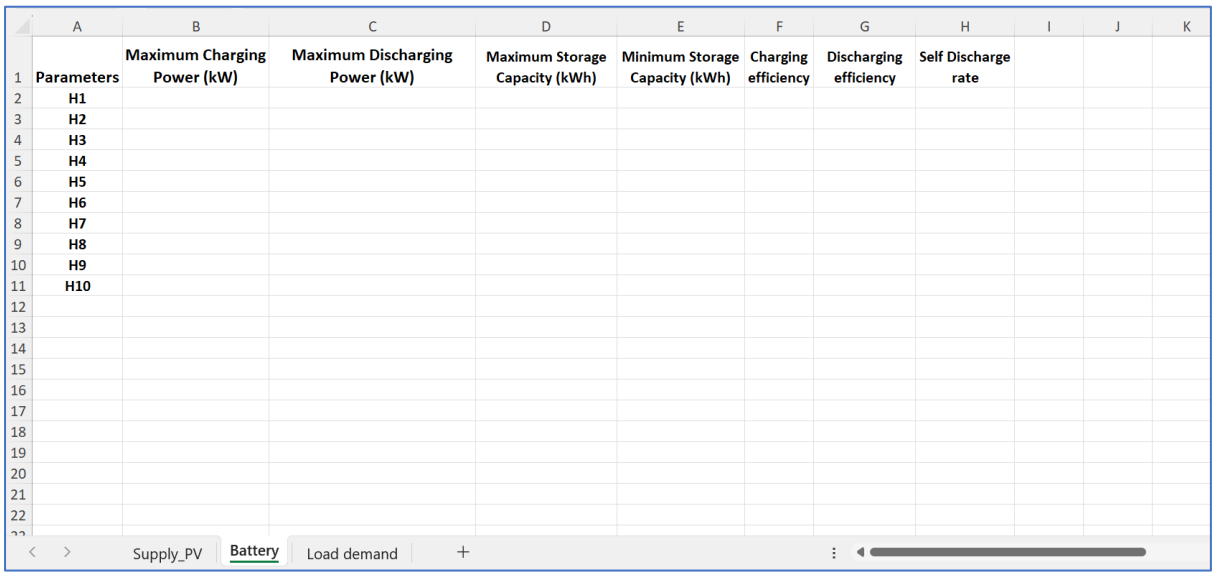

Figure 5.8: Excel Workbook for entering energy storage data for each household

5.5 Simulation Results and Discussion

5.5.1 Simulation Set-Up

The developed network optimization tool was applied to real data collected from Kitame village, where the mean monthly daily solar insolation was 6.0 kWh/m²/day. Given this relatively high and stable average insolation, it was considered appropriate to perform a one-week simulation using 6.0 kWh/m²/day as a representative value to approximate the system's performance over the entire year. A total of 50 households were visited to collect typical load, storage, geo-data and generations data. The cable specifications provided in Table 5.1 were obtained from manufacturers' data sheets, while the associated costs reflect current market prices in Tanzania. To have clarity in discussion and analysis of the results a sample of ten (10) households was considered for the simulation. The household positions were considered in a plane cartesian coordinates presented in Table 5.2 in which the distances are measured in meters from the centre of the house. Household 1 (H1) was taken as the reference point for the entire village sample.

Table 5.1: Cable Particulars

Parameters	Type 1	Type 2	Type 3
Cost per Length (TZS/m)	2,500	4,000	6,500
Capacity (kW)	6.9	8.74	12.65
Colour (For convenience)	Green	Red	Blue

Table 5.2: Household Locations

House	H1	H2	H3	H4	H5	H6	H7	H8	H9	H10
Position(m)	(0,0)	(0,7)	(12,20)	(3,4)	(8,12)	(7,10)	(2,5)	(40,35)	(4,7)	(7,0)

The electrical loads, generation, and energy storage system for each household involved in the simulation are provided in Table 5.3. The corresponding supply and demand profile for a week is presented in Figure 5.10. The load curves used to generate this profile were obtained from a collected 24-hour load profile. To reflect realistic household consumption behaviour and introduce variability between households and time periods, a random variation of ±20% was applied to the base 24-hour load values. This stochastic adjustment allows the simulation to capture fluctuations in daily electricity demand that typically occur due to differences in user behaviour, appliance usage, and other uncertain factors. As a result, the generated load curves represent more realistic demand patterns for the weekly simulation. The maximum charging

and discharging power were set to 1.2 kW per each 1.2 kWh battery while the minimum energy level and self-discharge factor of the battery was set to at least 0.6 kWh and 0.5 % per day (Czerwiński et al., 2018), respectively. Summary of the battery characteristics used for simulation is presented in

Table *5.4*. Figure 5.9 shows a complete outlook of the Kitame village with the households in question being marked in red. These households were selected based on representativeness of demand patterns, and therefore not to include the entire village. The selection allows for a controlled and detailed analysis within the scope and constraints of this study. The tuning parameters of the developed model i.e., (a, b) were initialized to (0,0) and a total of 30 iterations were carried out. The model was allowed to forecast demand for at most 2 hrs ahead. Simulation results for independent households and for household in the SG are presented in Section 5.5.2.

Table 5.3: Load, Generation and Storage status at each household

Household Name	**Loads**	**Generation and Storage**
H2, H3, H4 & H5	Three 6 W LED lights, Phone charging, 200 W Radio 70 W Electric fan	320 W solar panel Two 1.2 kWh batteries
H6, H7 & H8	Six 6 W LED lights, Phone charging, 200 W Radio 70 W Electric fan	
H1	Eight 6 W LED lights, Phone charging, 1000 W Radio 750 W Refrigerator 45 W Hair Cutting Saloon 70 W Electric fan 30 W TV	Four 320 W solar panels Three 1.2 kWh batteries
H9 & H10	Four 6 W LED lights, Phone charging, 1000 W Radio 750 W Refrigerator 70 W Electric fan 30 W TV	Three 320 W solar panels Three 1.2 kWh and One 0.84 kWh batteries

Table 5.4: Battery Characteristics for Residential Applications*(Rand & Moseley, 2015)*

	Charging efficiency (η_c,)	Discharging efficiency (η_d)	Self-Discharge factor (β)
Typical Values	80 - 95%	80 - 90%	2–5%, up to 15–25% per month
Value Used	95%	90%	15% equivalent to 0.5% per day

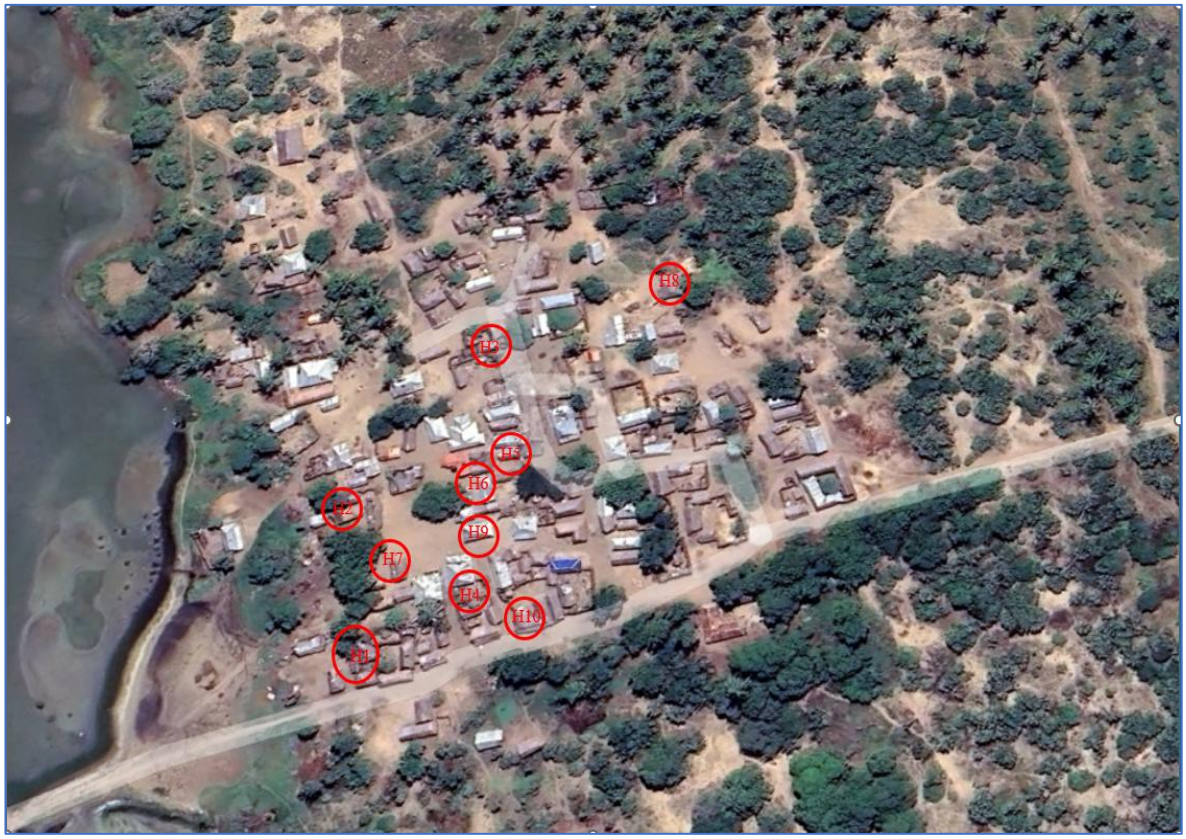

Figure 5.9: Outlook of Kitame Village with ten houses (in red) used for simulation

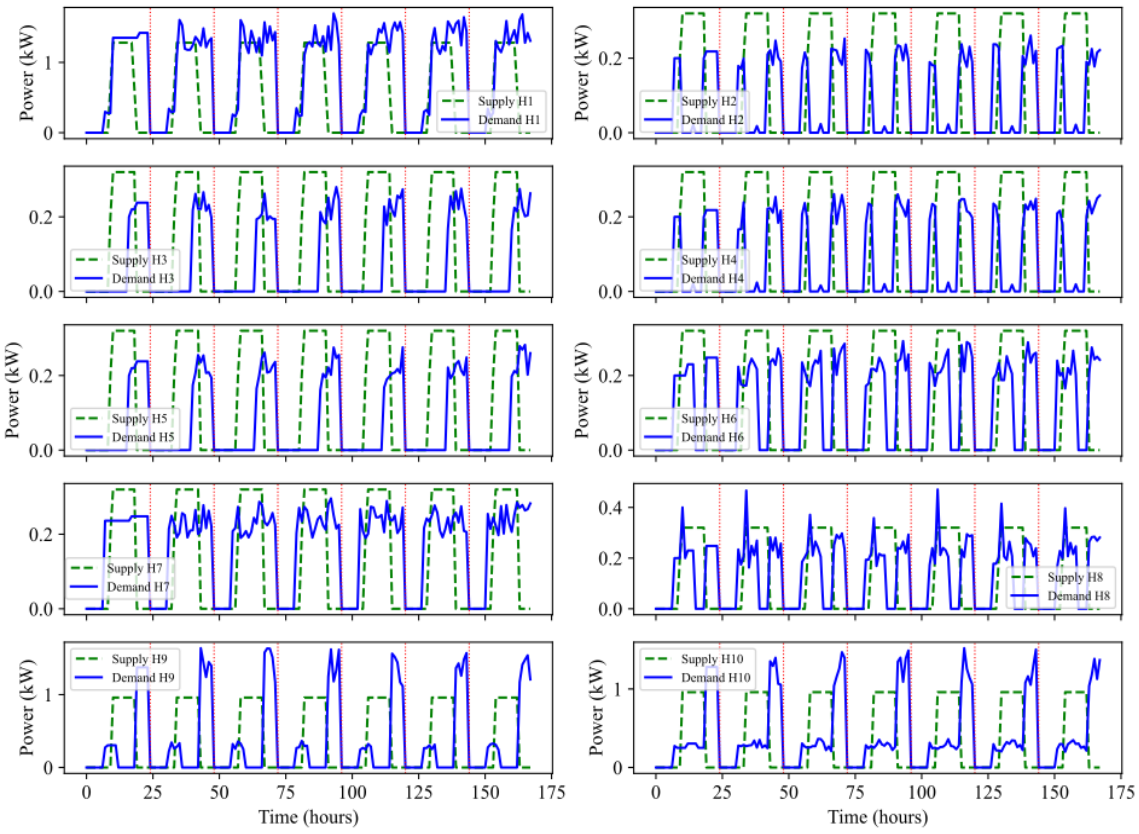

Figure 5.10: Demand and Supply Profile for Each Household

5.5.2 Simulation Results

(a). Individual Solar Home Systems, SHS

In this subsection, the demand and surplus status of individual households (prior to the formation of the SG network) are presented. This serves as a benchmark for evaluating the transition toward the SG network implementation. The households' unmet demand and surplus, as well as net power profiles over the simulation period, are illustrated in Figure 5.11 and Figure 5.12, respectively.

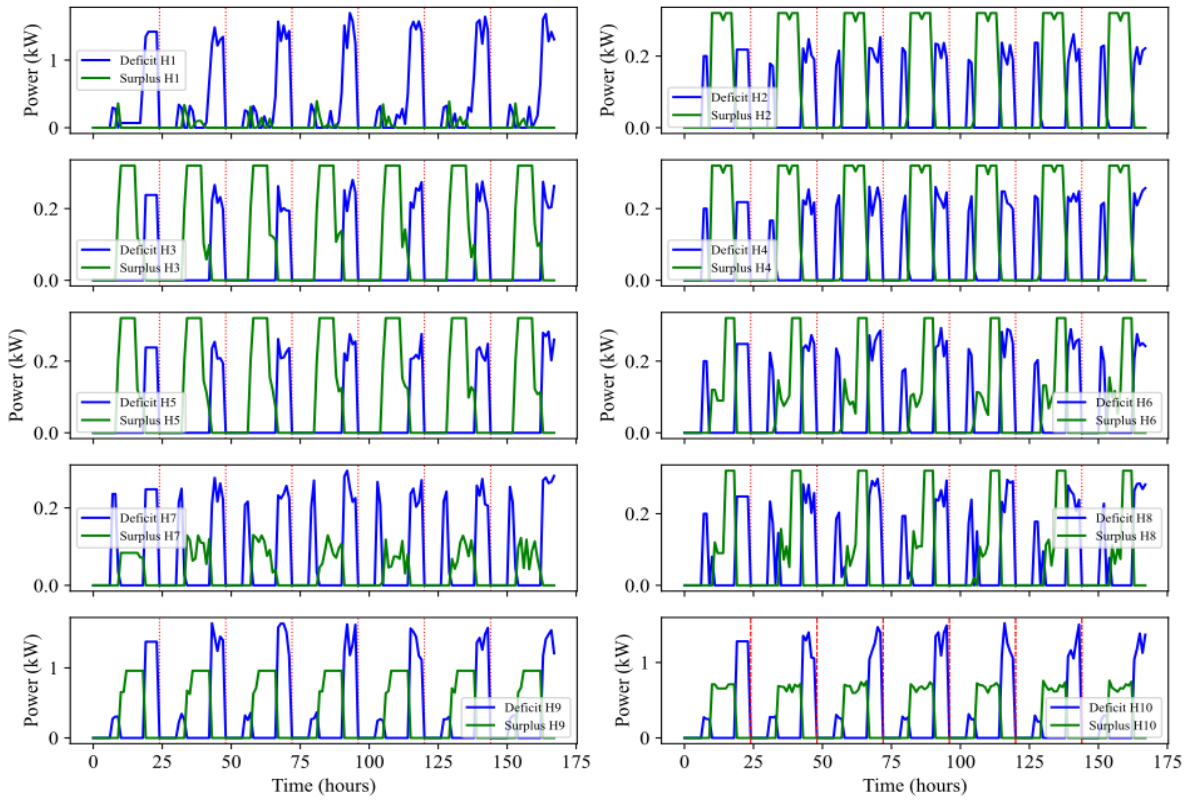

Figure 5.11:Unmet demand and surplus before SG

From these two figures, it is evident that all households experience surplus energy production during the daytime and energy deficits from the evening through the night. The primary difference lies in the duration of the time window during which either surplus or deficit occurs. Household H1 exhibits the shortest surplus production window, whereas Household H3 shows the shortest deficit period.

The aggregated hourly surplus and deficit across all households are presented in Figure 5.13. In this case, the total daily surplus energy amounts to 27.018 kWh, while the total deficit reaches 32.332 kWh. It can also be observed that there are points at which the two curves intersect, indicating the simultaneous occurrence of surplus and deficit across different households which can be shared or traded between houses to reduce the available demand.

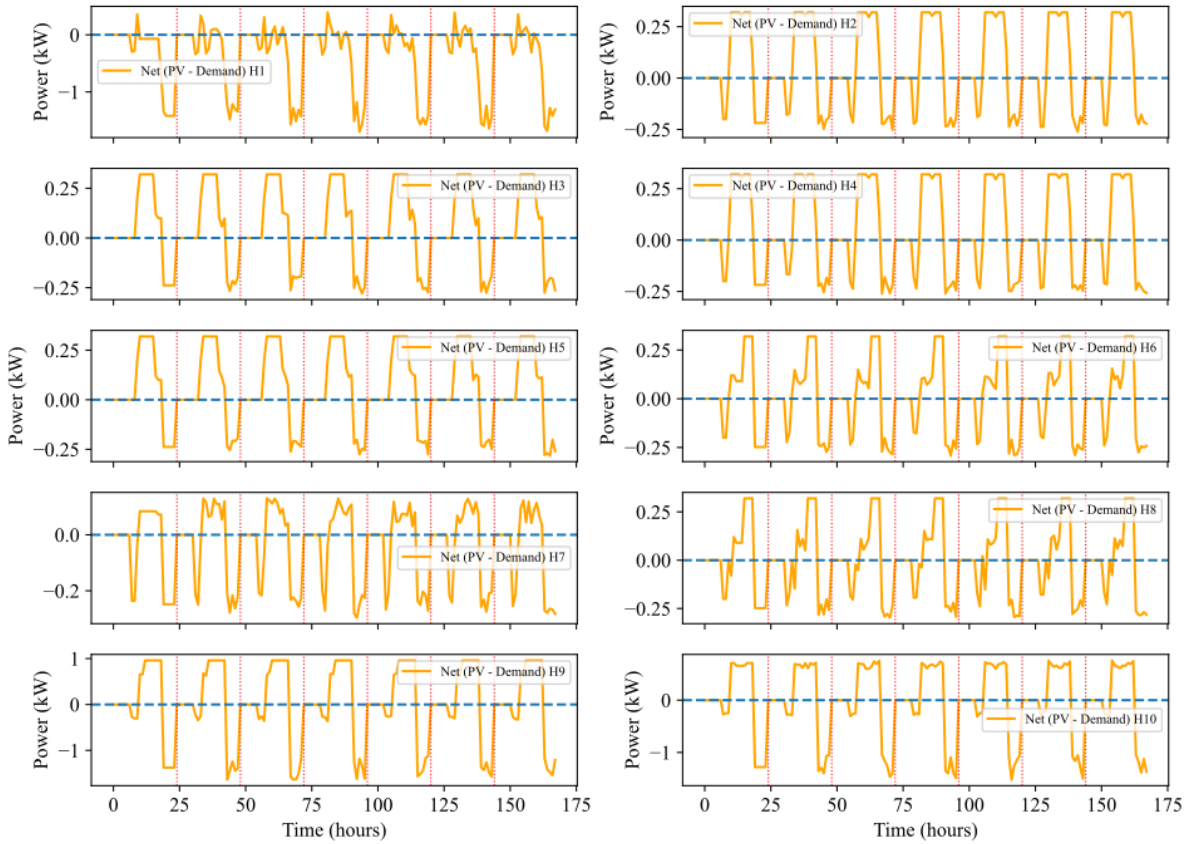

Figure 5.12: Net power profile before SG

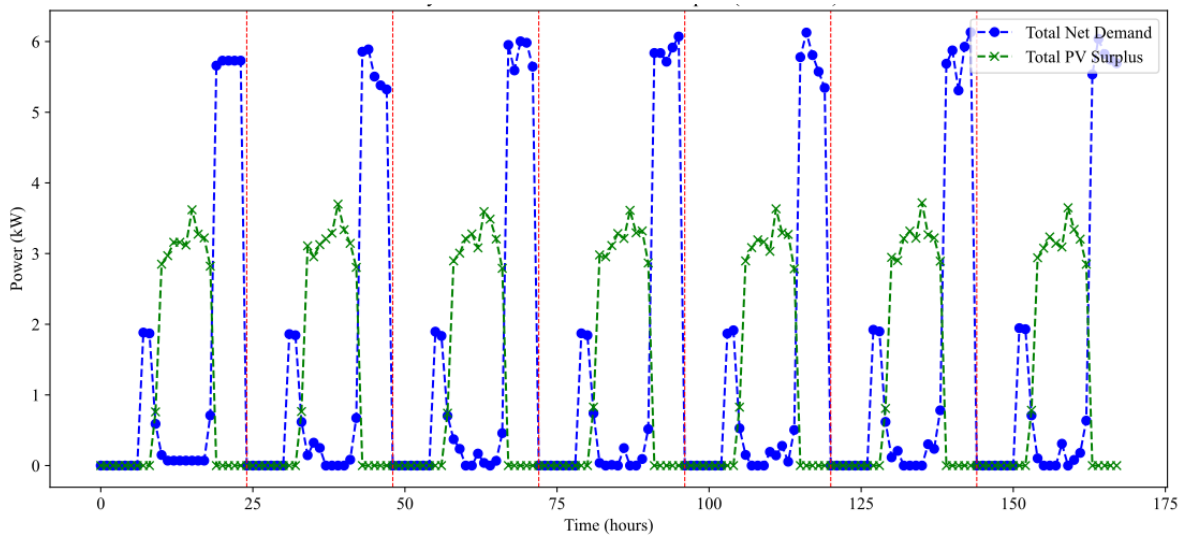

Figure 5.13: Total unmet Demand and Surplus before SG

(b).Optimized Swarm Grid Network

The result in Figure 5.14 shows how the model managed to create a swarm grid consisting of 9 out of 10 households. The household number 8 was not connected due to high deployment cost required for it to be in the grid. The model yields the minimum achievable cost with optimal levels of deficit and surplus production, enabling the efficient deployment of the SG

network with a well-defined connection pattern. Demand and supply status and analysis on the deployed grid was then conducted to determine how much is the reliability and stability of the network.

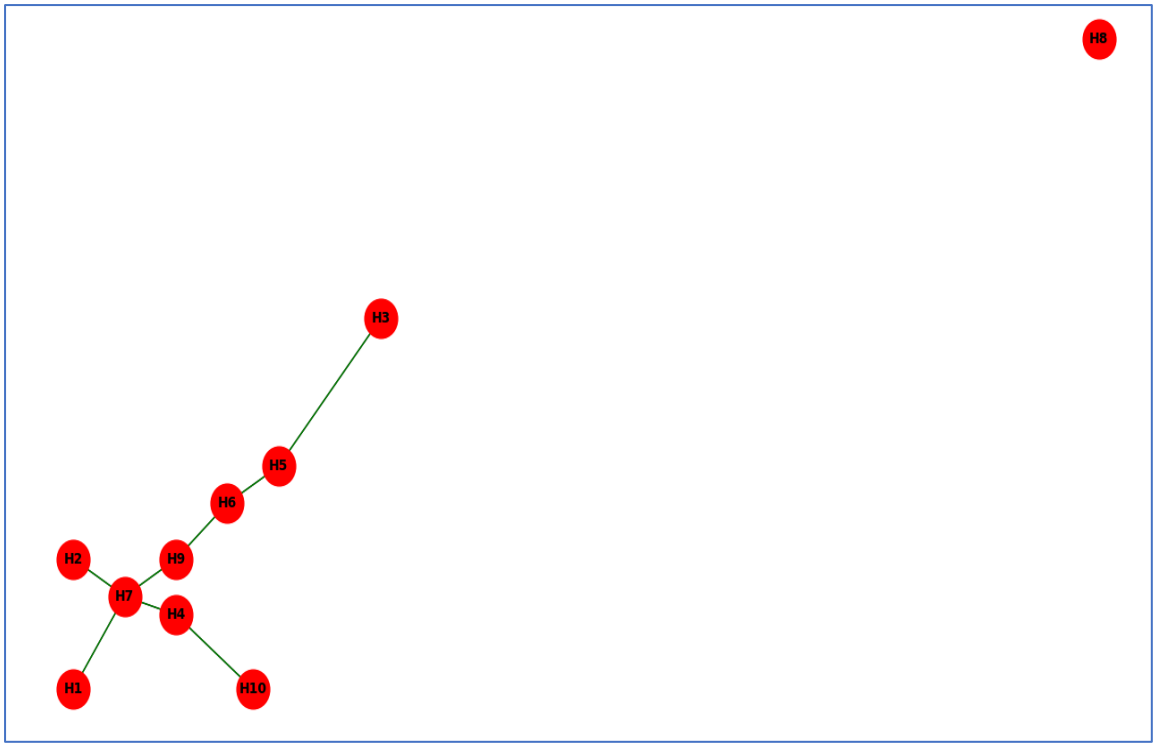

Figure 5.14: Optimized Swarm Grid (SG) Network layout

Figure 5.15 and Figure 5.16 show that the battery energy levels sometimes supply energy to the grid and at other times extract energy from it, which represents the expected operational behaviour of batteries within swarm grid networks. A prominent pattern can be observed during the day, when solar power generation is abundant. During this period, all batteries charge toward their maximum energy capacity, and no discharging occurs. From evening onward, when solar generation is no longer available, the batteries begin to discharge to supply the loads present in the network until when the batteries reach their allowable minimum energy limits and are therefore unable to provide further supply. The battery energy profile of household H8 differs from that of the other households because it is not connected to the network; consequently, its operation depends solely on its individual PV generation and demand.

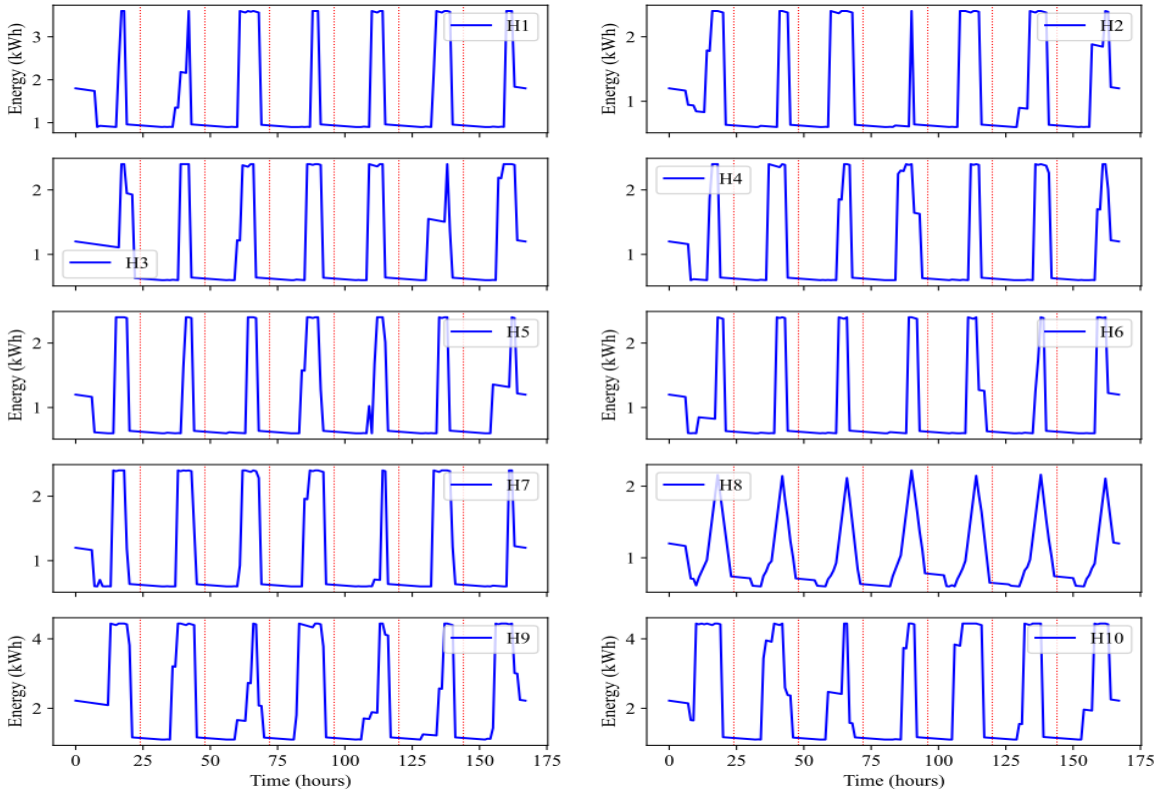

Figure 5.15: Battery energy level over time in SG

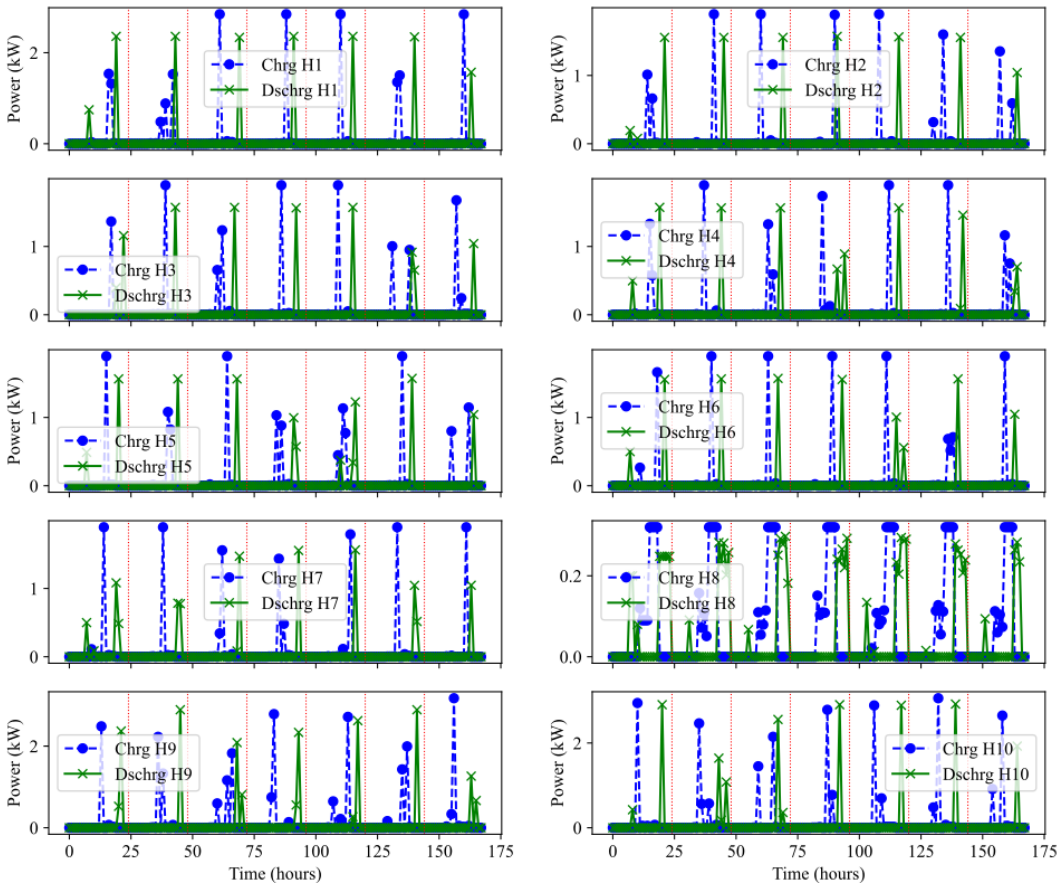

Figure 5.16: Battery charging and discharging in SG

Figure 5.17 and Figure 5.18 present the deficit and surplus energy at both the household level and the aggregated hourly level, respectively. During the afternoon, when solar generation is high, surplus energy is produced within the network which covers the available demands. From around 17:00 hours, household demands are largely met using the energy stored in the energy storage system until approximately 22:00 hours, when the stored energy reaches its minimum allowable limit; this process repeats each day of the week.

All houses except for household H7 have deficit at either late night or morning. The model decided to collect all surplus at household H7 because it's the hub node of the network, as shown in Figure 5.14. Moreover, the daily deficit and surplus is observed to have been highly improved for all households in the SG as compared to the situation before the introduction of SG. The average deficit and surplus for the week are 14.157 kWh and 4.129 kWh, respectively.

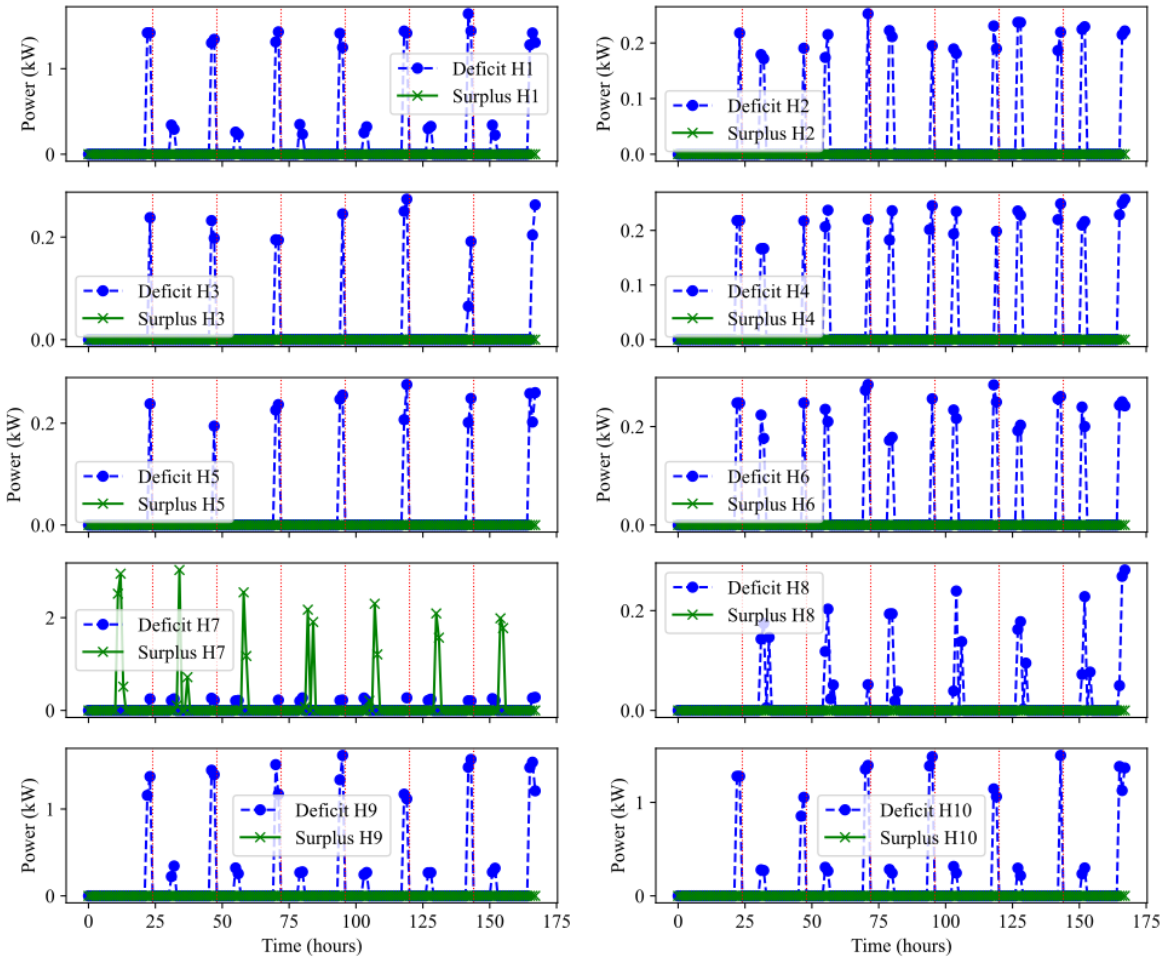

Figure 5.17: Individual Household deficit and Surplus in SG

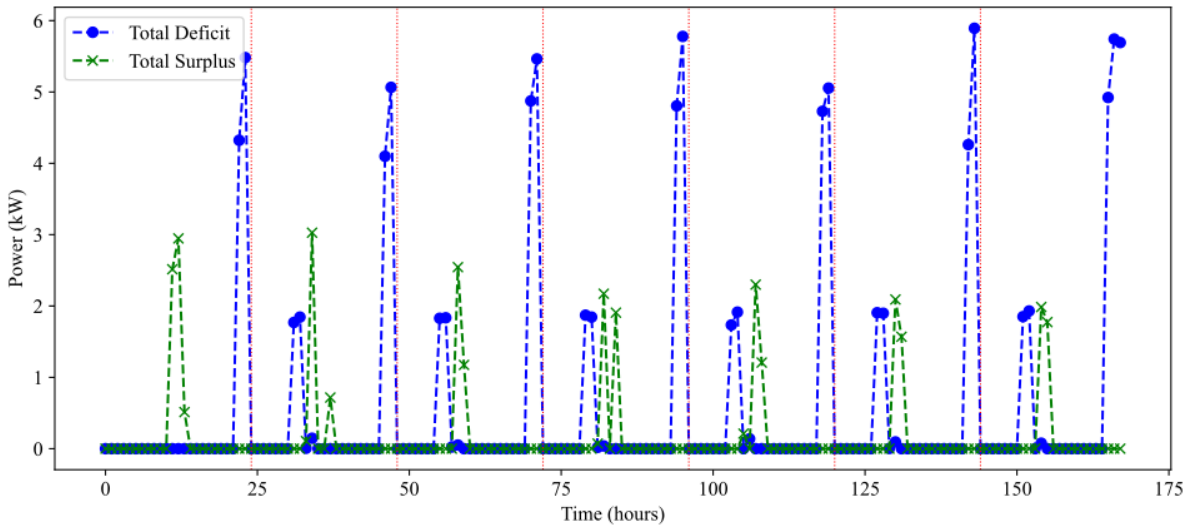

Figure 5.18: Overall deficit and surplus in SG

(c). Sensitivity Analysis

While the previous sections illustrated the system operation before and after the introduction of the SG using the developed model, this section presents a sensitivity analysis of the objective function. Equation (5.1) includes two tuning parameters, *a* and *b*, which weight the penalties associated with unmet demand and surplus generation, respectively. Parameter *a* represents the penalty cost assigned to unserved energy, thereby prioritizing household connectivity and demand satisfaction. Parameter *b*, on the other hand, represents the penalty associated with excess generation or inefficient energy utilization.

To evaluate the influence of these parameters, *a* and *b* were varied systematically, and the resulting number of connected households was recorded, as shown in Figure 5.19. The results indicate that increasing *a* significantly increases the number of connected households. This occurs because a higher penalty on unmet demand forces the optimizer to allocate available generation capacity more aggressively toward serving additional households, even if it requires higher infrastructure utilization. In contrast, variations in *b* produce only a moderate effect on connectivity. This suggests that surplus energy management is less critical to network expansion decisions than demand satisfaction under the studied conditions.

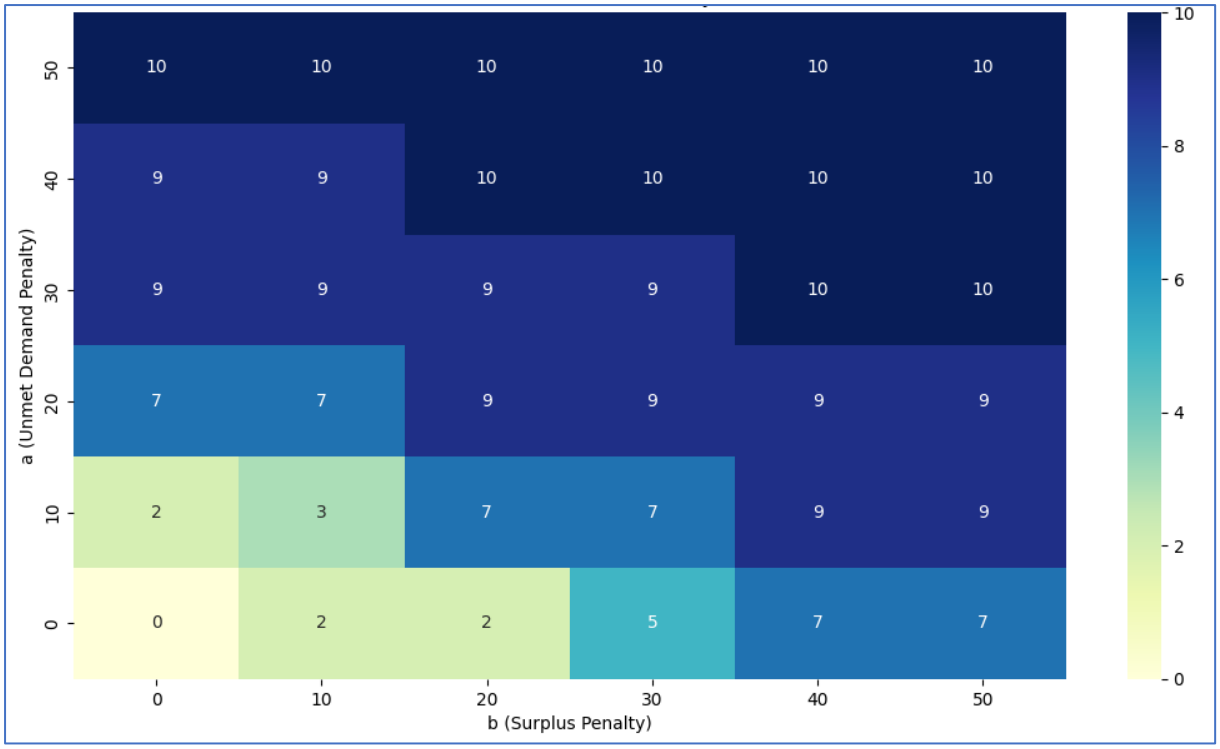

Figure 5.19: Sensitivity of the Model to the tunning parameters

When $(a, b) = (0,0)$, meaning that no penalties are imposed for surplus energy or unmet demand, the resulting configuration corresponds to isolated systems resembling individual Solar Home Systems (SHS), as illustrated in Figure *5.9*. As the penalty values increase, households begin to connect with neighbouring houses to reduce the costs associated with energy deficits and surplus generation, although this occurs at the expense of higher deployment costs. The first inter-house connection appears at $(a, b) = (10,9)$(Figure *5.20*). Further increases in the penalty parameters lead to progressively denser network configurations, with the structure shown in Figure *5.14* emerging at $(a, b) = (20,20)$, and full connectivity across the sample village achieved at $(a, b) = (30,40)$, as presented in Figure *5.21*

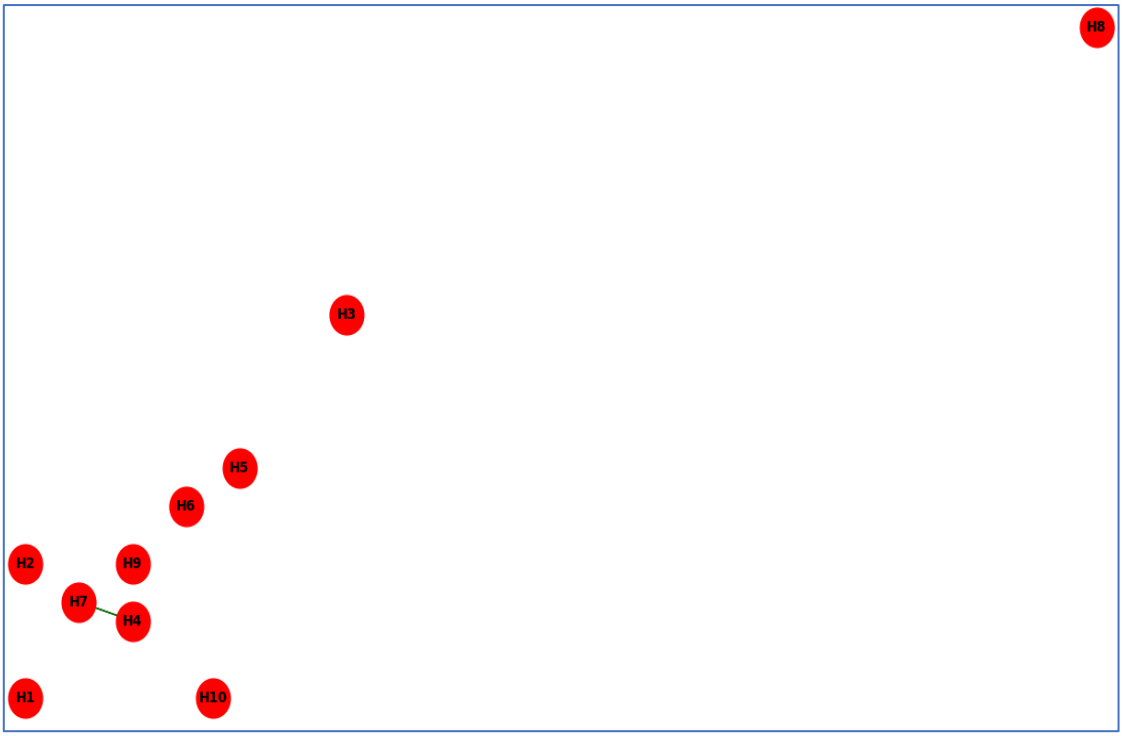

Figure 5.20: First connection between Houses, occurred at (a, b) = (10,9)

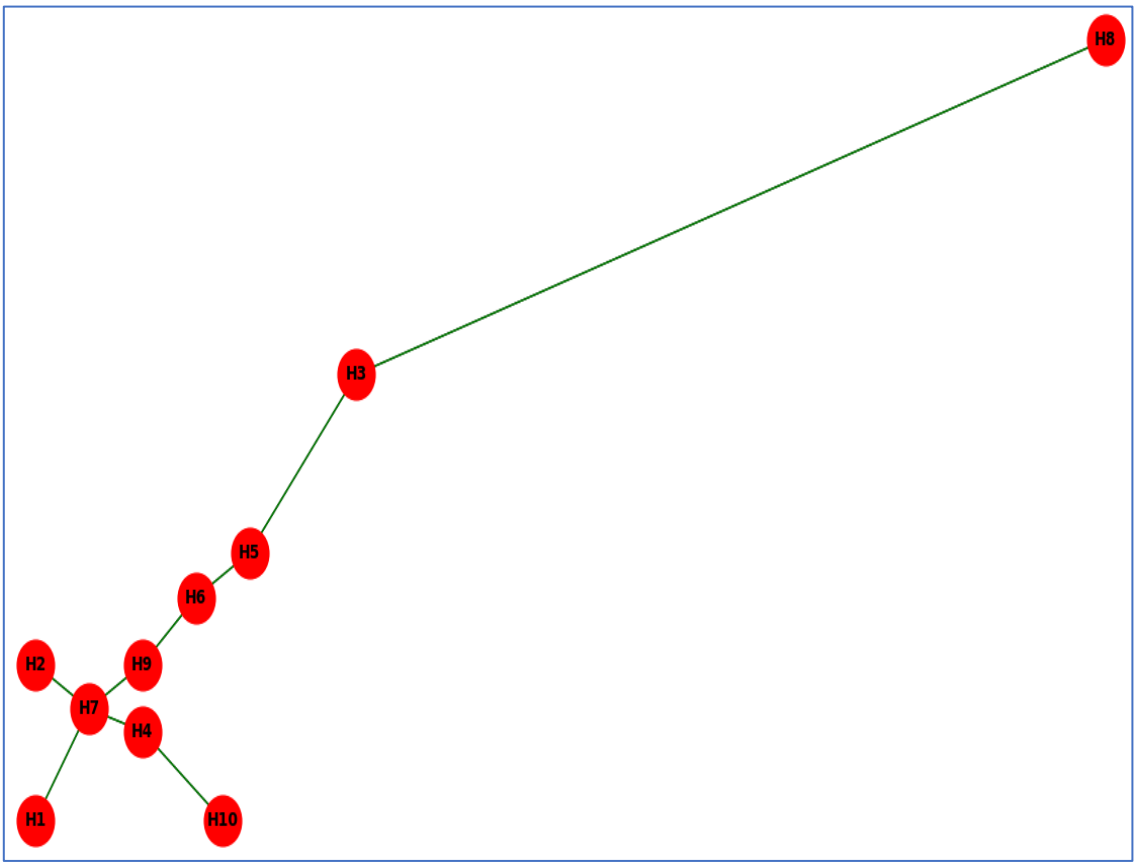

Figure 5.21: Fully connected of the village sample, occurred at (a, b) = (30,40)

Overall, the sensitivity analysis show that the model is particularly responsive to the weighting of unmet demand. The choice of parameter *a* therefore plays a crucial role in determining network connectivity and overall system performance. From a planning perspective, this implies that policymakers and system designers must carefully select penalty weights to reflect their priorities-whether maximizing household access or optimizing energy efficiency-since these choices directly influence the resulting network configuration.

(d).Grid stability Control – Introduction of ESS

To ensure the SG is stable as previously explained, here the simulation results for the two approaches discussed in section 5.3 are presented. The charging and discharging of the centralized battery are presented in Figure 5.22. In Figure 5.23 the energy levels of the optimal centralized ESS is presented, in which the maximum energy maximum is around 17.22 kWh (according to simulated value) and the minimum energy is zero. Practically the ESS cannot be discharged to its zero value, hence taking this into consideration using the depth of discharge (DoD) of 75%, the required optimal capacity value is approximately 24 kWh.

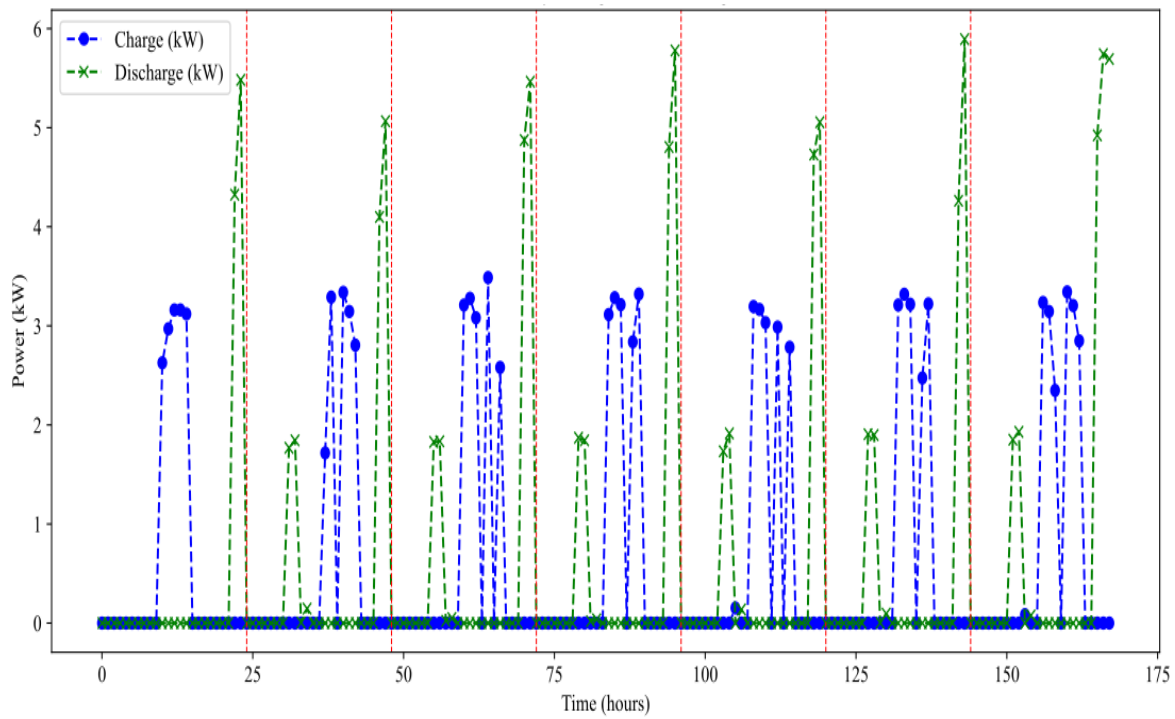

Figure 5.22: Charging and Discharging of the Centralized ESS

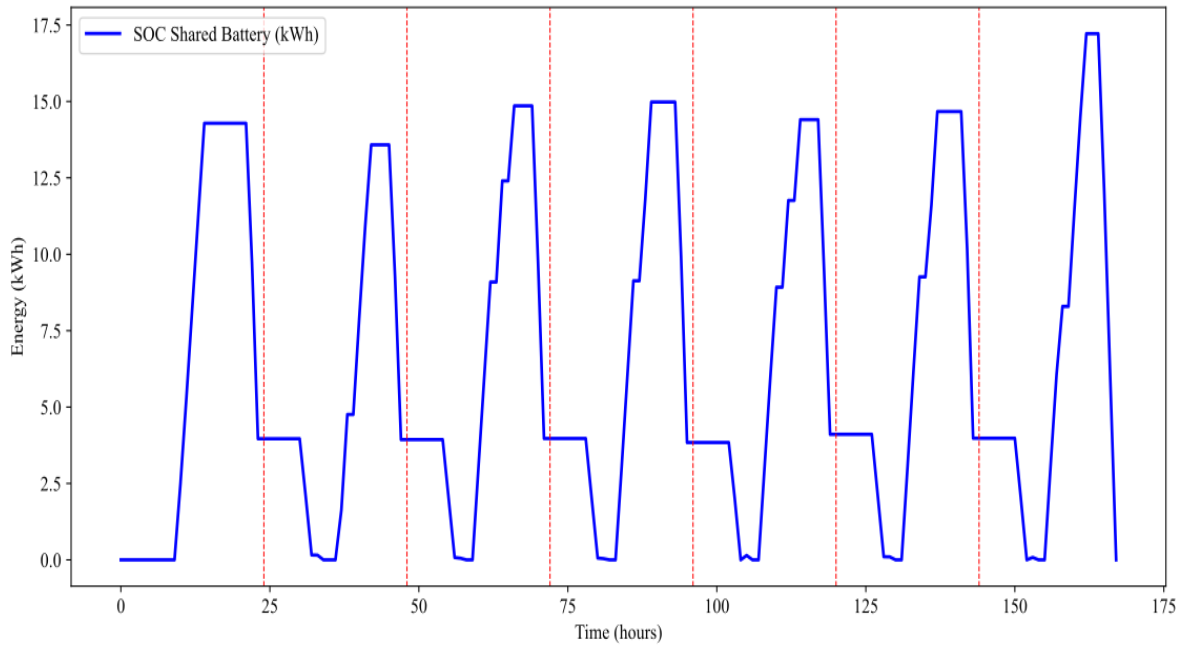

Figure 5.23: Energy levels of the Centralized ESS

To validate the size of the centralized Energy Storage System (ESS), the optimal placement model was first applied to determine the most suitable location for its installation. The optimization results identified house number 7 as the optimal location for placing the centralized ESS. The SG was subsequently simulated with the integrated ESS to evaluate its operational performance within the network.

As illustrated in Figure 5.24, the ESS exhibits an expected charging and discharging pattern, charging predominantly during daytime hours when photovoltaic (PV) generation is high and discharging during the evening and night periods when demand increases and PV generation is unavailable. Consequently, the centralized ESS was able to fully compensate for the energy deficits observed across the houses within the grid, as shown in Figure 5.25.

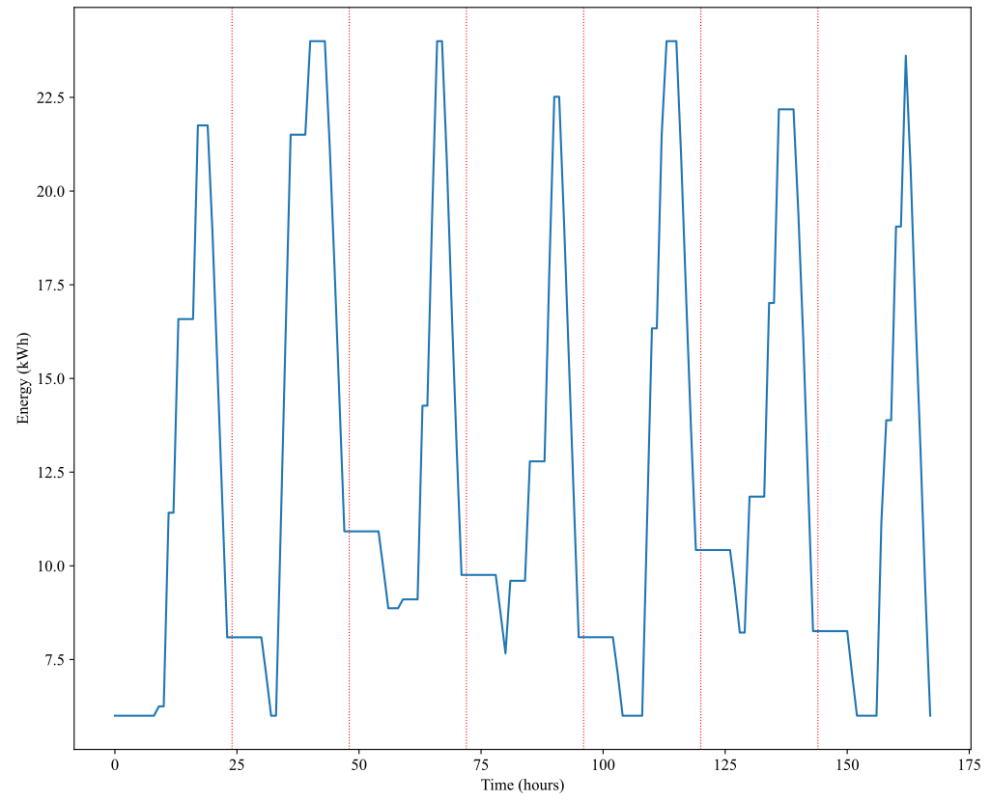

Figure 5.24: Energy Storage status in ESS

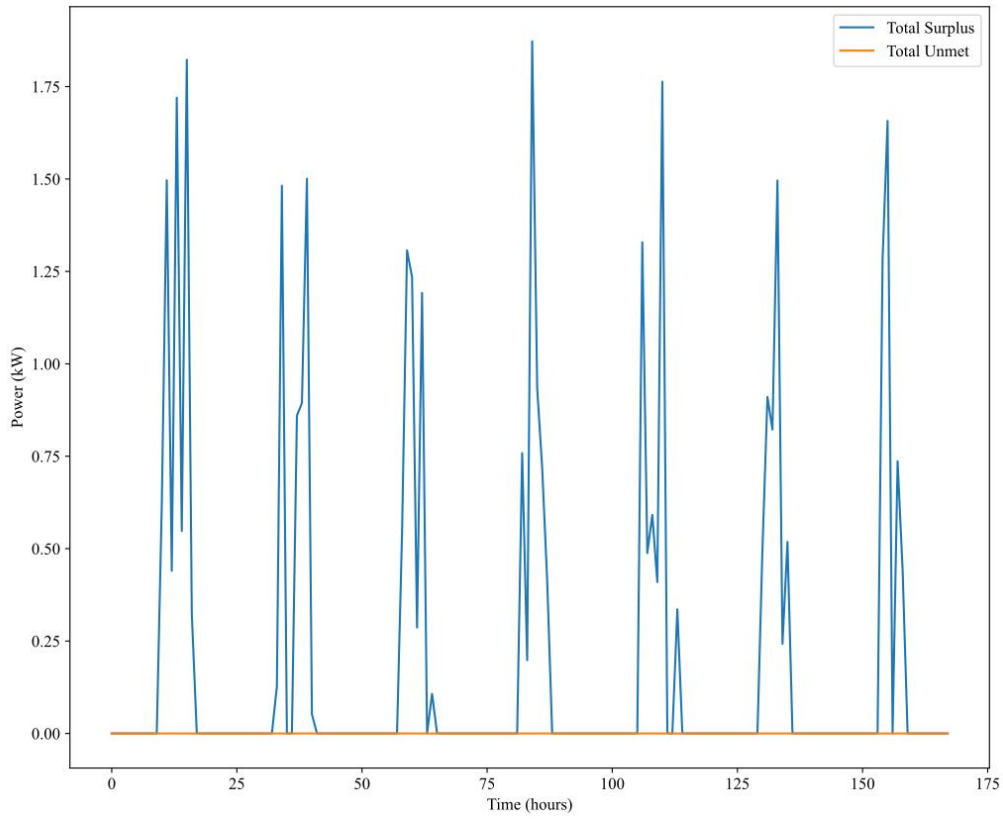

Figure 5.25: Overall surplus and Deficit in SG with ESS

Despite this improvement in deficit mitigation, surplus energy remains at house number 7. Since this is now a larger node, the model tends to consolidate the surplus there, as indicated in Figure 5.26. This residual surplus could potentially be utilized by introducing small additional loads at the respective households, thereby improving the overall energy utilization within the system.

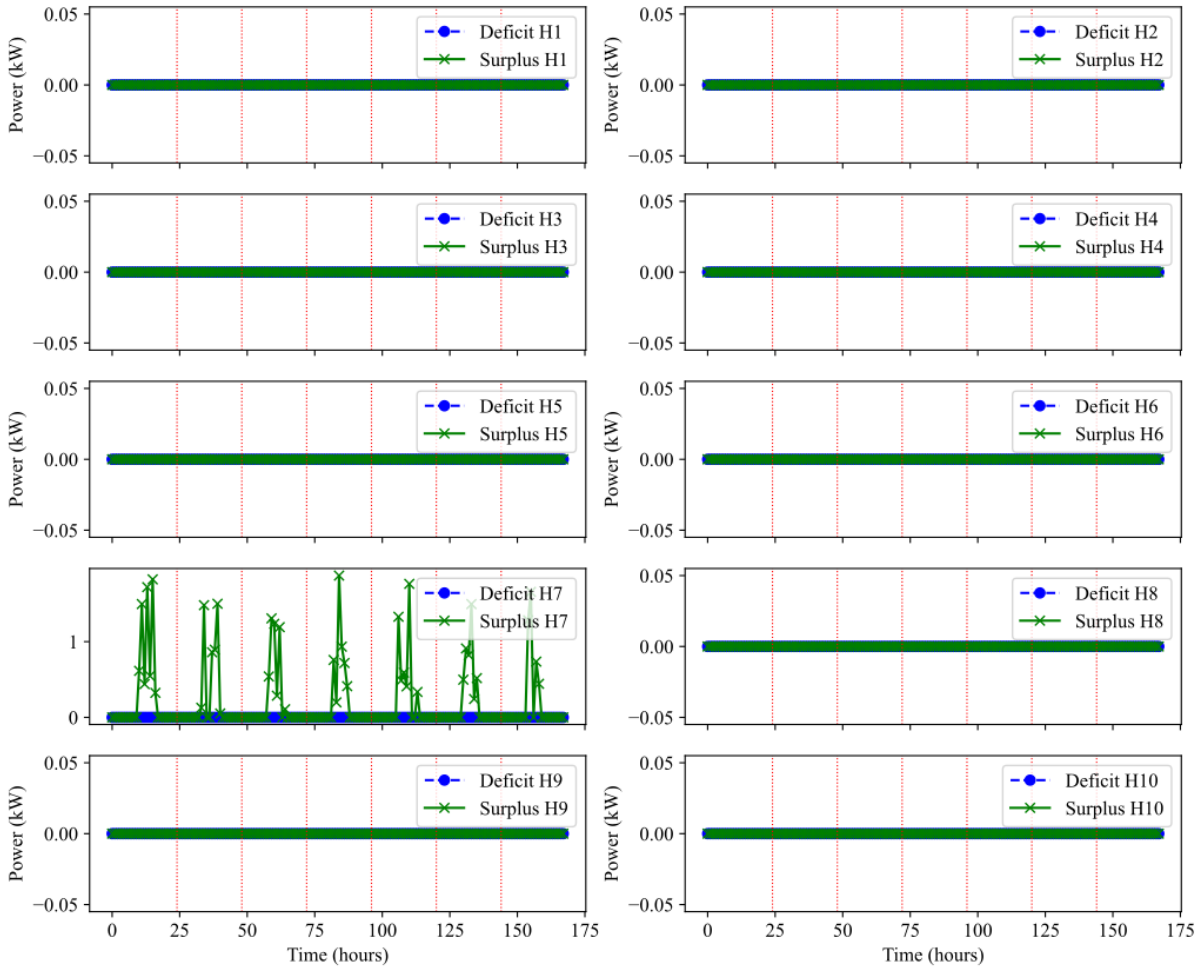

Figure 5.26: Deficit and Surplus in SG with ESS

State of energy in each house's battery was observed to be smooth as per the case of SG without ESS indicating that the introduction of centralized ESS did not affect the operation of the individual batteries but the deficit, see Figure 5.27. Also, the household batteries were normally charged and discharged during the day and day, respectively as illustrated in Figure *5.28*.

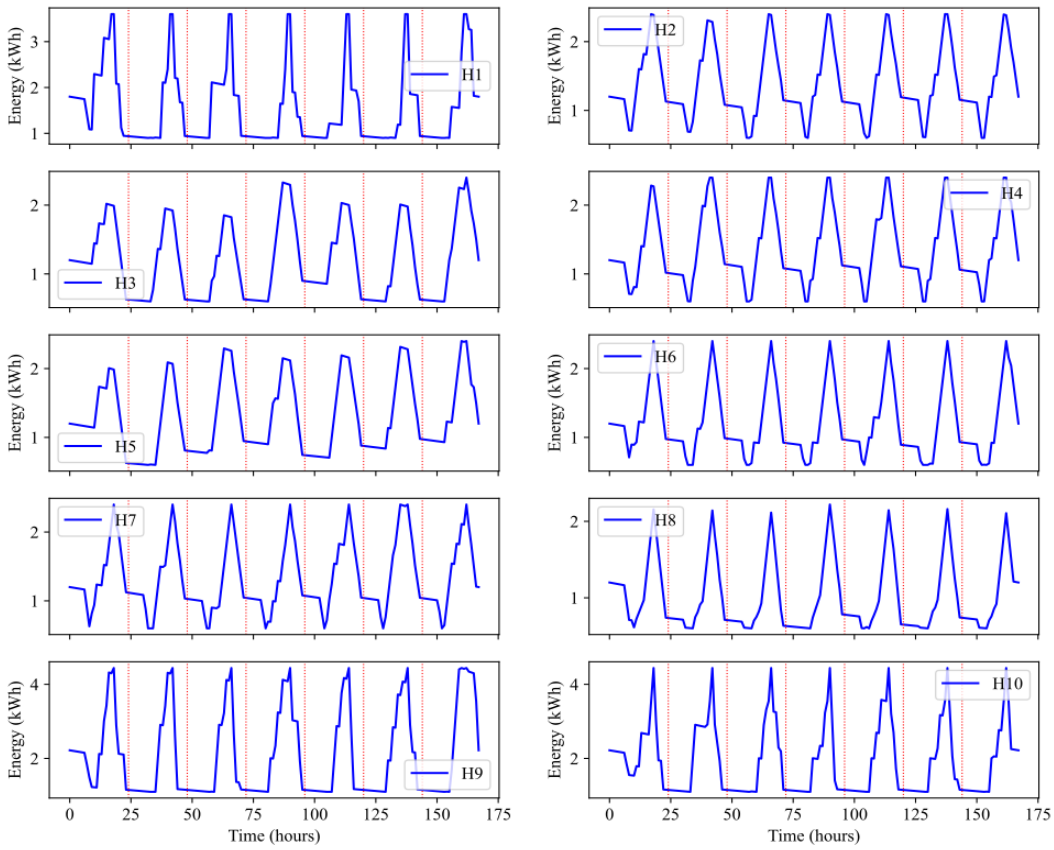

Figure 5.27: Energy level in each household batteries

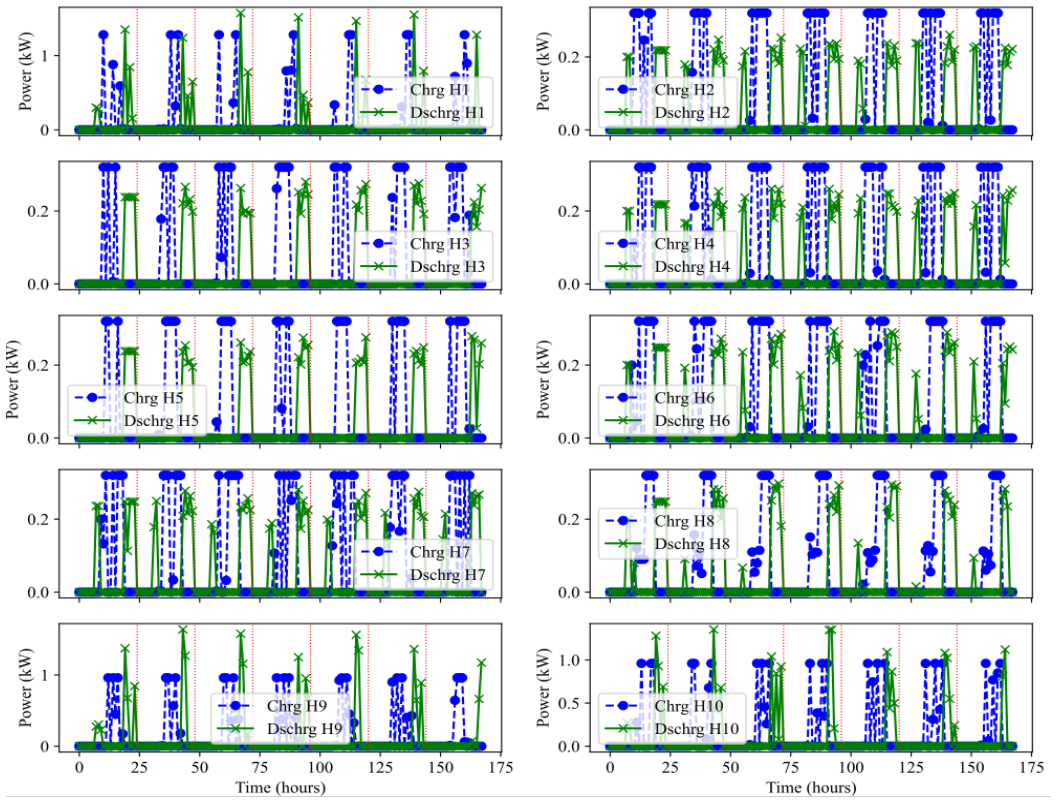

Figure 5.28: Battery charging and discharging at each house

(e). Grid stability Control – Introduction of DSM

Again, the other mechanism used to ensure stability and reliability of the grid is the introduction of demand side management (DSM). In this section the impact of applying DSM on the generated SG network are presented. The DSM applied is called load shifting that involve incentivizing users from shifting their loads. At First the total demand and supply availability in the network are calculated and presented in Figure 5.29. To match the demand and supply so that to reduce energy deficit the load shifting was performed using high penalty for not meeting the demand. Figure 5.30 illustrates the combination of the original and shifted demand while Figure 5.31 shows the original demand, shifted demand and PV supply.

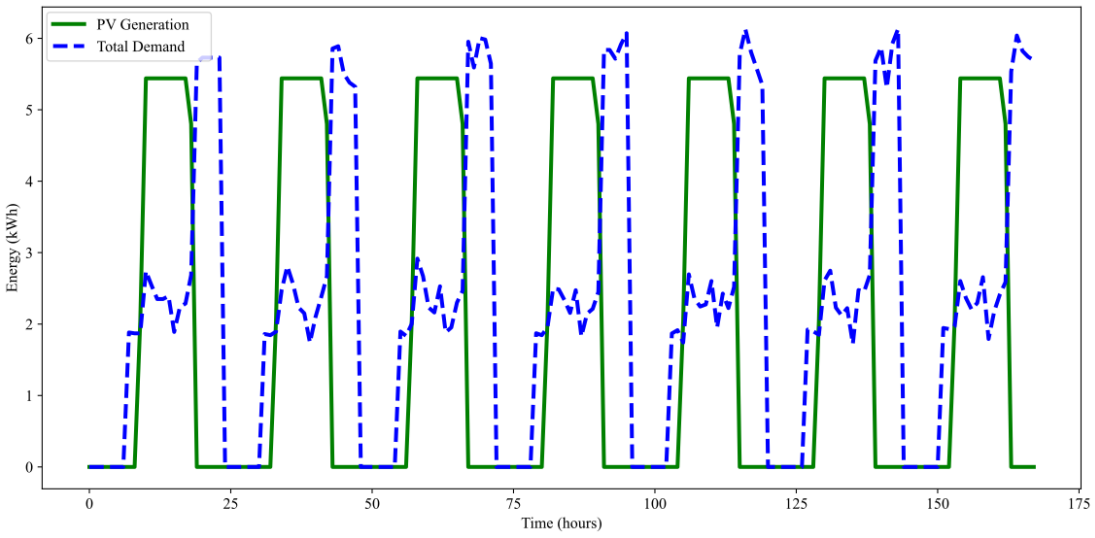

Figure 5.29: Total Demand and Supply in the entire Village

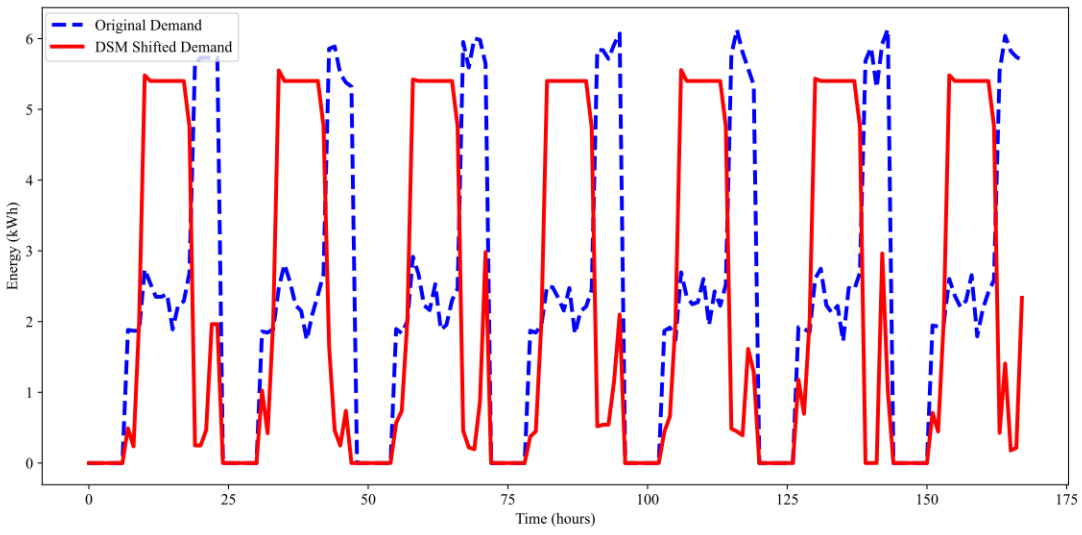

Figure 5.30: Original and Shifted Demand

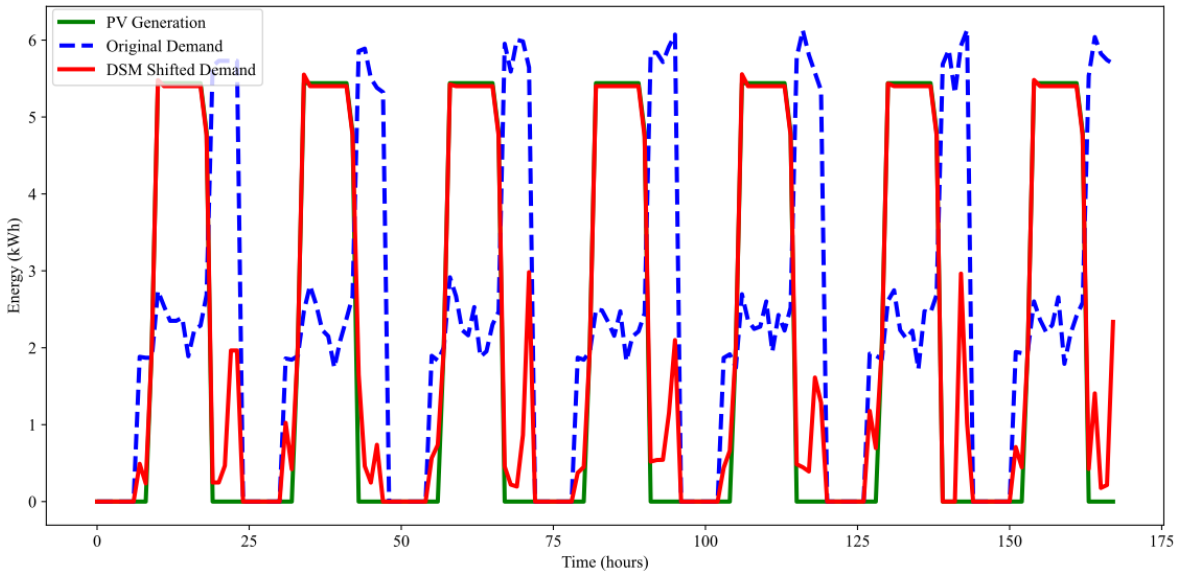

Figure 5.31: Supply (PV), Original and Shifted Demand

As shown in Figure 5.31 after most of the demand is shifted to periods of high PV production (i.e., daytime), the total unmet demand is significantly reduced to a daily average of 6.203 kWh, as illustrated in Figure 5.29. Similarly, the entire PV supply is effectively utilized, resulting in zero surplus.

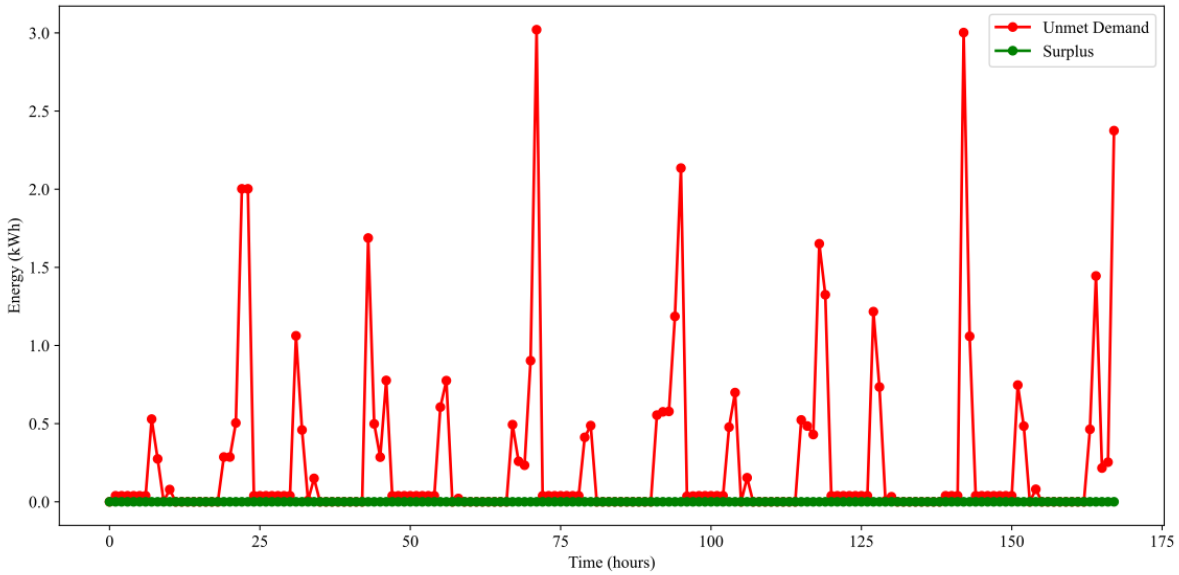

Figure 5.32: Deficit and Surplus after introduction of DSM

5.5.3 Discussion

The simulation results demonstrate that the introduction of the Swarm Grid (SG) significantly improves both surplus energy utilization and unmet demand reduction at the household and

network levels. Prior to SG implementation, the coexistence of substantial midday surplus generation and evening unmet demand highlights a well-documented challenge in decentralized photovoltaic (PV) systems: the temporal mismatch between generation and consumption. This phenomenon has been widely reported in off-grid solar home systems (SHS), where peak solar production occurs at midday while peak household demand typically arises in the evening hours, as discussed by Mandelli et al. (2016) and Bhattacharyya (2012)

After the introduction of the SG, the daily average deficit decreased from 32.322 kWh to 14.144 kWh equivalent to 56.2% improvement. Similarly, the daily average surplus dropped from 27.326 kWh to 4.119 kWh equivalent to 84.9%. These findings are consistent with the broader literature on peer-to-peer energy sharing and community microgrids, which shows that interconnected systems improve reliability and resource utilization through spatial aggregation of demand and generation diversity (Parag & Sovacool, 2016; Tushar et al., 2020). Similarly, Mengelkamp et al. (2018) on cooperative microgrids report that inter-household energy exchange reduces both curtailment and load shedding by leveraging diversity in demand profiles and storage states. Table 5.5 presents the detailed daily unmet demand and surplus before and after the introduction of the SG.

Table 5.5: Deficit and Surplus - Before and After SG

	Before SG		**After SG**	
Day	**Total Deficit (kWh)**	**Total Surplus (kWh)**	**Total Deficit (kWh)**	**Total Surplus (kWh)**
1	32.429	27.018	9.8053	5.9749
2	31.924	28.165	12.9298	3.8505
3	33.783	25.067	14.0758	3.7184
4	32.783	27.017	14.3571	4.1497
5	31.687	28.005	13.5699	3.717
6	31.763	28.006	14.057	3.6597
7	31.882	28.004	20.2152	3.7602

The fact that no household experienced increased unmet demand after joining the SG is particularly noteworthy. In some decentralized energy trading models, poorly coordinated sharing can negatively affect certain participants and cause a potential of such scenario in the network (Sousa et al., 2019). However, the present results indicate that accurate demand forecasting and coordinated dispatch within the SG prevented adverse redistribution effects.

This supports arguments in the literature that information transparency and coordinated control mechanisms are critical for equitable peer-to-peer energy systems (Zhang et al., 2017).

Nevertheless, the persistence of unmet demand after SG implementation underscores the structural limitation imposed by insufficient storage capacity or proper demand side management strategy. The simultaneous presence of midday surplus and night-time deficits confirms that interconnection alone cannot fully resolve temporal imbalances. This finding is in line with Luthander et al. (2015), who emphasize that while spatial aggregation improves balancing across users, temporal balancing requires either additional storage capacity or demand-side flexibility.

Furthermore, from a system design perspective, two principal strategies emerge to deal with such a challenge: increasing storage capacity or introducing demand-side management mechanisms. While expanding battery storage seems to be a direct technical solution, studies show that storage expansion may become economically inefficient under growing demand due to high capital costs and diminishing marginal returns (Zakeri & Syri, 2015). In this study a model for determination of energy storage system (ESS) capacity was developed and applied in the case study. The ESS capacity was found to be around 24 kWh. This support concern of high costs taking into the nature of the village in question where all the participants have their ESS with capacity less than 5 kWh. However, this study has proved that there is an optimal ESS size for the village sample at which there could be no deficit in the SG.

An alternative to introducing energy storage systems (ESS) is the implementation of demand side management (DSM), which can shift loads to periods of peak generation. In this study, an incentive-based load shifting approach was employed to move consumption to high-generation periods. The approach is like time-of-use and real-time pricing schemes, helps to reduce peak deficits without requiring a proportional increase in storage capacity, as discussed by Albadi & El-Saadany (2008). The load shifting has shown much improvement in the system stability from the system deficit of 32.322 kWh to 6.141 kWh equivalent to 81% while the surplus is recued to zero. Table 5.6 presents details for the daily surpluses before and after application of the two grid stability measures.

Table 5.6: Daily deficit and Surplus in SG with and without Stability measures

Day	Normal SG		SG with ESS		SG with DSM	
	Total Deficit (kWh)	Total Surplus (kWh)	Total Deficit (kWh)	Total Surplus (kWh)	Total Deficit (kWh)	Total Surplus (kWh)
1	9.8053	5.9749	0	6.965	6.198	0
2	12.9298	3.8505	0	4.915	5.236	0
3	14.0758	3.7184	0	4.668	6.581	0
4	14.3571	4.1497	0	4.894	6.198	0
5	13.5699	3.717	0	4.916	6.009	0
6	14.057	3.6597	0	4.487	6.435	0
7	20.2152	3.7602	0	4.119	6.333	0

According to the discussion above, using penalties (which basically costs) for surplus and demand, introduction of the ESS and application of DSM none of them has guaranteed both cost effectiveness and network stability. This is in line with the No Free lunch theorem whenever there is more than one variable of consideration. The combination of the three approaches is then encouraged for cost effectiveness and network stability. By inspecting Table 5.6, it is can easily be deduced that once the combination of the three approaches is applied the optimal centralized battery required would be 8.8 kWh. However, depending on which aspect needs to be addressed much, one could choose among the three approaches.

The sensitivity analysis further strengthens the interpretation of the model's behaviour. The stronger responsiveness to parameter *a* (penalty for unmet demand) compared to *b* (penalty for surplus energy) reflects real-world rural electrification priorities, where reliability and energy access typically outweigh efficiency considerations. Service reliability is widely recognized as a primary determinant of user satisfaction and productive energy use (Bhattacharyya, 2012; Tenenbaum et al., 2014). Contextually, the coefficient *a* can be interpreted as the socio-economic cost of electricity shortages. In households engaged in productive activities, the value of lost load corresponds to forgone income, as emphasized in the productive uses of energy. Conversely, coefficient *b* represents the cost associated with surplus energy management, including battery degradation and storage investment costs. Calibrating *a* and *b* based on local diesel generation costs, SHS expansion costs, or battery replacement costs therefore enables the model to reflect realistic socio-economic trade-offs.

Overall, the findings of this study align with existing microgrid and peer-to-peer energy sharing approaches, confirming that SHSs interconnection to form an SG enhances both efficiency and

reliability in decentralized PV systems. However, they also reinforce the consensus that interconnection alone cannot eliminate deficits without complementary storage or demand-side strategies. The proposed modelling framework thus contributes to ongoing research advocating integrated approaches that combine spatial energy sharing, storage optimization, and economic incentives for sustainable rural electrification.

5.6 Chapter Summary

This chapter aimed to develop a planning and design tool for the deployment of swarm grids to help mitigate energy access challenges in underserved areas. The tool consists of a mathematical optimization model integrated within MS Excel.

The model incorporates both investment and operational costs, as well as local technical parameters. A Gurobi-based optimization model was developed to determine the optimal network layout, followed by a grid stability analysis. Simulation results showed that the developed model was able to generate an optimal network configuration while reducing total unmet demand by 56.2% and surplus production by 84.7%. However, the coexistence of surplus energy and unmet demand highlighted the need for additional stability control measures, such as increasing storage capacity or introducing demand side management (DSM) mechanisms.

To address this issue, a model for determining the optimal size of an energy storage system (ESS) was developed and tested. The results showed significant improvements in reducing both energy deficit and surplus; however, the required ESS capacity was relatively large, leading to high investment costs. Alternatively, a load-shifting DSM model was developed and implemented. The DSM approach demonstrated considerable improvement in managing surplus energy, although some level of unmet demand persisted.

Overall, the results indicate that while both ESS and DSM approaches improve system performance, achieving an optimal balance between reliability and cost may require a coordinated combination of storage solutions and demand-side management strategies.

Moreover, the sensitivity analysis revealed that the developed network optimization model is more responsive to changes in the unmet demand penalty (a) than to the surplus penalty (b). These results indicate that electricity demand is the primary driver for establishing grid interconnections, whereas the utilization of surplus energy largely depends on the availability of PV generation and energy storage capacity.

Chapter 6: CONCLUSION AND FUTURE WORKS

6.1 Overview

This chapter summarizes the key outcomes of the study, highlights the main scientific contributions, discusses challenges encountered during the research process, and outlines possible directions for future work. The study aimed to develop a smart transceiver for swarm grid implementation and design a planning and deployment tool for optimized rural electrification using renewable energy resources.

6.2 Main Contributions

The scientific contribution of this study can be categorized into two main areas:

6.2.1 Smart Energy Transceiver Development

A Smart Energy Transceiver was developed to enable efficient energy dispatch within the swarm grid. The transceiver utilizes LoRa wireless communication technology, which provides reliable long-range communication suitable for rural environments at a low operational cost.

Key features include:

- Real-time sensing of household energy status and adaptive response capabilities.
- Energy exchange reports for billing and monitoring.
- Reconfigurability for deployment in other isolated renewable systems such as mini-grids and micro-grids, with potential applications in demand-side management (DSM).

By leveraging LoRa, the transceiver avoids high communication costs associated with GSM or other commercial networks, offering a scalable and cost-effective solution for rural electrification.

6.2.2 Swarm Grid Planning and Deployment Tool

An innovative swarm grid planning and deployment tool was developed to assist swarm grid implementers in designing optimized network layouts based on: - Energy generation and demand Patterns, Separation between SG participants, Material specifications and costs, and Network stability requirements.

The tool was integrated with Microsoft Excel, making it user-friendly and accessible even for non-experts. It also includes sensitivity analysis features that evaluate how changes in costs

affect the number of connected nodes in forming a swarm-grid network. Additionally, a swarm-grid stabilization mechanism has been proposed to ensure stable grid operation.

6.3 Comparison with Existing Literatures

The results and methodological approach of this study were compared with those from previous works, notably (Unger & Kazerani, 2012), (Groh et al., 2014) and (Kirchhoff, 2015).

In Unger & Kazerani (2011), all houses within a village were assumed to be interconnected, without considering deployment costs, operational costs, or power losses. In contrast, the present study incorporates material costs and accounts for power losses in the deployment of the swarm grid, while a smart, low-cost transceiver helps keep operational costs low.

Groh et al. (2014) acknowledged their inability to quantify how inter-house connections reduce surplus energy. This study addresses that limitation by providing both graphical and numerical analyses that demonstrate how surplus energy can be redistributed to meet existing demand within the network, followed by an evaluation of network stability after deployment.

While Kirchhoff (2015) proposed a model to estimate rural electrification costs using aerial imagery and demand forecasts, this work advances that approach by employing real-world field data to develop a practical and data-driven optimization tool for rural grid planning.

6.4 Answers to Research Questions

The study sought to answer the following key research questions:

i. How can a smart transceiver for swarm grid implementation be developed using a communication technology suitable for rural settings?

   The study demonstrated that a smart transceiver can be developed using LoRa communication technology to transmit control information. LoRa offers low cost, strong security, low noise, long range, and low power consumption, making it well suited for rural environments. The transceiver design incorporates energy-efficient protocols to ensure continuous operation with minimal maintenance while supporting energy trading and sharing within the swarm grid. With the developed transceiver, low-cost operation and maintenance of the swarm grid are ensured. The design and performance evaluation of the transceiver are presented in Chapter 4.

ii. How can a solar swarm grid be planned under consideration of investment and operation costs as well as local specifications?

a. Which tools are applicable for effective and efficient deployment of solar swarm grids?

Optimization and simulation tools such as Gurobi for network optimization and Python-based modelling frameworks were identified as highly effective. These tools enable planners to evaluate multiple configurations, analyse energy flows, and determine the optimal placement of energy storage and distribution lines under both cost and technical constraints. In this study, a Python-based model using mixed-integer linear programming (MILP) was developed and evaluated, as presented in Chapter 5.

b. How to integrate the tool with common computer application program, enabling easy interaction and use by novice?

The developed tool has been integrated into MS Excel for data input and output. The integration has been done using the Visual Basic Application (VBA). This approach allows users without deep programming knowledge to perform scenario analysis, visualize and adjust planning parameters conveniently. Detailed integration processes have been presented in Chapter 5.

6.5 Future Work

While the proposed transceiver and swarm grid planning tool demonstrated effectiveness under simulated and laboratory conditions, real-world deployment would introduce additional challenges such as: Dynamic communication delays, Real time varying household load profiles, and potential system adversarial behaviours. Future research may extend this work by:

- Integrating dynamic pricing mechanisms inside the developed transceiver to reflect real-time process and enable demand-side management.
- Developing the real village model and conduct optimal network deployment followed by installation of the developed transceiver to get understanding of combining the two.
- Applying machine learning-based anomaly detection for fault prediction and adaptive control in the deployed network
- Conducting laboratory testing of the transceiver using at least 10 units, with a time step measured in seconds instead of hours, as used in this study to gain more understanding and observation in the applicability of the transceiver.

- Conducting long-term field trials to evaluate resilience, scalability, and system robustness under diverse rural conditions.

6.6 Conclusion

In summary, this study developed and validated two key innovations: a Smart Energy Transceiver and a Swarm Grid Planning Tool - that together advance the feasibility of decentralized, cost-efficient rural electrification. The integration of communication technology, optimization modelling, and user-friendly deployment tools provides a strong foundation for scalable and sustainable rural energy systems**.** The findings indicate the potential of smart, data-driven, and locally adaptable approaches to enhance energy accessibility and operational efficiency in off-grid communities. However, as this study is based on a single laboratory test and one case study simulation, the results represent only a partial exploration of possible solutions and require further investigation and validation

List of Figures

List of Tables

NOMENCLATURE

The representation used throughout this study is confirmed here for quick reference.

A. Subscripts and Superscripts

i	House number ranging from *1 to N*
j	House number ranging from *1 to N*
k	Cable type connecting the houses, ranging from *1 to K*
d	Design parameter

B. Symbols and Parameters

N	Number of houses in the village
K	Number of cable type required to be installed
C_k	Cost of the cable of type k (TZS/m)
C_c	Capacity of the cable of type c (kW)
$d_{i,j}$	Distance between i-th house and the j-th house (m)
cp	Cost of the pole (TZS/pole)
$mp_{i,j}$	Number of poles required to connect house-i and house-j
$y_{i,j}$	Decision variable to whether the pole between house i and house j is required
$x_{i,j,k}$	Decision variable whether the cable connection between house i and house j using conductor type k is required
f_{ji}	Power flow from house j to house i (W)
f_{ij}	Power flow from house i to house j (W)
B_i	Power supplied by battery of house i (W)
PV_i	Power supplied direct from the solar Photo Voltaic of house i (W)

D_i	Electrical demand of house i (W)
$S_{i,t}^{bat(chg)}$	Charging of the battery at house i in time t
$S_{i,t}^{bat(dis)}$	Discharging of the battery at house i in time t
$D_{i,t}$	Demand due to load at node i at time t
$P_{i,t}^{D}$	Unmet demand penalty (kW)
$P_{i,t}^{S}$	Surplus penalty (kW)
$S_{i,t}^{pv}$	Supply from the solar PV at node *i* at time *t*
$E_{i,t+1}^{b}$	Stored energy in the battery at node i at time t+1 (kWh)
$E_{i,t}^{b}$	Stored energy in the battery at node i at time t (kWh)
η_c, η_d	Battery charging and discharging efficiency, respectively
β	Battery self-discharge factor
E_i^{bmin}	Minimum allowable battery energy of node i (kWh)
$E_{i,t}^{b}$	Battery energy of node i at time t (kWh)
E_i^{bmax}	Maximum allowable battery energy of node i (kWh)
$C_i^{bat(dis)}$	Maximum battery discharge power (kW)
$C_i^{bat(chg)}$	Maximum battery charging power (kW)
$A_{i,j}$	Element in adjacency matrix drawn from the optimized grid
a and b	Constants values for the unmet demand and surplus production, respectively
Δt	Change in time (h)
t	Time period (h)
$P_{i,d}^{D}$	Design unmet demand penalty for house i (W)

$P_{i,d}^{s}$	Design surplus penalty for house i (W)
ω	Penalty to ensure the deficit is covered by the introduced centralized ESS
$U_{i,t}$	Deficit of house i in time t after introduction of ESS
λ	Cost of the introduced ESS
B	Capacity in kWh of the introduced ESS
$S_t^{PV\_surplus}$	Surplus solar power required to charge the introduced ESS
CB_t^{chg}	Charging of the introduced centralized ESS
CB_t^{dis}	Discharging of the introduced centralized ESS
P_t^{total}	Total unmet demand for the entire grid at time t
$Q_{i,t}$	Amount of demand that can be shifted in house i at time t
c^u	Cost of unmet demand after failing to shift
c^Q	Cost of shifted demand
c^s	Cost for not using surplus energy
$D_{i,t}^{Q}$	Shifted demand in house i at time t
$PV_{i,t}^{use}$	Amount of solar PV energy consumed in house i at time t

C. Acronyms and Abbreviation

HHs	House Holds
SHSs	Solar home systems
Solar PV	Solar Photo Voltaic
TZS	Tanzanian Shillings
UNSDG	United Nation Sustainable Development Goals
UDSM	University of Dar es Salaam
MS	Microsoft
VB	Visio Basic

HEET	Higher Education for Economic Transformation
TOU	Time of use
ESS	Energy Storage System
CMST	Capacitated Minimum Spanning Tree
MST	Minimum Spanning Tree
MAC	Media Access Control
P2P	Peer-to-Peer
SG	Swarm Grid
PSO	Particle Swarm Optimizations
GWO	Grey Wolf Optimizations
LoRa WAN	Long-Range Wireless Access Network
CoET	College of Engineering and Technology
GSM	Global Standards for Mobile communications
Wi-Fi	Wireless Fidelity
IoT	Internet of Things
LoRa	Long-Range
CSS	Chirp Spread Spectrum
TDOA	Time Difference of Arrival
LOS	Line of sight
nLOS	No line of sight
DSM	Demand side management
PLC	Programmable Logic controller
HOMER	Hybrid Optimization of Multiple Energy Resources
GA	Genetic Algorithm

SSA	Sub-Saharan Africa
LCOE	Levelized Cost of Energy
BLE	Bluetooth Low Energy
SIM	Subscriber Identifier Module
3G	Third Generation
4G	Fourth Generation
ISM	Industrial, Scientific and Medicine
Nb	Narrow band
MILP	Mixed Integer Linear Programming
MoPSO	Multi-objectives Particle Swarm Optimization
NSR	Neighbourhood Search Routine
GUI	Graphical User Interface
PAYGO	Pay-as-you-go
CB	Community battery or Centralized battery
RTP	Real time pricing

REFERENCES

Adame, T., Bel, A., Bellalta, B., Barcelo, J., & Oliver, M. (2014). IEEE 802.11AH: The WiFi approach for M2M communications. *IEEE Wireless Communications*, *21*(6). https://doi.org/10.1109/MWC.2014.7000982

Adenle, A. A. (2020). Assessment of solar energy technologies in Africa-opportunities and challenges in meeting the 2030 agenda and sustainable development goals. *Energy Policy*, *137*. https://doi.org/10.1016/j.enpol.2019.111180

Agrawal, R., Faujdar, N., Romero, C. A. T., Sharma, O., Abdulsahib, G. M., Khalaf, O. I., Mansoor, R. F., & Ghoneim, O. A. (2023). Classification and comparison of ad hoc networks: A review. In *Egyptian Informatics Journal* (Vol. 24, Number 1). https://doi.org/10.1016/j.eij.2022.10.004

Albadi, M. H., & El-Saadany, E. F. (2008). A summary of demand response in electricity markets. In *Electric Power Systems Research* (Vol. 78, Number 11). https://doi.org/10.1016/j.epsr.2008.04.002

Alfaris, F. E., & Almutairi, F. (2024). Performance Assessment User Interface to Enhance the Utilization of Grid-Connected Residential PV Systems. *Sustainability (Switzerland)* , *16*(5). https://doi.org/10.3390/su16051825

Ashetehe, A. A., Shewarega, F., Gessesse, B. B., Biru, G., & Lakeou, S. (2024). A stochastic approach to determine the energy consumption and synthetic load profiles of different customer types of rural communities. *Scientific African*, *24*. https://doi.org/10.1016/j.sciaf.2024.e02172

Asif, M., & Muneer, T. (2007). Energy supply, its demand and security issues for developed and emerging economies. In *Renewable and Sustainable Energy Reviews* (Vol. 11, Number 7, pp. 1388–1413). https://doi.org/10.1016/j.rser.2005.12.004

Augustin, A., Yi, J., Clausen, T., & Townsley, W. M. (2016). A study of Lora: Long range & low power networks for the internet of things. *Sensors (Switzerland)*, *16*(9). https://doi.org/10.3390/s16091466

Bhattacharyya, S. C. (2012). Energy access programmes and sustainable development: A critical review and analysis. In *Energy for Sustainable Development* (Vol. 16, Number 3). https://doi.org/10.1016/j.esd.2012.05.002

Borenstein, S., & Holland, S. (2005). On the efficiency of competitive electricity markets with time-invariant retail prices. *RAND Journal of Economics*, *36*(3).

Bowes, J., Booth, C., & Strachan, S. (2017). System interconnection as a path to bottom up electrification. *2017 52nd International Universities Power Engineering Conference, UPEC 2017*, *2017-January*. https://doi.org/10.1109/UPEC.2017.8232018

Cabello-Vargas, J. E., Escobedo-Izquierdo, A., & Morales-Acevedo, A. (2021). Review on rural energy access policies. *International Journal of Energy Economics and Policy*, *11*(5). https://doi.org/10.32479/ijeep.11268

Centenaro, M., Vangelista, L., Zanella, A., & Zorzi, M. (2016). Long-range communications in unlicensed bands: The rising stars in the IoT and smart city scenarios. *IEEE Wireless Communications*, *23*(5). https://doi.org/10.1109/MWC.2016.7721743

Czerwiński, A., Wróbel, J., Lach, J., Wróbel, K., & Podsadni, P. (2018). The charging-discharging behavior of the lead-acid cell with electrodes based on carbon matrix. *Journal of Solid State Electrochemistry*, (9), 2703–2714. https://doi.org/10.1007/s10008-018-3981-4

Daniel Philipp, Hannes Kirchhoff, Brian Edlefsen, & Joseph Theune. (2020). *Swarm Electrification - A Paradigm Change: Building a Micro-Grid from the Bottom-up - energypedia*. Energypedia. https://energypedia.info/wiki/Swarm_Electrification_-_A_Paradigm_Change:_Building_a_Micro-Grid_from_the_Bottom-up

Devalal, S., & Karthikeyan, A. (2018). LoRa Technology - An Overview. *Proceedings of the 2nd International Conference on Electronics, Communication and Aerospace Technology, ICECA 2018*. https://doi.org/10.1109/ICECA.2018.8474715

Ebrahim, E. A., Maged, N. A., Abdel-Rahim, N., & Bendary, F. (2021). Open Energy Distribution System-Based on Photo-voltaic with Interconnected- Modified DC-Nanogrids. *Advances in Science, Technology and Engineering Systems Journal*, *6*(1), 982–988. https://doi.org/10.25046/aj0601108

Fairley, P. (2018). "swarm electrification" powers villages [Resources-Startups]. In *IEEE Spectrum* (Vol. 55, Number 4). https://doi.org/10.1109/MSPEC.2018.8322040

Fuchs, I., Balderrama, S., Quoilin, S., del Granado, P. C., & Rajasekharan, J. (2023). Swarm electrification: Harnessing surplus energy in off-grid solar home systems for universal electricity access. *Energy for Sustainable Development*, *77*. https://doi.org/10.1016/j.esd.2023.101342

Georges Akhras. (2000). Smart materials and smart systems for the future. *Canadian Military Journal 1.3*, 25–31.

Giraneza, M., Abo-Al-Ez, K. M., & Kahn, M. T. (2021). Nanogrid Based Energy Trading System for a Rural Off-Grid Communityin Africa. *SSRN Electronic Journal*. https://doi.org/10.2139/ssrn.3735389

Groh, S., Philipp, D., Lasch, B. E., & Kirchhoff, H. (2014, July 21). Swarm electrification-suggesting a paradigm change through building microgrids bottom-up. *Proceedings of 2014 3rd International Conference on the Developments in Renewable Energy Technology, ICDRET 2014*. https://doi.org/10.1109/icdret.2014.6861710

Hollberg, P. (2015). *Swarm grids - Innovation in rural electrification*. https://urn.kb.se/resolve?urn=urn:nbn:se:kth:diva-172846

Huang, Z., Zhu, T., Gu, Y., Irwin, D., Mishra, A., & Shenoy, P. (2014). Minimizing electricity costs by sharing energy in sustainable microgrids. *BuildSys 2014 - Proceedings of the 1st ACM Conference on Embedded Systems for Energy-Efficient Buildings*. https://doi.org/10.1145/2676061.2674063

Inam, W., Strawser, D., Afridi, K. K., Ram, R. J., & Perreault, D. J. (2015). Architecture and system analysis of microgrids with peer-to-peer electricity sharing to create a marketplace which enables energy access. *9th International Conference on Power Electronics - ECCE Asia: "Green World with Power Electronics", ICPE 2015-ECCE Asia*, 464–469. https://doi.org/10.1109/ICPE.2015.7167826

Indicator | Access to electricity (% of population) | World Bank Data360. (n.d.). Retrieved June 5, 2025, from https://data360.worldbank.org/en/indicator/WB_SE4ALL_EG_ACS_ELEC?view=map&urbanisation=RUR

Javadi, F. S., Rismanchi, B., Sarraf, M., Afshar, O., Saidur, R., Ping, H. W., & Rahim, N. A. (2013). Global policy of rural electrification. In *Renewable and Sustainable Energy Reviews* (Vol. 19). https://doi.org/10.1016/j.rser.2012.11.053

Kerboua, A., Boukli-Hacene, F., & Mourad, K. A. (2020). Particle swarm optimization for micro-grid power management and load scheduling. *International Journal of Energy Economics and Policy*, *10*(2). https://doi.org/10.32479/ijeep.8568

Kirchhoff, H. (2013). The Swarm Electrification Concept. *Berlin: Research Group Microenergy Systems*.

Kirchhoff, H. (2015). *Identifying Hidden Resources in Solar Home Systems as the Basis for Bottom-Up Grids* (pp. 23–32). https://doi.org/10.1007/978-3-319-15964-5_2

Kirchhoff, H., & Strunz, K. (2019). Key drivers for successful development of peer-to-peer microgrids for swarm electrification. *Applied Energy*, *244*. https://doi.org/10.1016/j.apenergy.2019.03.016

Kulkarni, S., Piper, S., Liptak, S., & Divan, D. (2019). Implementing Pay-as-You-Go Functionality in Microgrids using Mobile Ad-Hoc Networks. *2019 IEEE Decentralized Energy Access Solutions Workshop, DEAS 2019*. https://doi.org/10.1109/DEAS.2019.8758756

Luthander, R., Widén, J., Nilsson, D., & Palm, J. (2015). Photovoltaic self-consumption in buildings: A review. In *Applied Energy* (Vol. 142). https://doi.org/10.1016/j.apenergy.2014.12.028

Magnasco, A., Kirchhoff, H., Chowdhury, S., & Groh, S. (2016). Data Services for Real Time Optimization of DC Nanogrids with Organic Growth. *Energy Procedia*, *103*, 369–374. https://doi.org/10.1016/j.egypro.2016.11.301

Mandelli, S., Barbieri, J., Mereu, R., & Colombo, E. (2016). Off-grid systems for rural electrification in developing countries: Definitions, classification and a comprehensive literature review. *Renewable and Sustainable Energy Reviews*, *58*, 1621–1646. https://doi.org/10.1016/j.rser.2015.12.338

Maria Mahmud, M., Foong Wong, S., Qazi, A., Fazlin Mohd Ramli, N., Fauziana Zakaria, S., Alam, S., & Rusli, R. (2024). *Excel-ling in Data Visualization: Evaluating Microsoft Excel's User-Friendliness, Visual Appeal, and Reputation Impact*. https://doi.org/10.1109/ICIET60671.2024.10542793

Masenge, I., & Mwasilu, F. (2020). Hybrid Solar PV-Wind Generation System Coordination Control and Optimization of Battery Energy Storage System for Rural Electrification. *2020 IEEE PES/IAS PowerAfrica, PowerAfrica 2020*. https://doi.org/10.1109/PowerAfrica49420.2020.9219890

Mekki, K., Bajic, E., Chaxel, F., & Meyer, F. (2019). A comparative study of LPWAN technologies for large-scale IoT deployment. *ICT Express*, *5*(1). https://doi.org/10.1016/j.icte.2017.12.005

Mengelkamp, E., Gärttner, J., Rock, K., Kessler, S., Orsini, L., & Weinhardt, C. (2018). Designing microgrid energy markets: A case study: The Brooklyn Microgrid. *Applied Energy*, *210*. https://doi.org/10.1016/j.apenergy.2017.06.054

Mergel, D. (n.d.). *Physics with Excel and Python Using the Same Data Structure Volume I: Basics, Exercises and Tasks*.

Mishra, S., & Palu, I. (2016). A user interface tool for ramping behavior analysis of renewable energy. *10th International Conference - 2016 Electric Power Quality and Supply Reliability, PQ 2016, Proceedings*. https://doi.org/10.1109/PQ.2016.7724109

Murdyantoro, E., Nugraha, A. W. W., Wardhana, A. W., Fadli, A., & Zulfa, M. I. (2019). A review of LoRa technology and its potential use for rural development in Indonesia. *AIP Conference Proceedings*, *2094*. https://doi.org/10.1063/1.5097480

Mwammenywa, I., Petrov, D., Holle, P., & Hilleringmann, U. (2022). LoRa Transceiver for Load Monitoring and Control System in Microgrids. *8th International Conference on Engineering and Emerging Technologies, ICEET 2022*. https://doi.org/10.1109/ICEET56468.2022.10007274

Narvios, W. M. O., Archival, J. N., & Nguyen, Y. Q. (2021). An internet of things (IoT) based swarm electrification for solar powered households. *AIP Conference Proceedings*, *2406*. https://doi.org/10.1063/5.0066561

Parag, Y., & Sovacool, B. K. (2016). Electricity market design for the prosumer era. *Nature Energy*, *1*(4). https://doi.org/10.1038/NENERGY.2016.32

Paserba, J., & Cunningham, J. J. (2024). DC Survival: Myth of the War of the Currents [History]. *IEEE Power and Energy Magazine*, *22*(3), 104–109. https://doi.org/10.1109/MPE.2024.3379454

Peters, J., Sievert, M., & Toman, M. A. (2019). Rural electrification through mini-grids: Challenges ahead. *Energy Policy*, *132*. https://doi.org/10.1016/j.enpol.2019.05.016

Prechtl, M. H. G. (2023). UN Sustainable Development Goal 7: clean energy - a holistic approach towards a sustainable future through hydrogen storage. In *RSC Sustainability* (Vol. 1, Number 7). https://doi.org/10.1039/d3su90036c

Ramesh, L., & Chowdhury, S. (2009). Minimization of power Loss in distribution networks by different techniques. *International Journal of Electrical and Electronics Engineering*, *2*.

Rand, D. A. J., & Moseley, P. T. (2015). Energy Storage with Lead–Acid Batteries. *Electrochemical Energy Storage for Renewable Sources and Grid Balancing*, *13*(2), 201–222. https://doi.org/10.1016/B978-0-444-62616-5.00013-9

Rasheed, M. B., Qureshi, M. A., Javaid, N., & Alquthami, T. (2020). Dynamic Pricing Mechanism with the Integration of Renewable Energy Source in Smart Grid. *IEEE Access*, *8*. https://doi.org/10.1109/ACCESS.2020.2967798

Reynders, B., Meert, W., & Pollin, S. (2016). Range and coexistence analysis of long range unlicensed communication. *2016 23rd International Conference on Telecommunications, ICT 2016*. https://doi.org/10.1109/ICT.2016.7500415

Samende, C., Bhagavathy, S. M., & McCulloch, M. (2021). Power Loss Minimization of Off-Grid Solar DC Nano-Grids-Part I: Centralized Control Algorithm. *IEEE Transactions on Smart Grid*, *12*(6). https://doi.org/10.1109/TSG.2021.3108236

Sheridan, S., Sunderland, K., & Courtney, J. (2023). Swarm electrification: A comprehensive literature review. In *Renewable and Sustainable Energy Reviews* (Vol. 175). Elsevier Ltd. https://doi.org/10.1016/j.rser.2023.113157

Solomon, S., Plattner, G. K., Knutti, R., & Friedlingstein, P. (2009). Irreversible climate change due to carbon dioxide emissions. *Proceedings of the National Academy of Sciences of the United States of America*, *106*(6). https://doi.org/10.1073/pnas.0812721106

Soltowski, B., Campos-Gaona, D., Strachan, S., & Anaya-Lara, O. (2019). Bottom-up electrification introducing new smart grids architecture-concept based on feasibility studies conducted in Rwanda. *Energies*, *12*(12). https://doi.org/10.3390/en12122439

Sousa, T., Soares, T., Pinson, P., Moret, F., Baroche, T., & Sorin, E. (2019). Peer-to-peer and community-based markets: A comprehensive review. In *Renewable and Sustainable Energy Reviews* (Vol. 104). https://doi.org/10.1016/j.rser.2019.01.036

Starke, M., Tolbert, L. M., & Ozpineci, B. (2008). AC vs. DC distribution: A loss comparison. *Transmission and Distribution Exposition Conference: 2008 IEEE PES Powering Toward the Future, PIMS 2008*. https://doi.org/10.1109/TDC.2008.4517256

Steven Nolan, Scott Strachan, Puran Rakhra, & Damien Frame. (2017). *Optimized Network Planning of Mini-Grids for the Rural Electrification of Developing Countries*. IEEE.

Stojanovski, O., Thurber, M., & Wolak, F. (2017). Rural energy access through solar home systems: Use patterns and opportunities for improvement. *Energy for Sustainable Development*, *37*. https://doi.org/10.1016/j.esd.2016.11.003

Temesgen, A. L., Wassie, Y. T., & Ahlgren, E. O. (2024). Analyzing grid extension suitability: A case study of Ethiopia using OnSSET. *Energy Strategy Reviews*, *52*, 101292. https://doi.org/10.1016/j.esr.2023.101292

Tenenbaum, B., Greacen, C., Siyambalapitiya, T., & Knuckles, J. (2014). From the Bottom Up: How Small Power Producers and Mini-Grids Can Deliver Electrification and Renewable Energy in Africa. In *From the Bottom Up: How Small Power Producers and Mini-Grids Can Deliver Electrification and Renewable Energy in Africa*. https://doi.org/10.1596/978-1-4648-0093-1

Tushar, W., Saha, T. K., Yuen, C., Smith, D., & Poor, H. V. (2020). Peer-to-Peer Trading in Electricity Networks: An Overview. *IEEE Transactions on Smart Grid*, *11*(4). https://doi.org/10.1109/TSG.2020.2969657

UART Interface 868/915 MHz LoRa® Antenna Transceiver Module Datasheet. (2021).

Unger, K., & Kazerani, M. (2011). Simulation of rural electrification via cellular-enabled micro-inverter. *Proceedings - 2011 IEEE Global Humanitarian Technology Conference, GHTC 2011*, 1–6. https://doi.org/10.1109/GHTC.2011.9

Unger, K., & Kazerani, M. (2012). Organically grown microgrids: Development of a solar neighborhood microgrid concept for off-grid communities. *IECON Proceedings (Industrial Electronics Conference)*. https://doi.org/10.1109/IECON.2012.6389060

Van Der Meer, S., Steglich, S., & Arbanowski, S. (n.d.). *User-Centric Communications*.

Watson, S., Bian, D., Sahraei, N., Winter, A. G., Buonassisi, T., & Peters, I. M. (2018). Advantages of operation flexibility and load sizing for PV-powered system design. *Solar Energy*, *162*. https://doi.org/10.1016/j.solener.2018.01.022

Zakeri, B., & Syri, S. (2015). Electrical energy storage systems: A comparative life cycle cost analysis. In *Renewable and Sustainable Energy Reviews* (Vol. 42). https://doi.org/10.1016/j.rser.2014.10.011

Zhang, C., Wu, J., Long, C., & Cheng, M. (2017). Review of Existing Peer-to-Peer Energy Trading Projects. *Energy Procedia*, *105*. https://doi.org/10.1016/j.egypro.2017.03.737

Zhu, T., Xiao, S., Ping, Y., Towsley, D., & Gong, W. (2011). A secure energy routing mechanism for sharing renewable energy in smart microgrid. *2011 IEEE International Conference on Smart Grid Communications, SmartGridComm 2011*, 143–148. https://doi.org/10.1109/SmartGridComm.2011.6102307

Appendix 1: List of Publications

The following articles have been published during the PhD journey.

1. **Mwakijale, J. S**., Safin, K. H., & Hilleringmann, U. (2024, October). Smart and Low-Cost Transceiver for Energy Sharing and Billing in the Implementation of Swarm Grids. In *2024 IEEE PES/IAS PowerAfrica* (pp. 1-4). IEEE.

2. **Mwakijale, J. S.,** & Hilleringmann, U. (2024, October). Is AC or DC Distribution Line the Way Forward for Solar Swarm Grid Implementation? In *2024 IEEE PES/IAS PowerAfrica* (pp. 1-4). IEEE.

3. **Mwakijale, J. S.,** Mwammenywa, I., & Hilleringmann, U. (2023, November). LoRa-based Swarm Grid Implementation for Rural Electrification in Africa. In *2023 IEEE PES/IAS PowerAfrica* (pp. 1-4). IEEE.

4. Mwammenywa, I. A., **Mwakijale, J. S.,** & Krishna, M. (2025). Techno-Economic Analysis of Hybrid PV-Wind-Diesel Generator Swarm Grid for Rural Electrification in Tanzania. *Tanzania Journal of Engineering and Technology*, *44*(3), 49-68.

Appendix 2: Model Testing and Verification

The correctness of the developed network optimization model was first verified using simplified test scenario comprised of four households as depicted in Figure 0.1. From the figure parameters i.e., PV, battery, demand, charging and discharging efficiency, penalties were supplied as shown in the sample code below. A 24-hour simulation was conducted, and the results were manually computed to verify the effectiveness of the model. Three-time stamp was used to perform the verification: Morning, day and night. Retrospectively the time step of 8, 14 and 22 hrs for Morning, day and night were used.

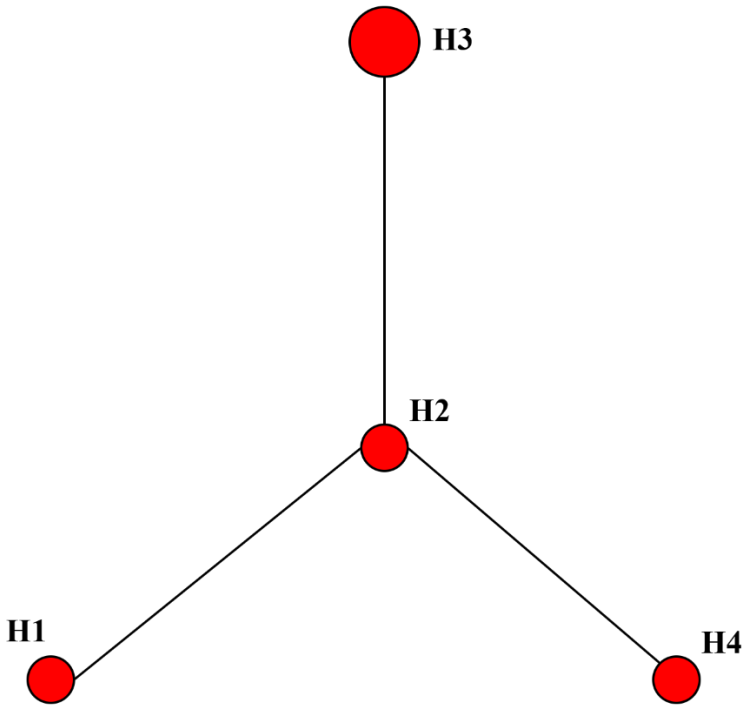

Figure 0.1: Sample network for Model's Constraints Verification

Sample code for model constraint and variable verification

```
import gurobipy as gp
from gurobipy import GRB
import pandas as pd
import numpy as np

# ====================================
# SETS
# ====================================

houses = ["H1", "H2", "H3","H4"]

T = range(24) # 24 hours simulation time

# ====================================
# PV GENERATION (kWh)
# ====================================

S_pv = {(i,t): 2 if 10 <= t <= 17 else 0
        for i in houses for t in T}

# ====================================
# DEMAND (kWh)
# ====================================

D = {(i,t): 3 if 18 <= t <= 22 else 1
     for i in houses for t in T}

# ====================================
# ADJACENCY MATRIX
# ====================================

A = {(i,j): 1 if i != j else 0
     for i in houses for j in houses}

# For NO connection between H1 and H3, H1 and H4, also H4
and H3
A["H1","H3"]=0
```

```
A["H3","H1"]=0
A["H3","H4"]=0
A["H4","H3"]=0
A["H1","H4"]=0
A["H4","H1"]=0

# ====================================
# BATTERY PARAMETERS
# ====================================

C_bat_chg = {i:2 for i in houses}
C_bat_dis = {i:2 for i in houses}

E_b_min = {i:0 for i in houses}
E_b_max = {i:5 for i in houses}

initial_SOC = 0.5

eta_c = 0.95
eta_d = 0.9
eta_s = 0.995

flow_capacity = 3

# penalties
pen_unmet = 10000
pen_surplus = 10

# ====================================
# MODEL
# ====================================

model = gp.Model("SwarmGrid_Test")

# ====================================
# VARIABLES
# ====================================
```

```
flows = model.addVars(houses, houses, T, lb=0,
ub=flow_capacity)

S_bat_chg = model.addVars(houses, T, lb=0)
S_bat_dis = model.addVars(houses, T, lb=0)

E_b = model.addVars(houses, T, lb=0)

P_D = model.addVars(houses, T, lb=0)   # unmet demand
P_S = model.addVars(houses, T, lb=0)   # surplus

z = model.addVars(houses, T, vtype=GRB.BINARY)
w = model.addVars(houses, houses, T, vtype=GRB.BINARY,
name="flow_one_direction_at_time")

# ====================================
# FLOW CONSTRAINTS
# ====================================

for i in houses:
    for j in houses:
        if A[i,j] == 0:
            for t in T:
                model.addConstr(flows[i,j,t] == 0)

# ====================================
# FLOW CONSTRAINTS
# ====================================


for i in houses:
    for j in houses:
     if i!=j:
      for t in T:
        model.addConstr(flows[i, j, t] <= flow_capacity *
A[i,j] * w[i, j, t])
        model.addConstr(flows[j, i, t] <= flow_capacity *
A[i,j] * (1 - w[i, j, t]))
# ====================================
```

```
# POWER BALANCE
# ====================================

for i in houses:
    for t in T:

        inflow = gp.quicksum(flows[j,i,t] for j in houses if
j != i)
        outflow = gp.quicksum(flows[i,j,t] for j in houses
if j != i)

        model.addConstr(

            S_pv[i,t]
            + S_bat_dis[i,t]
            + inflow
            + P_D[i,t]

            ==

            D[i,t]
            + S_bat_chg[i,t]
            + outflow
            + P_S[i,t]

        )


for i in houses:
    model.addConstr(E_b[i, T[-1]] == E_b[i, 0])

# ====================================
# BATTERY SOC DYNAMICS
# ====================================

for i in houses:
    for t in T:

        if t == 0:
```

```
            model.addConstr(
                E_b[i,t]
                ==
                initial_SOC
                + eta_c * S_bat_chg[i,t]
                - (1/eta_d) * S_bat_dis[i,t]
            )
        else:
            model.addConstr(
                E_b[i,t]
                ==
                eta_s * E_b[i,t-1]
                + eta_c * S_bat_chg[i,t]
                - (1/eta_d) * S_bat_dis[i,t]
            )
# ====================================
# BATTERY LIMITS
# ====================================
for i in houses:
    for t in T:
        model.addConstr(E_b[i,t] <= E_b_max[i])
        model.addConstr(E_b[i,t] >= E_b_min[i])
```

```
        model.addConstr(S_bat_chg[i,t] <= C_bat_chg[i] *
z[i,t])
        model.addConstr(S_bat_dis[i,t] <= C_bat_dis[i] * (1
- z[i,t]))

        # Prevent discharging more than stored energy
        model.addConstr(S_bat_dis[i,t] <= E_b[i,t])
        model.addConstr(P_D[i,t] <= D[i,t])
        model.addConstr(P_S[i,t] <= S_pv[i,t])

# ====================================
# OBJECTIVE FUNCTION
# ====================================

model.setObjective(

    gp.quicksum(pen_unmet * P_D[i,t] for i in houses for t
in T)
    +
    gp.quicksum(pen_surplus * P_S[i,t] for i in houses for t
in T),

    GRB.MINIMIZE
)

# ====================================
# SOLVE
# ====================================

model.optimize()

# ====================================
# RESULTS
# ====================================

import pandas as pd

# ==============================
```

```
# COLLECT RESULTS INTO DATAFRAME
# ==============================

rows = []

for t in range(22,23):
    for i in houses:

        rows.append({
            "Hour": t,
            "House": i,
            "PV": S_pv[i,t],
            "Demand": D[i,t],
            "Unmet_Demand": P_D[i,t].X,
            "Surplus": P_S[i,t].X
        })

results_df = pd.DataFrame(rows)

print("\nEnergy Results Table")
print(results_df)

flow_rows = []

for t in range(22,23):
    for i in houses:
        for j in houses:
            if i != j:

                val = flows[i,j,t].X

                if val > 1e-6:
                    flow_rows.append({
                        "Hour": t,
                        "From": i,
                        "To": j,
                        "Energy Flow (kWh)": round(val,2)
                    })
```

```
flows_df = pd.DataFrame(flow_rows)

print("\nFlow Table")
print(flows_df)


import pandas as pd

# Prepare list to store SOC data
soc_data = []

for i in houses:
    initial_soc = E_b[i, 0].X   # SOC at the first timestep
    final_soc   = E_b[i, 23].X  # SOC at the last timestep
(hour 23)
    soc_data.append({
        'House': i,
        'Initial SOC (kWh)': round(initial_soc, 2),
        'Final SOC (kWh)': round(final_soc, 2)
    })

df_soc = pd.DataFrame(soc_data)
print(df_soc)



Battery_rows=[]
for i in houses:
    for t in range(22,23):
        val = E_b[i,t].X
        Battery_rows.append({
                        "Hour": t,
                        "From": i,
                        "Battery Energy level (kWh)":
round(val,2),
                        "Maximum Battery Cap (kWh)":
round(E_b_max[i],2)
                    })
```

```
battery_df = pd.DataFrame(Battery_rows)

data = []

for t in range (22,23):
    for i in houses:
        val1 = S_bat_chg[i, t].X
        val2 = S_bat_dis[i, t].X
        # Append as a dictionary for easy DataFrame creation
        data.append({
            'House': i,
            'Time': t,
            'Charge (kW)': round(val1, 1),
            'Discharge (kW)': round(val2, 1)
        })

df_battery = pd.DataFrame(data)

print(df_battery)

# Name of the output file
output_file =
"C:/Users/mwaki/Desktop/Research/Thesis/Optimization
Model/Script/milp_results.txt"

with open(output_file, "w") as f:
    # Table 1: Energy Result Table
    f.write("=== Table 1: Energy Result Table ===\n")
    f.write(results_df.to_string(index=False))
    f.write("\n\n")  # extra space between tables

    # Table 2: Power flow)
    f.write("=== Table 2: Power Flow (kWh) ===\n")
    f.write(flows_df.to_string(index=False))
    f.write("\n\n")

    # Section 2: Battery State of Charge (SOC)
    f.write("=== Table 3: Battery SOC (kWh) ===\n")
```

```
    f.write(df_soc.to_string(index=False))
    f.write("\n\n")

    # Table 1: Energy Result Table
    f.write("=== Table 4: Battery Charge and Discharge logic
===\n")
    f.write(df_battery.to_string(index=False))
    f.write("\n\n")  # extra space between tables

    # Table 1: Energy Result Table
    f.write("=== Table 5: Maximum Storage not exceeded
===\n")
    f.write(battery_df.to_string(index=False))
    f.write("\n\n")  # extra space between tables

print(f"All results saved to {output_file}")
```

Case 1: Morning

The snapshot for morning simulation is shown in Figure 0.2. From the supplied inputs during this time are., PV= 0, demand =1. Since there is no PV and the initial condition of the battery's energy was set 0.5. Then, recall energy balance equation

$$S_{i,t}^{pv} + S_{i,t}^{bat(dis)} + \sum_{j \in N} f_{j,i,t} + P_{i,t}^{D} = D_{i,t} + S_{i,t}^{bat(chg)} + \sum_{j \in N} f_{i,j,t} + P_{i,t}^{s} \quad (0.1)$$

```
=== Table 1: Energy Result Table ===
 Hour House  PV  Demand  Unmet_Demand  Surplus
    8    H1   0       1      0.999423      0.0
    8    H2   0       1      0.998847      0.0
    8    H3   0       1      1.000000      0.0
    8    H4   0       1      0.999423      0.0

=== Table 2: Power Flow (kWh) ===
 Hour From To  Energy Flow (kWh)
    8   H3 H2               0.0

=== Table 3: Battery SOC (kWh) ===
House  Initial SOC (kWh)  Final SOC (kWh)
   H1              0.24             0.24
   H2              0.24             0.24
   H3              0.24             0.24
   H4              0.24             0.24

=== Table 4: Battery Charge and Discharge logic ===
House  Time  Charge (kW)  Discharge (kW)
   H1     8         0.0             0.0
   H2     8         0.0             0.0
   H3     8         0.0             0.0
   H4     8         0.0             0.0

=== Table 5: Maximum Storage not exceeded ===
 Hour From  Battery Energy level (kWh)  Maximum Battery Cap (kWh)
    8   H1                         0.0                         5
    8   H2                         0.0                         5
    8   H3                         0.0                         5
    8   H4                         0.0                         5
```

Figure 0.2: Morning (*at t=8hrs*) simulation

Table 0.1: Energy Balance constraint Verification

Expectation	***Model Results***
R.H.S: $0 + 0 + 0 + 1 = 1$	R.H.S: $0 + 0 + 0 + 0.999423 \cong 1$
L.H.S: $1 + 0 + 0 + 0 \ = \ 1$	L.H.S: $1 + 0 + 0 + 0 \ = \ 1$
∴R.H.S =L.H.S	∴R.H.S =L.H.S

According to Table 0.1, the model adhered with the energy balance constraint. By doing inspection on Figure 0.2, the recycling battery energy constraint is obeyed as shown in Table 3. Avoidance of the simultaneous battery charging and discharging is shown in Table 4 of the same figure in which now there is neither charging nor discharging, which is an acceptable condition. Similarly, in Table 5 no battery energy has exceeded the maximum value set. The bidirectional power flow is also obeyed as there is no power flow happening twice between the same pair of nodes in all three cases, see Table 2 in Figure 0.2, Figure 0.3, and Figure 0.4. Recall that the flow capacity of the cable was limited to 3 kWh, and the constraint for not to exceed the capacity was set and obeyed as seen in Table 2 where none of the flow is beyond 3 kWh.

Case 2: Day

```
=== Table 1: Energy Result Table ===
 Hour House  PV  Demand  Unmet_Demand  Surplus
   14    H1   2       1           0.0      1.0
   14    H2   2       1           0.0      0.0
   14    H3   2       1           0.0      0.0
   14    H4   2       1           0.0      0.0

=== Table 2: Power Flow (kWh) ===
 Hour From To  Energy Flow (kWh)
   14   H2 H1                2.0
   14   H2 H4                1.0

=== Table 3: Battery SOC (kWh) ===
House  Initial SOC (kWh)  Final SOC (kWh)
   H1               0.24             0.24
   H2               0.24             0.24
   H3               0.24             0.24
   H4               0.24             0.24

=== Table 4: Battery Charge and Discharge logic ===
House  Time  Charge (kW)  Discharge (kW)
   H1    14          2.0             0.0
   H2    14          0.0             2.0
   H3    14          1.0             0.0
   H4    14          2.0             0.0

=== Table 5: Maximum Storage not exceeded ===
 Hour From  Battery Energy level (kWh)  Maximum Battery Cap (kWh)
   14   H1                         5.00                         5
   14   H2                         2.75                         5
   14   H3                         4.79                         5
   14   H4                         5.00                         5
```

Figure 0.3: Daytime (*at t=14*) Simulation

Case 3: Night

```
=== Table 1: Energy Result Table ===
 Hour House  PV  Demand  Unmet_Demand  Surplus
   22    H1   0       3      2.912276      0.0
   22    H2   0       3      3.000000      0.0
   22    H3   0       3      2.956138      0.0
   22    H4   0       3      2.956138      0.0

=== Table 2: Power Flow (kWh) ===
 Hour From To  Energy Flow (kWh)
   22   H2 H1               0.00

=== Table 3: Battery SOC (kWh) ===
House  Initial SOC (kWh)  Final SOC (kWh)
   H1               0.24             0.24
   H2               0.24             0.24
   H3               0.24             0.24
   H4               0.24             0.24

=== Table 4: Battery Charge and Discharge logic ===
House  Time  Charge (kW)  Discharge (kW)
   H1    22          0.0             0.0
   H2    22          0.0             0.0
   H3    22          0.0             0.0
   H4    22          0.0             0.0

=== Table 5: Maximum Storage not exceeded ===
 Hour From  Battery Energy level (kWh)  Maximum Battery Cap (kWh)
   22   H1                         0.24                          5
   22   H2                         0.24                          5
   22   H3                         0.24                          5
   22   H4                         0.24                          5
```

Figure 0.4: Nighttime (*at t=22*) Simulation

Appendix 3: List of Supervised Students

The following students were supervised and successfully completed their studies during the PhD journey.

1. **Kamrul Hassan Safin**
   - Title: Design and Development of Energy Transceiver Using LoRa Wireless Technology for Solar Swarm Grids
   - Type: Master Project
   - Year: 2024

2. **Neky Vinodkumar Chaniyara**
   - Title: Improved Latency for Satellite Communication using Dynamic Routing and Machine Learning Algorithm
   - Type: Master Thesis
   - Year: 2025

3. **Monish Krishna Ogirala**
   - Title: Designing, Modelling, and Simulation of Hybrid Energy Sources for off-grid Swarm Grid using MATLAB/Simulink and HOMER
   - Type: Master Thesis
   - Year: 2025

4. **Rostand Tagne Kungne**
   - Title: Smart and cost-effective solution for Monitoring and Control of Remote Microgrid Using ESP32 and LoRa Network
   - Type: Master Thesis
   - Year: 2026